MDE-49-0386
DRF B11-00339
Class I
April 1986

JAMES A. FITZPATRICK NUCLEAR POWER PLANT REACTOR PRESSURE VESSEL SURVEILLANCE MATERIALS TESTING AND FRACTURE TOUGHNESS ANALYSIS

Prepared by: T. A. Caine 4/25/86

T. A. Caine, Senior Engineer
Structural Analysis Services

Verified by: B. J. Branlund 4/25/86

B. J. Branlund, Engineer
Structural Analysis Services

Approved by: S. Ranganath 4/25/86

S. Ranganath, Manager
Structural Analysis Services

IMPORTANT NOTICE REGARDING
CONTENTS OF THIS REPORT
PLEASE REAL CAREFULLY

This report was prepar d by General Electric solely for the use of the New York Power Authority. The information contained in this report is believed by General Electric to be an accurate and true representation of the facts known, obtained or provided to General Electric at the time this report was prepared.

The only undertakings f the General Electric Company respecting information in this document are contained in the contract governing New York Power Authority Purchase Order No. 025720-85 and nothing contained in this document shall be construed as changing said contract. The use of this information except as defined by said contract, or for any purpose other than that for which it is intended, is not authorized; and with respect to any such unauthorized use, neither General Electric Company nor any of the contributors to this document makes any representation or warranty (express or implied) as to the completeness, accuracy or usefulness of the information contained in this document or that such use of such information may not infringe privately owned rights; nor do they assume any responsibility for liability or damage of any kind which may result from such use of such information.

CONTENTS

		Page
	ABSTRACT	ix
	ACKNOWLEDGEMENTS	x
1.	INTRODUCTION	1-1
2.	SUMMARY AND CONCLUSIONS	2-1
	2.1 Summary of Results	2-1
	2.2 Conclusions	2-5
3.	SURVEILLANCE PROGRAM BACKGROUND	3-1
	3.1 Capsule Recovery	3-1
	3.2 RPV Materials and Fabrication Background	3-1
	3.2.1 Fabrication History	3-1
	3.2.2 Material Properties of RPV at Fabrication	3-2
	3.2.3 Specimen Chemical Composition	3-3
	3.2.4 Initial Reference Temperature	3-3
	3.3 Specimen Description	3-6
	3.3.1 Charpy Specimens	3-6
	3.3.2 Tensile Specimens	3-7
4.	PEAK RPV FLUENCE EVALUATION	4-1
	4.1 Flux Wire Analysis	4-1
	4.1.1 Procedure	4-1
	4.1.2 Results	4-2
	4.2 Determination of Lead Factors	4-3
	4.2.1 Procedure	4-4
	4.2.2 Results	4-5
	4.3 Estimate of End-of-Life Fluence	4-5
5.	CHARPY V-NOTCH IMPACT AND HARDNESS TESTING	5-1
	5.1 Impact Test Procedure	5-1
	5.2 Impact Test Results	5-2
	5.3 Irradiated Versus Unirradiated Charpy V-Notch Properties	5-3
	5.4 Rockwell Hardness Testing	5-3
6.	TENSILE TESTING	6-1
	6.1 Procedure	6-1
	6.2 Results	6-2
	6.3 Irradiated Versus Unirradiated Tensile Properties	6-3
7.	DEVELOPMENT OF OPERATING LIMITS CURVES	7-1
	7.1 Background	7-1
	7.2 Non-Beltline Regions	7-1
	7.3 Core Beltline Region	7-2
	7.4 Closure Flange Region	7-2
	7.5 Core Critical Operation Requirements of 10CFR50, Appendix G	7-3

CONTENTS (Continued)

		Page
7.6	Evaluation of Radiation Effects	7-4
	7.6.1 Measured Versus Predicted Surveillance Shift	7-5
	7.6.2 Modification of the Shift Relationship	7-5
	7.6.3 Radiation Shift Versus EFPY	7-5
	7.6.4 End-of-Life Conditions	7-6
7.7	Operating Limits Curves Valid to 16 EFPY	7-7
7.8	Reactor Operation Versus Operating Limits	7-7
8.	REFERENCES	8-1

APPENDICES

A.	CHARPY V-NOTCH FRACTURE SURFACE PHOTOGRAPHS	A-1

TABLES

Table	Title	Page
3-1	Chemical Composition of RPV Beltline Materials	3-8
3-2	Results of Fabrication Test Program for Selected RPV Locations	3-9
3-3	Plasma Emission Spectrometry Chemical Analysis of RPV Surveillance Plate and Weld Materials	3-10
3-4	Identification of Charpy and Tensile Specimens Removed from Surveillance Capsule	3-11
4-1	Summary of Daily Power History	4-6
4-2	Surveillance Capsule Location Flux and Fluence for Irradiation 1/26/75 to 2/15/85	4-7
5-1	Qualification Test Results Using U.S. Army Watertown Specimens (Tested in February 1986)	5-5
5-2	Charpy V-Notch Impact Test Results for Irradiated RPV Materials	5-6
5-3	Significant Results of Irradiated and Unirradiated Charpy V-Notch Data	5-7
5-4	Rockwell C Hardness Test Results	5-8
6-1	Tensile Test Results for Irradiated RPV Materials	6-4
6-2	Comparison of Unirradiated and Irradiated Tensile Properties at Room Temperature	6-5
7-1	Estimate of Upper Shelf Energy for Beltline Materials	7-8
7-2	Pressure-Temperature Values for Figure 7-5 (Curve A)	7-9
7-3	Pressure-Temperature Values for Figures 7-6 (Curve B) and 7-7 (Curve C)	7-10

ILLUSTRATIONS

Figure	Title	Page
2-1	Pressure Versus Minimum Temperature for Hydrostatic Pressure Tests for FitzPatrick	2-6
2-2	Pressure Versus Minimum Temperature for Non-Nuclear Heatup and Cooldown for FitzPatrick	2-7
2-3	Pressure Versus Minimum Temperature for Core Critical Operation for FitzPatrick	2-8
3-1	Surveillance Capsule Recovered from FitzPatrick Reactor	3-12
3-2	Schematic of the RPV Showing Arrangement of Vessel Plates and Welds	3-13
3-3	Fabrication Method for Base Metal Charpy Specimens	3-14
3-4	Fabrication Method for Weld Metal Charpy Specimens	3-15
3-5	Fabrication Method for HAZ Charpy Specimens	3-16
3-6	Fabrication Method for Base Metal Tensile Specimens	3-17
3-7	Fabrication [illegible]d for Weld Metal Tensile Specimens	3-18
3-8	Fabrication Met[illegible] for HAZ Tensile Specimens	3-19
4-1	Schematic of Model for Two-Dimensional Flux Distribution Analysis	4-8
5-1	FitzPatrick Irradiated Base Metal Impact Energy	5-9
5-2	FitzPatrick Irradiated Weld Metal Impact Energy	5-10
5-3	FitzPatrick Irradiated HAZ Metal Impact Energy	5-11
5-4	FitzPatrick Irradiated Base Metal Lateral Expansion	5-12
5-5	FitzPatrick Irradiated Weld Metal Lateral Expansion	5-13
5-6	FitzPatrick Irradiated HAZ Metal Lateral Expansion	5-14
5-7	FitzPatrick Irradiated versus Unirradiated Base Metal Impact Energy	5-15
5-8	FitzPatrick Irradiated verus Unirradiated Base Metal Lateral Expansion	5-16
6-1	Typical Engineering Stress versus Percent Strain for Irradiated RPV Materials	6-6

ILLUSTRATIONS

Figure	Title	Page
6-2	Strength versus Test Temperature for Irradiated Base, Weld, and HAZ Tensile Specimens	6-7
6-3	Ductility versus Test Temperature for Irradiated Base, Weld, and HAZ Tensile Specimens	6-8
6-4	Fracture Location, Necking Behavior, and Fracture Appearance for Irradiated Base Metal Tensile Specimens	6-9
6-5	Fracture Location, Necking Behavior, and Fracture Appearance for Irradiated Weld Metal Tensile Specimens	6-10
6-6	Fracture Location, Necking Behavior, and Fracture Appearance for Irradiated HAZ Metal Tensile Specimens	6-11
7-1	Components of Operating Limits Curve for Pressure Test (Curve A) for FitzPatrick	7-12
7-2	Components of Operating Limits Curve for Non-Nuclear Heatup/Cooldown (Curve B) for FitzPatrick	7-13
7-3	Components of Operating Limits Curve for Core Critical Operation (Curve C) for FitzPatrick	7-14
7-4	Adjusted Reference Temperature of Limiting Plate and Weld, Based on Surveillance Specimen Test Results for FitzPatrick	7-15
7-5	Pressure Versus Minimum Temperature for Hydrostatic Pressure Tests for FitzPatrick	7-16
7-6	Pressure Versus Minimum Temperature for Non-Nuclear Heatup and Cooldown for FitzPatrick	7-17
7-7	Pressure Versus Minimum Temperature for Core Critical Operation for FitzPatrick	7-18

ABSTRACT

A surveillance capsule was removed from the James A. FitzPatrick Nuclear Power Plant reactor at the end of Fuel Cycle 6. The capsule contained flux wires for neutron fluence measurement and Charpy and tensile test specimens for material property evaluation. A combination of flux wire testing and computer analysis was used to establish the vessel peak flux location and magnitude. Charpy V-Notch impact testing and uniaxial tensile testing were performed to establish the material properties of the irradiated vessel beltline. The irradiation effects were projected to the vessel end-of-life. The end-of-life conditions are less severe than the limits requiring vessel thermal annealing. Pressure-temperature operating limits curves valid to 16 effective full power years were developed to July 1983 requirements of 10CFR50 Appendix G (48FR24008).

ACKNOWLEDGMENTS

Flux wire testing was performed by G. C. Martin. D. R. Rogers provided the evaluation of flux distribution. The Charpy V-Notch impact testing was done by J. L. Bennett, and hardness testing was done by G. H. Hendersen. S. B. Wisner and G. H. Hendersen performed the tensile specimen testing. C. R. Judd performed the chemical composition testing.

1. INTRODUCTION

Part of the effort to assure reactor vessel integrity involves evaluation of the fracture toughness of the vessel ferritic materials. The key values which characterize a material's fracture toughness are the reference temperature of nil-ductility transition (RT_{NDT}) and the upper shelf energy (USE). These are defined in 10CFR50 Appendix G (Reference 1) and in Appendix G of the ASME Boiler and Pressure Vessel Code, Section III (Reference 2). These documents contain requirements used to establish the pressure-temperature operating limits which must be met to avoid brittle fracture.

Appendix H of 10CFR50 (Reference 3) and ASTM-E185 (Reference 4) establish the methods to be used for surveillance of the reactor vessel materials. In April, 1985 one of the surveillance specimen capsules required by Reference 3 was removed from the James A. Fitzpatrick Nuclear Power Plant (FitzPatrick) reactor after six fuel cycles of irradiation, or 5.98 effective full power years (EFPY) of operation. The surveillance capsule contained flux wires for neutron flux monitoring and Charpy V-Notch impact test specimens and uniaxial tensile test specimens fabricated from the vessel materials nearest the core (beltline). The impact and tensile specimens were tested to establish material properties for the irradiated vessel materials.

The results of surveillance specimen testing are presented in this report. The irradiated material properties are compared to available unirradiated properties from earlier tests. Predictions of the RT_{NDT} and USE at end of reactor life (EOL) are made for comparison with allowable values in Reference 1. Predictions of EOL properties were made based on surveillance test results, using Regulatory Guide 1.99, Revision 1 (Reference 5) as a guide.

Operating limits curves for the FitzPatrick reactor vessel are presented in this report. The curves account for recent new requirements of References 1 and 2. Geometric discontinuities and highly stressed regions, such as the feedwater nozzles and the closure flanges, are evaluated separately from the core beltline region. The operating limits developed consider the most limiting conditions of the discontinuity regions and the beltline region (including irradiation) to bound all operating conditions. The operating limits developed include irradiation shift in the beltline materials equivalent to 16 EFPY of operation, based on the results of the surveillance tests and the Reference 5 methods.

2. SUMMARY AND CONCLUSIONS

2.1 SUMMARY OF RESULTS

Surveillance capsule 1 was removed from the FitzPatrick reactor at the end of Fuel Cycle 6 and shipped to the General Electric Vallecitos Nuclear Center. The flux wires, Charpy V-Notch and tensile test specimens removed from the capsule were tested according to ASTM E185-82 (Reference 4). Revised operating limits curves were developed using the test results along with 10CFR50 Appendix G (Reference 1) and Appendix G of the ASME Code (Reference 2). The methods and results of the fracture toughness evaluation are presented in this report as follows:

a. Section 3: Surveillance Program Background

b. Section 4: Peak Vessel Fluence Evaluation

c. Section 5: Charpy V-Notch Impact and Hardness Testing

d. Section 6: Tensile Testing

e. Section 7: Operating Limits Curve Development

Photographs of fractured Charpy specimens are in Appendix A.

The significant results of the evaluation are summarized as follows:

a. Capsule 1 was removed from the 30° azimuth position of the reactor. The capsule contained 9 flux wires: 3 each of pure copper (Cu), iron (Fe), and nickel (Ni). There were 36 Charpy V-Notch specimens: 12 each of plate material, weld material and heat affected zone (HAZ) material. The 8 tensile specimens removed consisted of 3 plate, 2 weld and 3 HAZ metal specimens. All specimen materials were positively identified as being from the vessel beltline.

b. The chemical compositions of the beltline materials were identified through a combination of literature research and testing. The copper (Cu), phosphorus (P) and nickel (Ni) contents were determined for all heats of plate material and for representative longitudinal and girth seam welds in the beltline. The values for the limiting beltline plate are 0.13% Cu, 0.015% P and 0.60% Ni. For the limiting beltline weld, the values are 0.31% Cu, 0.015% P and 0.72% Ni.

c. Results from the fabrication program materials certification testing were located and adjusted to be equivalent to test results done to current standards. The initial RT_{NDT} values for locations of interest in the vessel were determined. They are 24°F for the limiting beltline plate, -22°F for the limiting beltline weld, 30°F for the closure flange region and 30°F for the recirculation inlet nozzle, which is the component with the highest RT_{NDT} in the non-beltline regions.

d. The flux wires were tested to determine the neutron flux at the surveillance capsule location. The fast flux (>1.0 MeV) measured was 1.4×10^{9} n/cm^2-sec. Based on the flux wire data, the surveillance specimens had received a best estimate fluence of 2.6×10^{17} n/cm^2 at removal.

e. The vessel peak inner surface and 1/4 T lead factors were established analytically using a reference analysis that combines two-dimensional and one-dimensional finite element computer analysis. The flux peak occurs at an azimuthal location 45° to either side of the vessel quadrant references. The lead factors for the surveillance capsule are 0.79 to the peak vessel surface and 1.05 to the peak 1/4 T depth location.

f. The maximum accumulated neutron fluence at the assumed vessel end-of-life (EOL) of 32 EFPY was determined at the peak 1/4 T location. The maximum 1/4 T vessel EOL fluence is 1.3×10^{18} n/cm^2 (best estimate) and 1.7×10^{18} n/cm^2 (upper bound).

g. The surveillance Charpy V-Notch specimens were impact tested at temperatures selected to define the transition of the fracture toughness curves of the plate, weld, and HAZ materials. Measurements were taken of absorbed energy, lateral expansion and percentage shear. Fracture surface photographs of each specimen are presented in Appendix A. From absorbed energy and lateral expansion results for the plate and weld materials the following values are extracted: index temperatures for 30 ft-lb, 50 ft-lb, and 35-mil lateral expansion (MLE) values and USE. The HAZ material data were not curve fit because of the significant scatter in the test results.

h. The irradiated plate impact energy curve is compared to unirradiated data from earlier studies to establish the RT_{NDT} irradiation shift for the surveillance program. The plate material shows a 23°F shift. Decrease in USE was estimated for the plate material also, showing a 6% decrease.

i. Rockwell C hardness tests were done on one broken half of each Charpy specimen. The average hardness for the base metal was 13.0 HRC. The weld metal specimens had an average hardness of 18.5 HRC. The average for the HAZ material was 18.8 HRC, indicating that the tests were done on the weld side of the HAZ specimens.

j. The irradiated tensile specimens were tested at room temperature (76°F), reactor operating temperature (550°F), and estimated onset to upper shelf temperature (185°F). The results tabulated for each specimen include yield and ultimate tensile strength uniform and total elongation, and reduction of area. The plate, weld, and HAZ specimens behave similarly for most properties.

k. The irradiated plate and weld material tensile test results are compared to unirradiated data from the vessel fabrication test program. The materials show increased strength and decreased ductility, as expected for irradiation embrittlement. The weld material shows a greater change in properties, which is consistent with its higher copper content relative to the plate.

l. As a part of the construction of the updated operating limits curves, the plate metal irradiation shift in RT_{NDT} was compared to predictions calculated with Regulatory Guide 1.99, Revision 1 (Reference 5). The surveillance test shift of 23°F in plate material RT_{NDT} for a fluence of 3.25×10^{17} n/cm^2 (upper bound) is slightly greater than the predicted shift of 19°F. Accounting for the small underprediction of plate material shift, the EOL adjusted reference temperature (ART = initial RT_{NDT} plus irradiation shift) of the plate is 86°F. The predicted ART at EOL for the weld metal is 104°F, so the weld is the limiting beltline material. However, the plate has a higher initial RT_{NDT} than the weld, so for the first 16 EFPY the plate is limiting. The larger irradiation shift of the weld, with its higher copper content, causes the weld ART to "overtake" the plate ART at about 17 EFPY. This is shown graphically in Figure 7-4 of the report.

m. The USE at EOL is predicted using the methods in Reference 5. The weld metal USE is predicted to be 72 ft-lb at EOL. The minimum plate USE is 89 ft-lb longitudinal at EOL. Branch Technical Position MTEB 5-2 (Reference 7) recommends 65% of the longitudinal USE as an estimate of transverse USE, so at EOL the plate USE would be 58 ft-lb transverse.

n. Operating limits curves were constructed for three reactor conditions: hydrostatic pressure tests, non-nuclear heatup and cooldown, and core critical operation. The curves are valid up to 16 EFPY of operation. The limiting regions of the vessel affecting the curves' shapes are the core beltline (shifted to account for irradiation), the feedwater nozzle, and the closure flange region. The bolt preload and minimum permissible operating temperatures on the curves of 90°F provide some additional margin in the closure flange region where a detectable flaw size of 0.24 inch is used instead of 1/4 T. The operating limits curves for FitzPatrick are shown in Figures 2-1 through 2-3.

2.2 CONCLUSIONS

The requirements of Reference 1 deal basically with EOL vessel conditions and with limits of operation designed to prevent brittle fracture. Based on the evaluation of surveillance testing, the following conclusions are drawn:

a. The adjusted reference temperature for the weld material of 104°F is the limiting beltline EOL value. This is below the Reference 1 allowable limit of 200°F, above which annealing is required. The EOL values of USE for the plate and weld materials are 58 ft-lb transverse and 72 ft-lb, respectively. These are above the Reference 1 allowable of 50 ft-lb, below which annealing is required. Therefore, provisions for annealing the reactor vessel before completing 32 EFPY of operation need not be considered.

b. Examination of the normal and upset operating conditions expected for the reactor shows that the worst pressure-temperature conditions expected from unplanned temperature transients are acceptable relative to the limits in Figures 2-1 through 2-3. Therefore, the only operating conditions for which the operating limits are a concern are those involving operator interaction, such as hydrotest and initiation of core criticality.

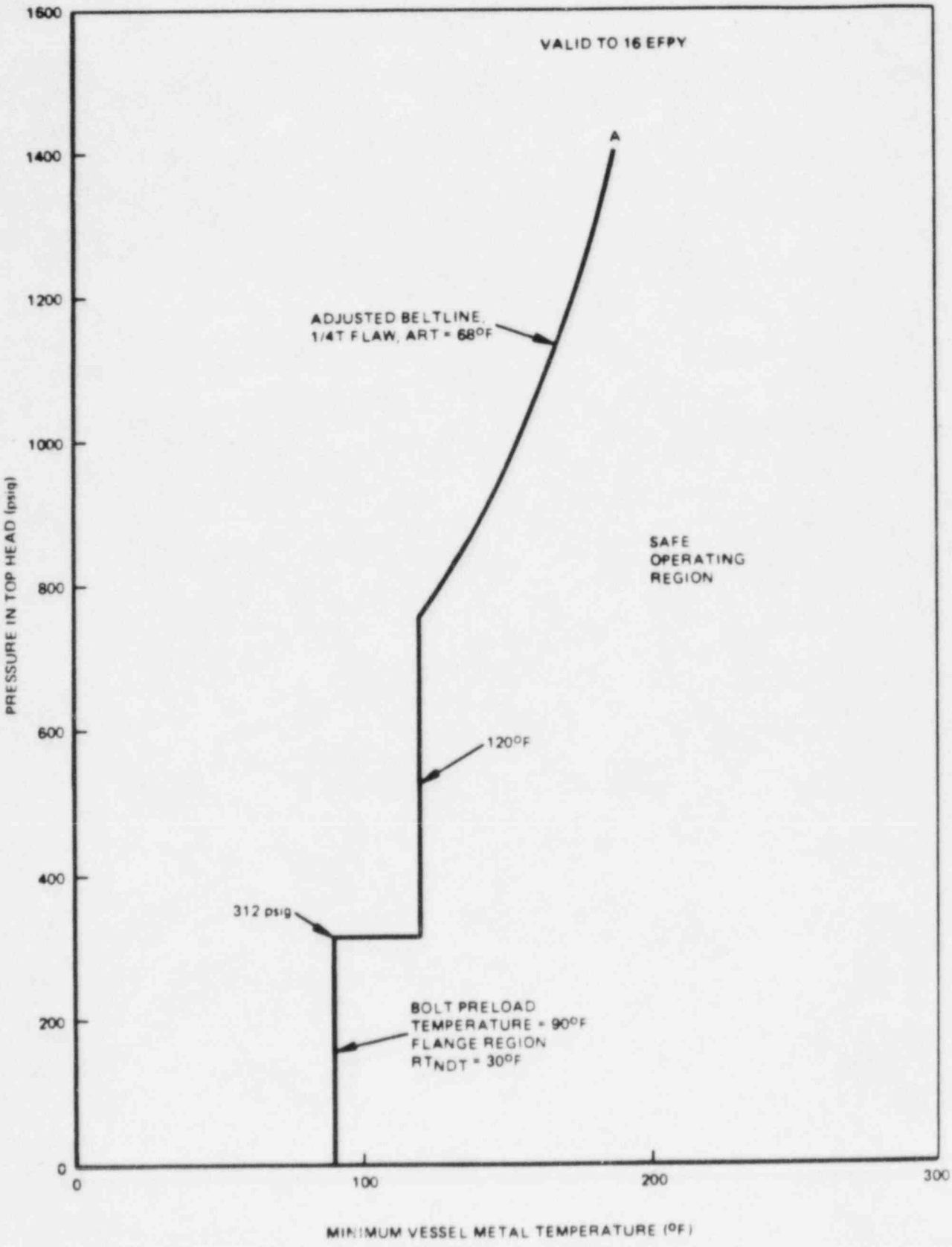

Figure 2-1. Pressure Versus Minimum Temperature for Hydrostatic Pressure Tests for FitzPatrick

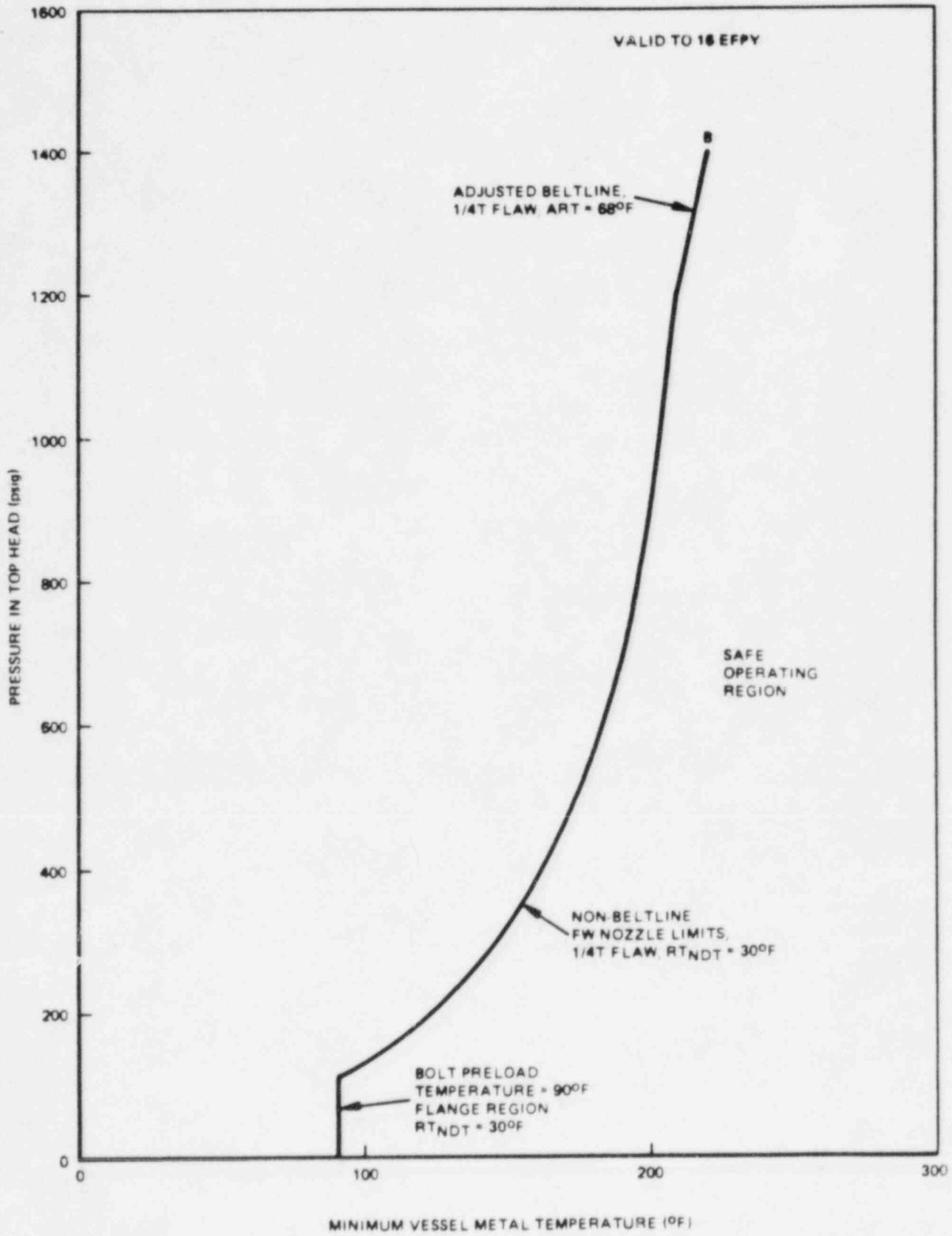

Figure 2-2. Pressure Versus Minimum Temperature for Non-Nuclear Heatup and Cooldown for FitzPatrick

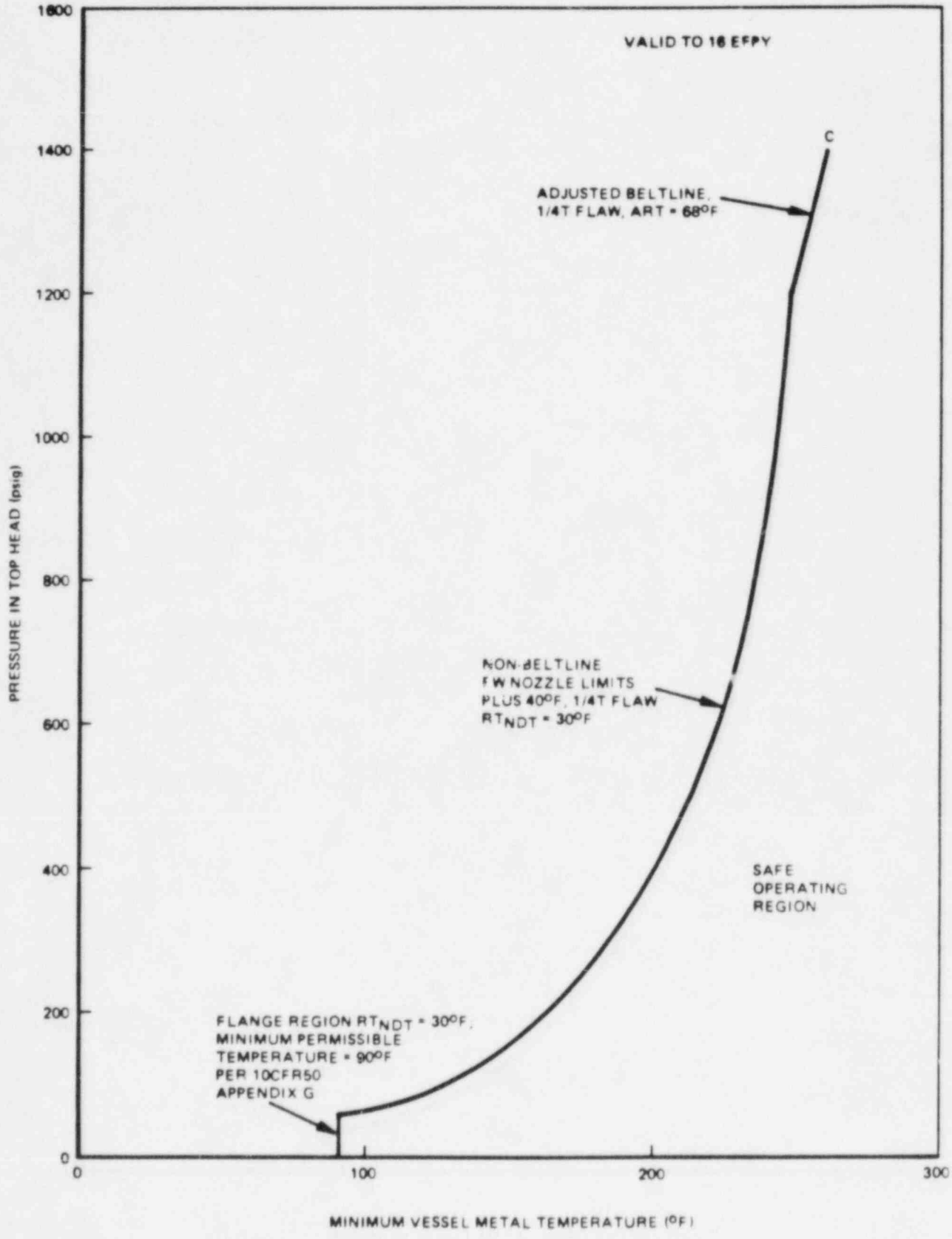

Figure 2-3. Pressure Versus Minimum Temperature for Core Critical Operation for FitzPatrick

3. SURVEILLANCE PROGRAM BACKGROUND

3.1 CAPSULE RECOVERY

The FitzPatrick reactor was shut down in February, 1985 for refueling and maintenance. The accumulated thermal power output was 5,318,900 MWd or 5.98 EFPY. The reactor pressure vessel (RPV) originally contained three surveillance capsules, at 30°, 120° and 300° azimuths at the core midplane. The specimen capsules are held against the RPV inside surface by a spring loaded specimen holder. Each capsule receives equal irradiation because of core symmetry. During the outage, Capsule 1 at 30° was removed. The capsule was cut from the holder assembly and shipped by a 200 Series cask to the General Electric Vallecitos Nuclear Center in Pleasanton, California.

Upon arrival at Vallecitos, the capsule was examined for identification. The reactor code of 29 and the basket code of 13 from Reference 8 were confirmed on the capsule, as shown in Figure 3-1. The capsule contained three Charpy specimen packets and four tensile specimen tubes. Each Charpy packet contained 12 Charpy specimens and 3 flux wires. The four tensile specimen tubes contained eight specimens. The specimen gage sections were protected by aluminum sleeves, and during removal of the sleeves, the threaded ends of the specimens were slightly damaged. The threads were later chased with a die-hex rethreading tool. The gage sections of the tensile specimens were not damaged during removal.

3.2 RPV MATERIALS AND FABRICATION BACKGROUND

3.2.1 Fabrication History

The FitzPatrick RPV is a 218-in. BWR/4. It was constructed by Combustion Engineering to the 1965 ASME Code with Addenda up to and including Winter 1966. The shell and head plates are ASME SA-533 Grade B, Class 1 low alloy steel (LAS). The nozzles and closure flanges are

ASTM A508 Class 2 LAS and the closure flange bolting materials are ASTM A540 Grade B24 LAS. The fabrication process employed quench and temper heat treatment immediately after hot forming, then submerged arc welding and post-weld heat treatment. The post-weld heat treatment was typically 6 hours at 1150°F ± 25°F. The arrangement of plates and welds relative to the core beltline and various nozzles is shown in Figure 3-2.

3.2.2 Material Properties of RPV at Fabrication

A search of General Electric Quality Assurance (QA) records was made to determine the chemical properties of the plates and welds in the RPV beltline. Table 3-1 shows the chemistry data obtained for the beltline materials. All data shown for the beltline plates were taken from QA records. Chemical composition of the beltline welds was obtained from Combustion Engineering (Reference 9), but as-welded data for the longitudinal seam welds was not available. Since the surveillance weld metal specimens were fabricated with the same weld procedure as was used in the longitudinal seam welds, samples from the specimens were analyzed to obtain a representative chemistry. The results are presented in Subsection 3.2.3.

A search of QA records was made to collect results of certification mechanical property tests performed during RPV fabrication, specifically tensile test, Charpy V-Notch and dropweight impact test results. Properties of the beltline materials and other locations of interest are presented in Table 3-2. The Charpy data collected were used to establish the RT_{NDT} values for each vessel component, as described in Subsection 3.2.4.

3.2.3 Specimen Chemical Composition

Samples were taken from tensile specimens 5CL and 5CM (base) and from 5DL and 5DM (weld) after they were tested. The tensile specimens were fabricated from the same plates and weld as were the Charpy specimens, as detailed in Subsection 3.3, so the samples chosen are representative of all surveillance specimens. Chemical analyses were performed using a plasma emission spectrometer. Each sample was decomposed and dissolved, and a portion prepared for evaluation by the spectrometer. The spectrometer was calibrated with a standard solution containing 700 ppm Fe, 8 ppm Mn, 2 ppm Cu, 5 ppm Ni, 5 ppm Mo, 5 ppm Cr, 1 ppm Si, 1 ppm Co, and levels of perchloric acid and lithium consistent with the test. The calibration for phosphorus was done by analyzing a series of seven National Bureau of Standards steels with known quantities of phosphorus. The chemical composition results are given in Table 3-3.

3.2.4 Initial Reference Temperatures

The requirements applicable to establishing the RT_{NDT} from the Winter 1966 Edition of the ASME Code can be summarized as follows for the RPV:

a. Test specimens shall be longitudinally oriented Charpy V-Notch specimens.

b. At the RT_{NDT}, no impact test result shall be less than 25 ft-lb, and the average of three test results shall be at least 30 ft-lb.

c. Pressure tests shall be conducted at a temperature at least 60°F above the acceptable RT_{NDT} for the vessel.

The current requirements for establishing RT_{NDT} are significantly different. For plants constructed to the ASME Code after Summer 1972, the requirements are as follows:

a. Charpy V-Notch specimens shall be oriented normal to the rolling direction (transverse).

b. RT_{NDT} is defined as the higher of the dropweight NDT or the temperature 60°F above which Charpy V-Notch 50 ft-lb energy and 35 mils lateral expansion are met.

c. Bolt-up in preparation for a pressure test or normal operation shall be performed at or above the RT_{NDT} or lowest service temperature (LST), whichever is greater.

Reference 1 states that for vessels constructed to a version of the ASME Code prior to the Summer 1972 Addendum, fracture toughness data and data analyses must be supplemented in an approved manner. General Electric has developed methods for analytically converting fracture toughness data for vessels constructed before 1972 to comply with current requirements. The methods used have been presented to the NRC in about 10 Final Safety Analysis Report updates. These were reviewed on a case by case basis and in each case approved (e.g., La Salle 1 and 2 and Nine Mile Point 2). These methods and example RT_{NDT} calculations for vessel plate, weld, weld HAZ, forging, and bolting material are summarized in the remainder of this subsection. Calculated RT_{NDT} values for selected RPV locations are given in Table 3-2.

For vessel plate material, the first step in calculating RT_{NDT} is to establish the 50 ft-lb transverse test temperature given longitudinal test specimen data. There are typically three energy values at a given test temperature. The lowest energy Charpy value is adjusted by adding 2°F per ft-lb energy to 50 ft-lb. For example, for the six beltline plates the limiting combination of test temperature and Charpy energy from Table 3-2 is 43 ft-lb at +40°F for Plate G-3415-3. The equivalent 50 ft-lb longitudinal test temperature is:

$$T_{50L} = 40°F + [(50 - 43)\ ft\text{-}lb * 2°F/ft\text{-}lb] = 54°F$$

The transition from longitudinal data to transverse data is made by adding 30°F to the test temperature. In this case, the 50 ft-lb transverse Charpy test temperature is $T_{50T} = 84°F$. The RT_{NDT} is the greater of NDT or (T_{50T} - 60°F). From Table 3-2, the NDT for G-3415-3 is -10°F. Therefore, the RT_{NDT} for the core beltline is 24°F.

For vessel weld material, the Charpy V-Notch results are usually limiting in establishing RT_{NDT}. The 50 ft-lb test temperature is established as for the plate material, but the 30°F adjustment to convert longitudinal data to transverse data is not applicable to weld metal. The limiting beltline weld Charpy V-Notch energy from Table 3-2 is 36 ft-lb at +10°F for weld 2-233. The corresponding transverse 50 ft-lb temperature is:

$$T_{50T} = T_{50L} = 10°F + [(50 - 36)\ ft\text{-}lb * 2°F/ft\text{-}lb] = 38°F$$

As shown in Table 3-2, there are no NDT data available for the weld metal. As long as the resulting RT_{NDT} is above -50°F, the RT_{NDT} is established as (T_{50T} - 60°F), or RT_{NDT} = -22°F for this core beltline weld.

For the vessel weld HAZ material, the RT_{NDT} is assumed the same as for the base material since ASME Code weld procedure qualification test requirements and post-weld heat treatment data indicate this assumption is valid.

For vessel forging material, such as nozzles and closure flanges the method for establishing RT_{NDT} is the same as for vessel plate material. The recirculation inlet nozzle, listed in Table 3-2, has a calculated value of T_{50T} = 40°F. However, the NDT reported in Table 3-2 is +30°F. Therefore, with the RT_{NDT} being the greater of NDT or (T_{50T} - 60°F), the RT_{NDT} is 30°F.

For bolting material, the current requirements define the LST as the temperature at which transverse Charpy V-Notch energy of 45 ft-lb and 25 mils lateral expansion (MLE) are achieved. If the required Charpy results are not met, or are not reported, but the Charpy V-Notch energy reported is above 30 ft-lb, the requirements of the ASME Code at construction are applied. As shown in Table 3-2, the limiting Charpy V-Notch energy for bolting material is 39 ft-lb at +10°F. The current requirements are not met, so the construction Code requirements are used.

The LST is defined as 60°F above the temperature at which 30 ft-lb Charpy V-Notch energy is achieved. Therefore, the LST of the closure bolting material is 70°F.

3.3 SPECIMEN DESCRIPTION

The surveillance capsule contained 36 Charpy specimens: base metal (12), weld metal (12), and HAZ (12). There were 8 tensile specimens: base metal (3), weld metal (2), and HAZ (3). The 9 flux wires recovered were iron (3), nickel (3) and copper (3). The chemistry and fabrication history for the Charpy and tensile specimens are described in this section.

3.3.1 Charpy Specimens

The fabrication of the Charpy specimens is described in the Surveillance Test Program description given in Reference 10. All materials used for specimens were beltline materials from the lower intermediate shell course.

The base metal specimens were cut from plate G-3414-2 from the beltline. The chemical analysis of this heat of low alloy steel is in Table 3-1. The test plate was heat treated for 40 hours at 1150°F ± 25°F to simulate the post-weld heat treatment of the vessel. The method used to machine the specimens from the test plate is shown in Figure 3-3. Specimens were machined from the 1/4 T and 3/4 T positions in the plate, in the longitudinal orientation (long axis parallel to the rolling direction). The identifications of the base metal Charpy specimens recovered from the surveillance capsule are shown in Table 3-4.

The weld metal and HAZ Charpy specimens were fabricated from trim-off pieces of plates G-3414-1 and G-3414-2 that were welded together with a weld identical to longitudinal seam weld 1-233 in the RPV beltline. The chemical analyses of the plates are given in Table 3-1. As-welded chemistry data were not reported in Reference 9 for the weld metal. The weld metal chemistry from two specimens is presented in Table 3-3.

The welded test plate for the weld and HAZ Charpy specimens received a heat treatment of 1150°F ± 25°F for 40 hours to conservatively simulate the fabricated condition of the RPV. The weld specimens and HAZ specimens were fabricated as shown in Figures 3-4 and 3-5, respectively. The base metal orientation in the weld and HAZ specimens was longitudinal. Contained in Table 3-4 are the identifications of the weld metal and HAZ Charpy specimens from the surveillance capsule.

3.3.2 Tensile Specimens

Fabrication of the surveillance tensile specimens is described in Reference 10. The chemical composition and heat treatment for the base, weld and HAZ tensiles are the same as those for the corresponding Charpy specimens. The identifications of the base, weld, and HAZ tensile specimens recovered from the surveillance capsule are given in Table 3-4. A summary of the fabrication methods is presented in the remainder of this section.

The base metal specimens were machined from material at the 1/4 T and 3/4 T depth in plate G-3414-2. The specimens, oriented along the plate rolling direction, were machined to the dimensions shown in Figure 3-6. The gage section was tapered to a minimum diameter of 0.250 inch at the center. The weld metal tensile specimen material was cut from the welded test plate, as shown in Figure 3-7. The specimens were machined entirely from weld metal, scrapping material that might include base metal. The fabrication method for the HAZ tensile specimens is illustrated in Figure 3-8. The specimen blanks were cut from the welded test plate such that the gage section minimum diameter was machined at the weld fusion line. The finished HAZ specimens are approximately half weld metal and half base metal oriented along the plate rolling direction.

Table 3-1

CHEMICAL COMPOSITION OF RPV BELTLINE MATERIALS

Identification	Heat/Lot No.	Composition by Weight Percent C	Mn	P	S	Si	Ni	Mo	Cu
Lower Plates:									
G-3415-1R	C3394-1	0.21	1.32	0.015	0.017	0.26	0.56	0.47	0.11
G-3415-3	C3376-2	0.22	1.33	0.015	0.017	0.22	0.60	0.48	0.13
G-3415-2	C3103-2	0.23	1.36	0.012	0.016	0.26	0.60	0.47	0.14
Lower-Intermediate Plates:									
G-3413-7	C3368-1	0.21	1.31	0.015	0.018	0.23	0.54	0.46	0.12
G-3414-2	C3278-2	0.20	1.26	0.011	0.016	0.23	0.60	0.48	0.13
G-3414-1	C3301-1	0.20	1.35	0.009	0.015	0.27	0.60	0.48	0.18
Lower Longitudinal Welds:									
2-233 A,B,C	Heat 27204, Flux 1092, Lot 3774				not available				
	Heat 12008, Flux 1092, Lot 3774				not available				
	Heat 8018 Lot EOAG	0.064	0.81	0.008	0.015	0.17	1.04	0.26	n/a
Lower-Intermediate Longitudinal Welds:									
1-233 A,B,C	Heat 13253, Flux 1092, Lot 3774				not available				
	Heat 12008, Flux 1092, Lot 3774				not available				
	Heat 8018 Lot EOAG				see above				
	Heat 8018 Lot LODG	0.081	1.02	0.009	0.011	0.49	0.93	0.21	n/a
Lower to Lower-Int. Girth Weld:									
1-240	Heat 305414, Flux 1092, Lot 3947	0.14	1.45	0.012	0.010	0.18	0.59	0.51	0.33
	Heat 8018 Lot BOBJ	0.080	1.03	0.012	0.012	0.40	0.91	0.24	0.02
	Heat 8018 Lot AOFJ	0.079	1.04	0.011	0.012	0.42	0.93	0.23	0.03

Table 3-2

RESULTS OF FABRICATION TEST PROGRAM FOR SELECTED RPV LOCATIONS

Location	Ident. Number	Heat Number	Tensile				Test Temp. (°F)	Charpy Energy (ft-lb)	NDT (°F)	$T_{50T}-60$ (°F)	RT_{NDT} (°F)
			Yield (ksi)	UTS (ksi)	Total Elong (%)	Area Reduc. (%)					
Lower Shell Plates	G-3415-1R	C3394-1	67.8	88.5	27.5	69.8	10	53,71,52	-10	-20	-10
	G-3415-3	C3376-2	67.0	88.3	27.0	68.6	40	43,51,49	-10	24	24
	G-3415-2	C3103-2	66.1	89.5	26.3	69.3	10	41,48,49	-10	-2	-2
Lower-Intermediate Shell Plates	G-3413-7	C3368-1	65.3	86.5	27.0	67.7	10	6i,55,45	-50	-10	-10
	G-3414-2	C3278-2	67.7	89.3	27.0	69.8	10	45,77,58	-30	-10	-10
	G-3414-1	C3301-1	70.9	92.6	26.5	67.9	10	60,63,49	-40	-18	-18
Longitudinal Weld	2-233	Ht. 27204 Lot 3774	78.9	93.5	24.0	66.1	10	49,48,36	n/a	-22	-22
Girth Weld	1-240	Ht. 305414 Lot 3947	72.1	87.7	25.5	66.8	10	82,66,80	n/a	-50	-50
Upper Shell Plate	G-3413-5	C3229-2	68.9	90.5	27.3	68.0	10	50,68,82	-10	-20	-10
Vessel Flange	G-3401	2V595	63.6	85.4	28.5	73.0	10	117,94,117	10	-20	10
Head Flange	G-3402	4P-1885	70.9	92.3	25.5	70.5	10	66,87,96	30	-20	30
Top Head Torus	G-3411-1	C3055-1	70.6	92.6	26.0	70.6	10	98,73,118	-10	-20	-10
Recirc. Inlet	G-3436-9	E21VW-104J5	75.8	93.8	26.0	71.5	10	73,116,118	30	-20	30
Closure Bolts	G-3134-1	37385	153.3	168.0	15.0	47.3	10	39,40,39	n/a	LST = 70°F	

Table 3-3

PLASMA EMISSION SPECTROMETRY CHEMICAL ANALYSIS OF RPV SURVEILLANCE PLATE AND WELD MATERIALS

Element	Base Metal Tensile 5CL	Base Metal Tensile 5CM	Weld Metal Tensile 5DL	Weld Metal Tensile 5DM
Mn	1.4	1.3	1.5	1.4
P	0.011	0.010	0.015	0.014
Cu	0.11	0.12	0.31	0.31
Si [a]	0.07	0.06	0.06	0.06
Ni	0.62	0.63	0.72	0.72
Mo	0.48	0.50	0.50	0.51
Cr	0.11	0.11	0.04	0.04
Co	0.011	0.011	0.020	0.019

[a] Si results may be low, due to precipitation during dissolution heating.

Table 3-4

IDENTIFICATION OF CHARPY AND TENSILE SPECIMENS REMOVED FROM SURVEILLANCE CAPSULE

Charpy Specimens

Base	Weld	HAZ
51B	541	572
51C	54B	57K
51D	54D	57T
51L	54L	57Y
51Y	54P	5A1
52A	552	5AA
52B	55A	5AC
52C	55D	5B4
52K	55J	5BL
52M	55U	5BM
52U	5GE	5BP
531	5GM	5BU

Tensile Specimens

Base	Weld	HAZ
5CL	5DL	5EB
5CM	5DM	5ED
5CT		5EM

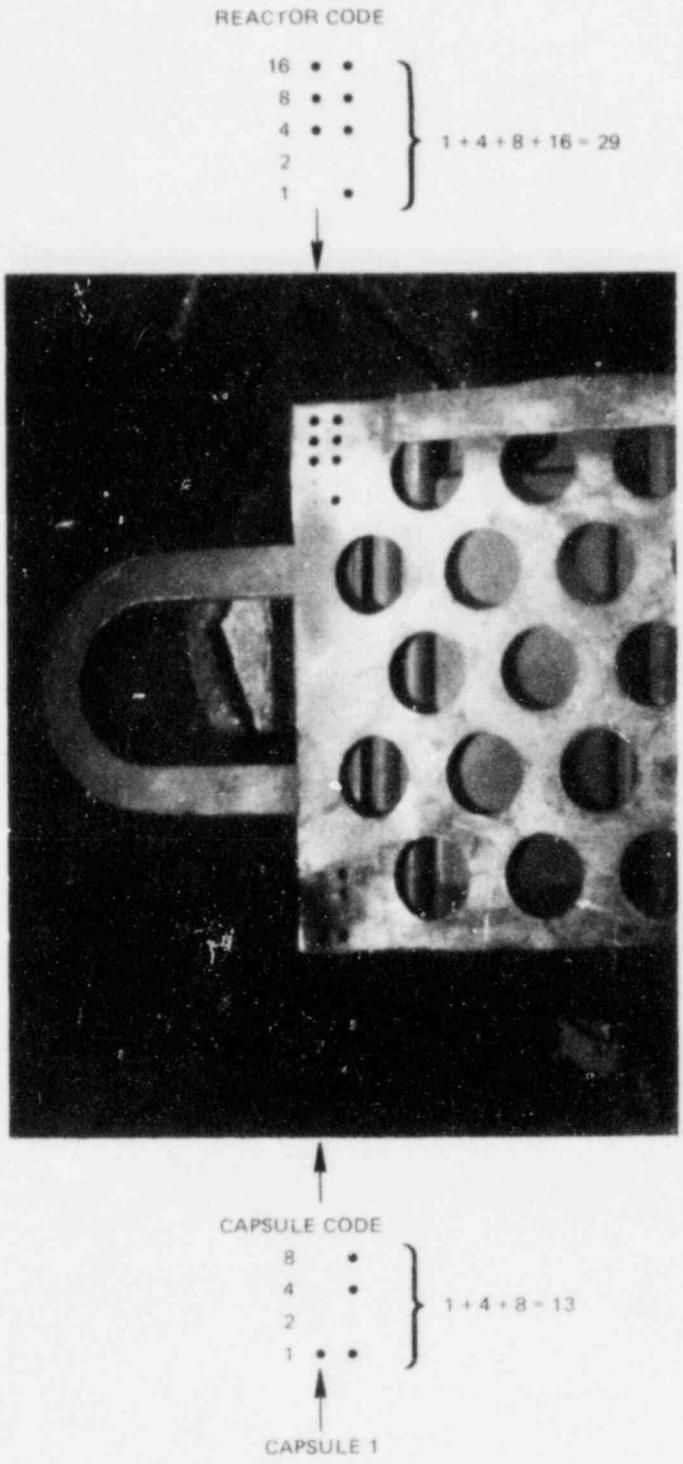

Figure 3-1. Surveillance Capsule Recovered from FitzPatrick Reactor

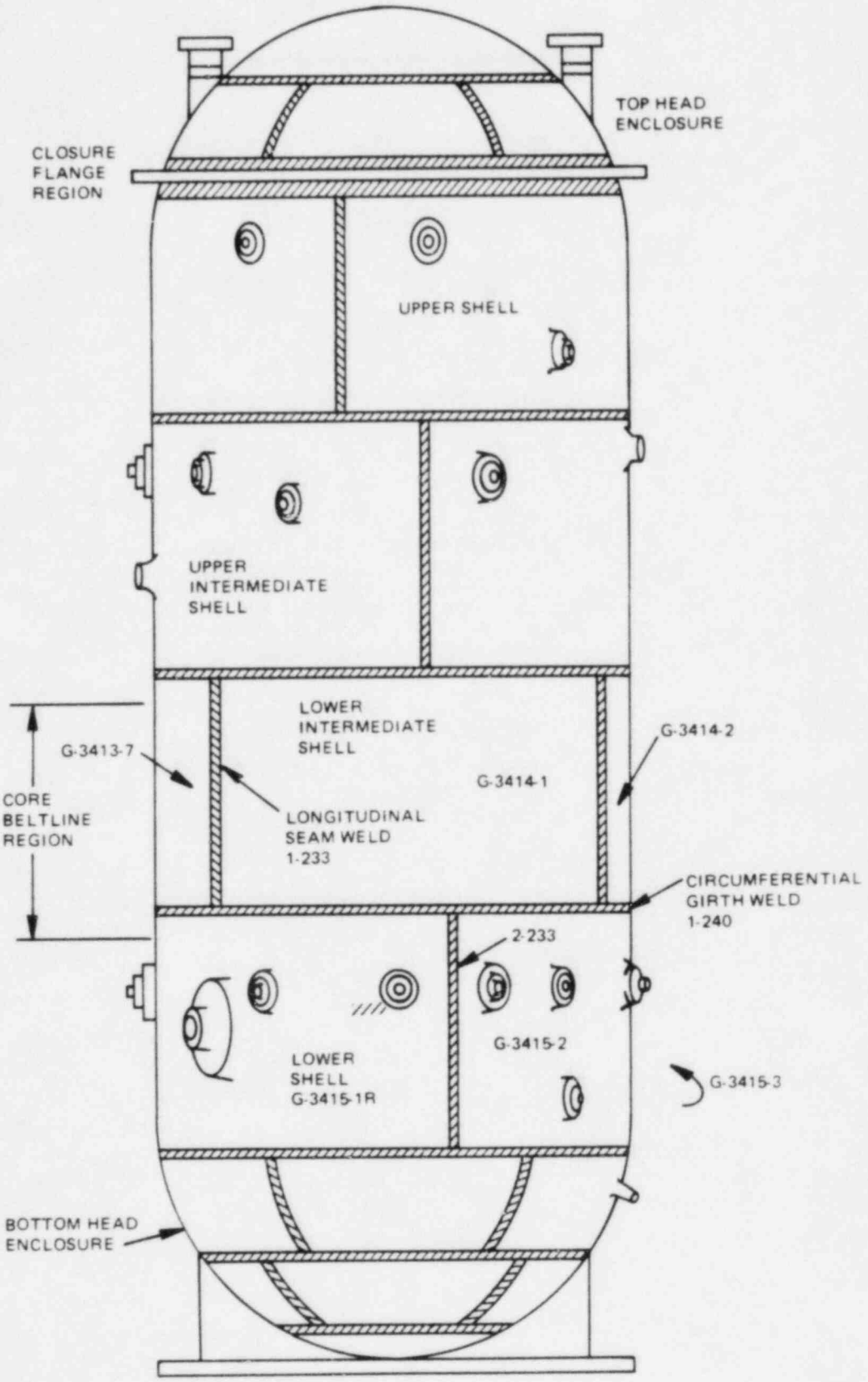

Figure 3-2. Schematic of the RPV Showing Arrangement of Vessel Plates and Welds

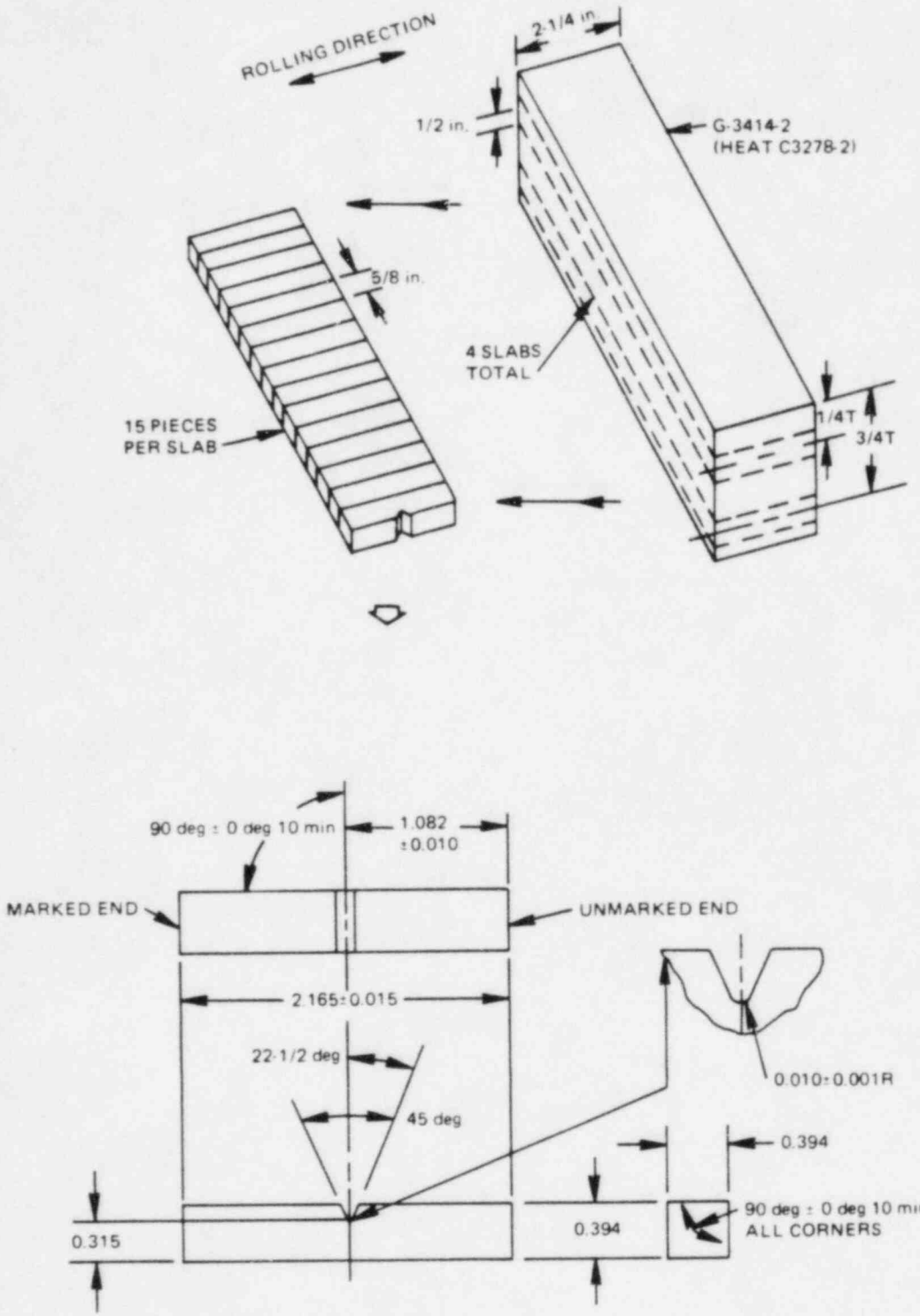

Figure 3-3. Fabrication Method for Base Metal Charpy Specimens

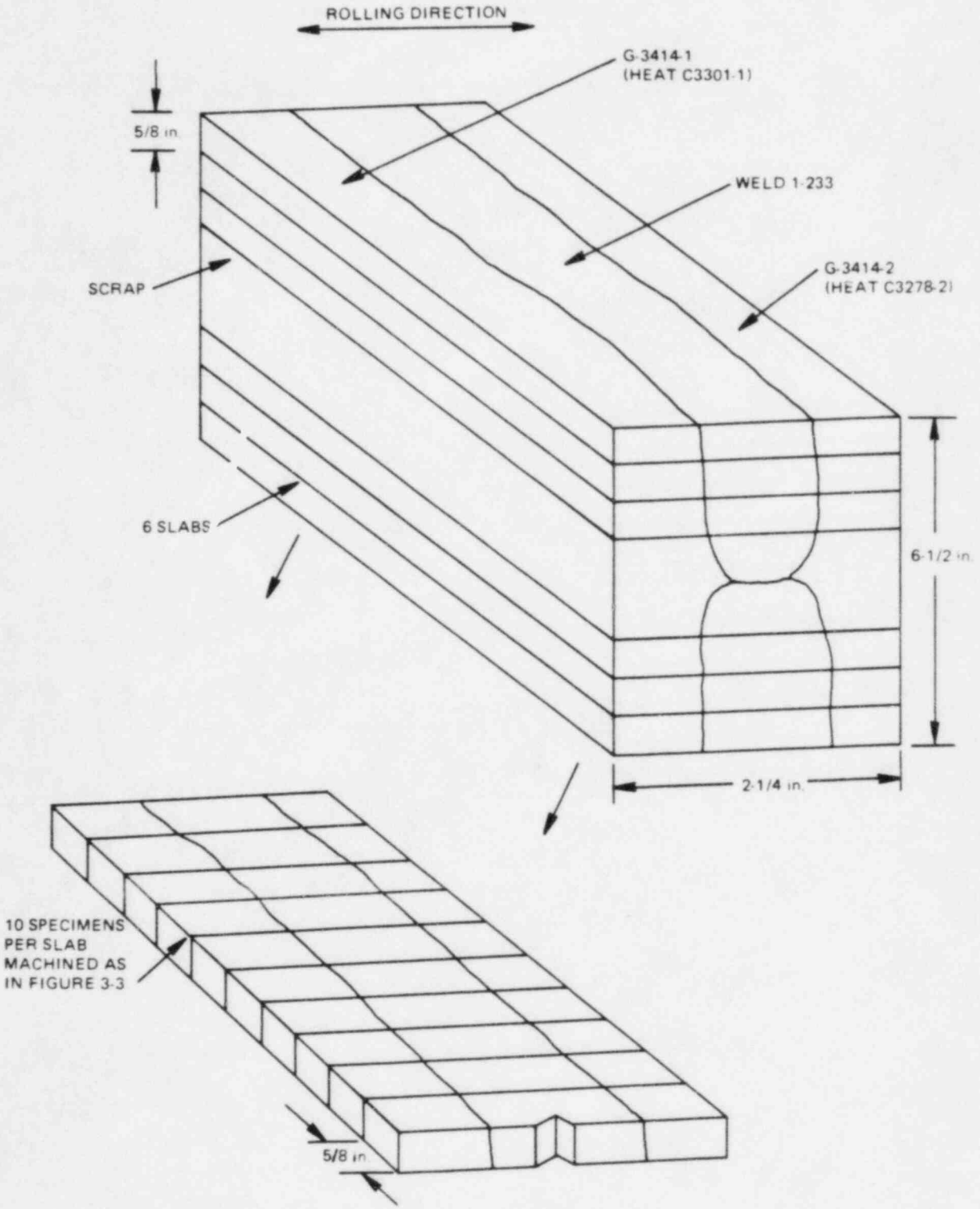

Figure 3-4. Fabrication Method for Weld Metal Charpy Specimens

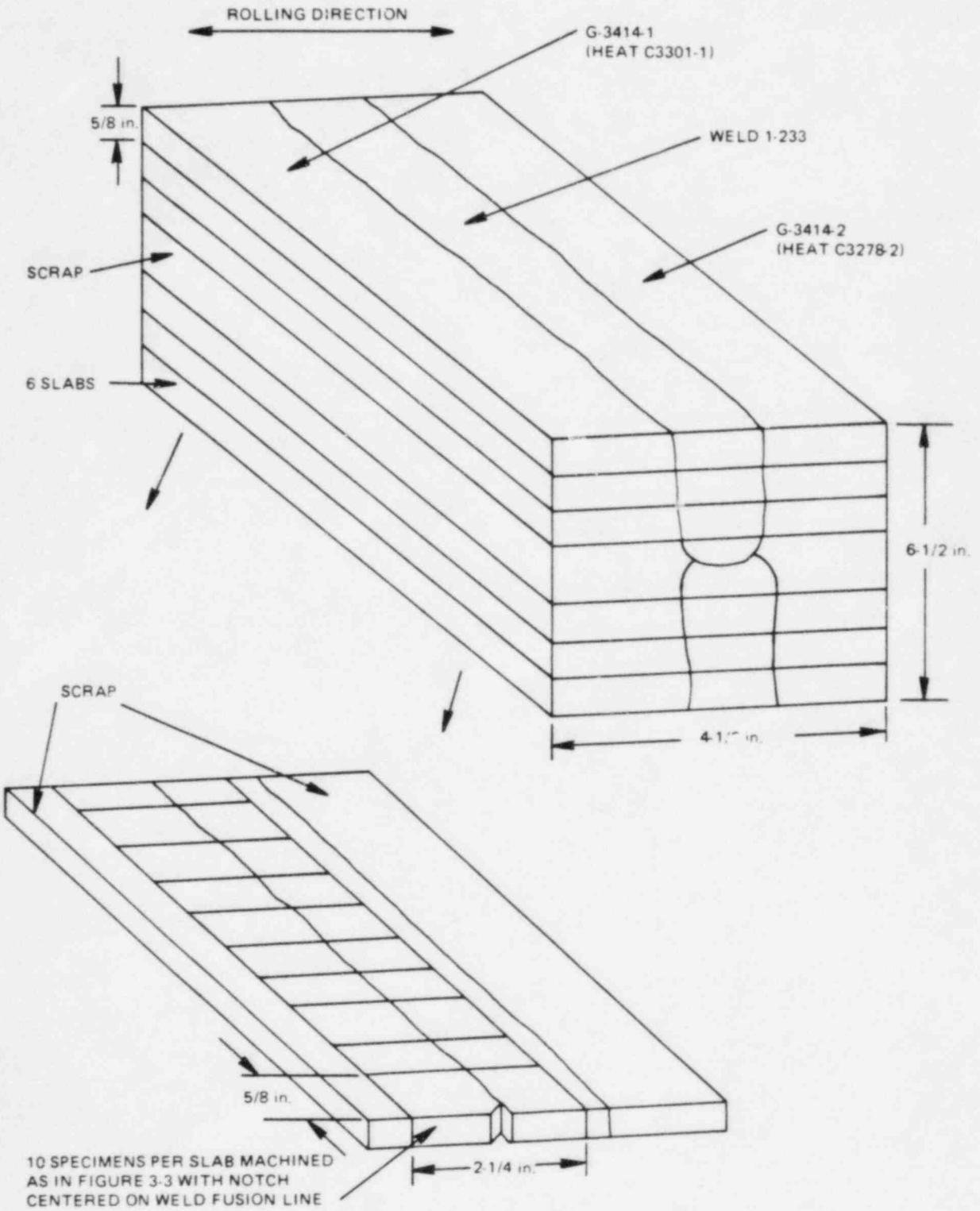

Figure 3-5. Fabrication Method for HAZ Charpy Specimens

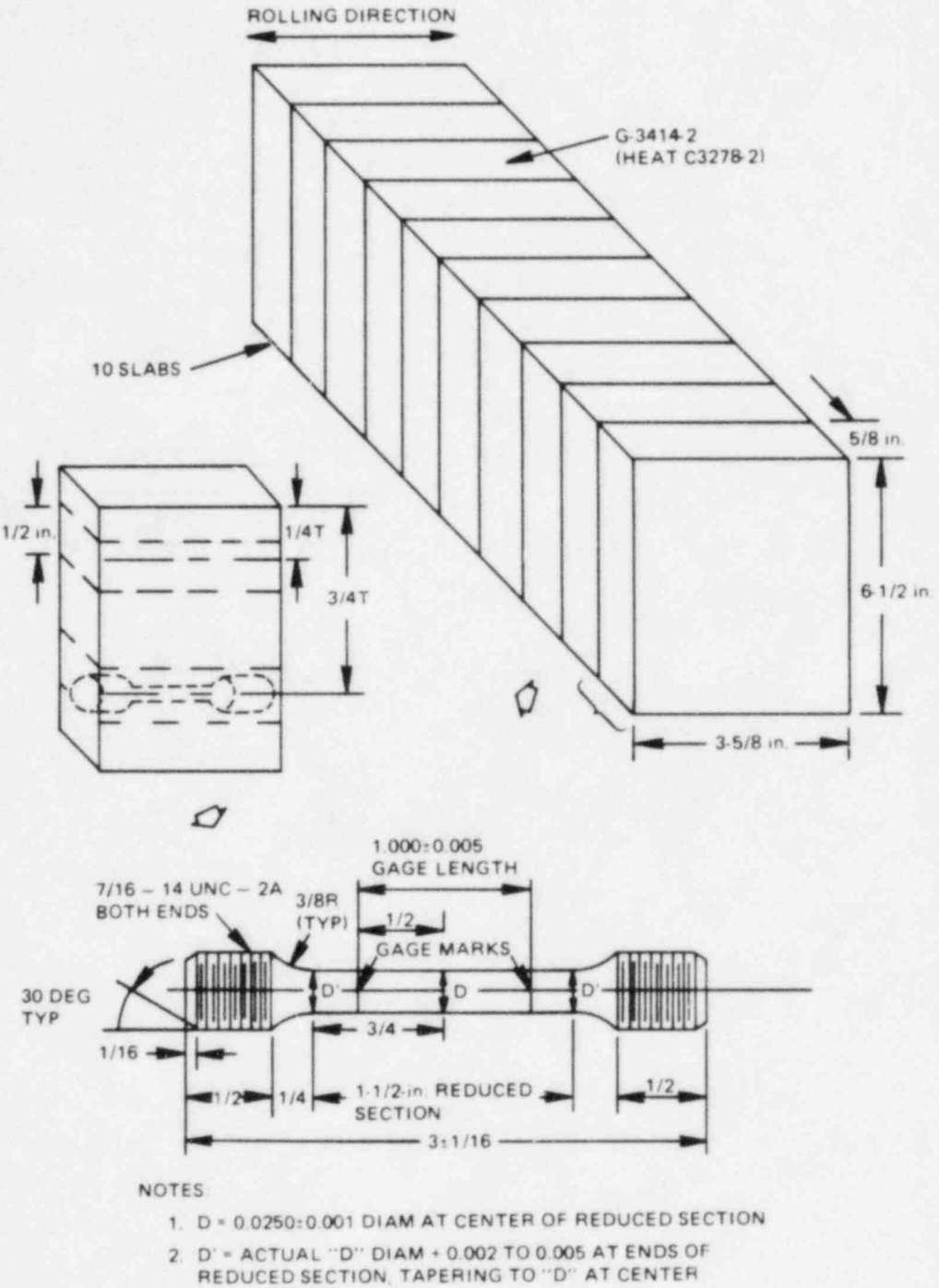

NOTES:

1. D = 0.0250±0.001 DIAM AT CENTER OF REDUCED SECTION
2. D' = ACTUAL "D" DIAM + 0.002 TO 0.005 AT ENDS OF REDUCED SECTION, TAPERING TO "D" AT CENTER

Figure 3-6. Fabrication Method for Base Metal Tensile Specimens

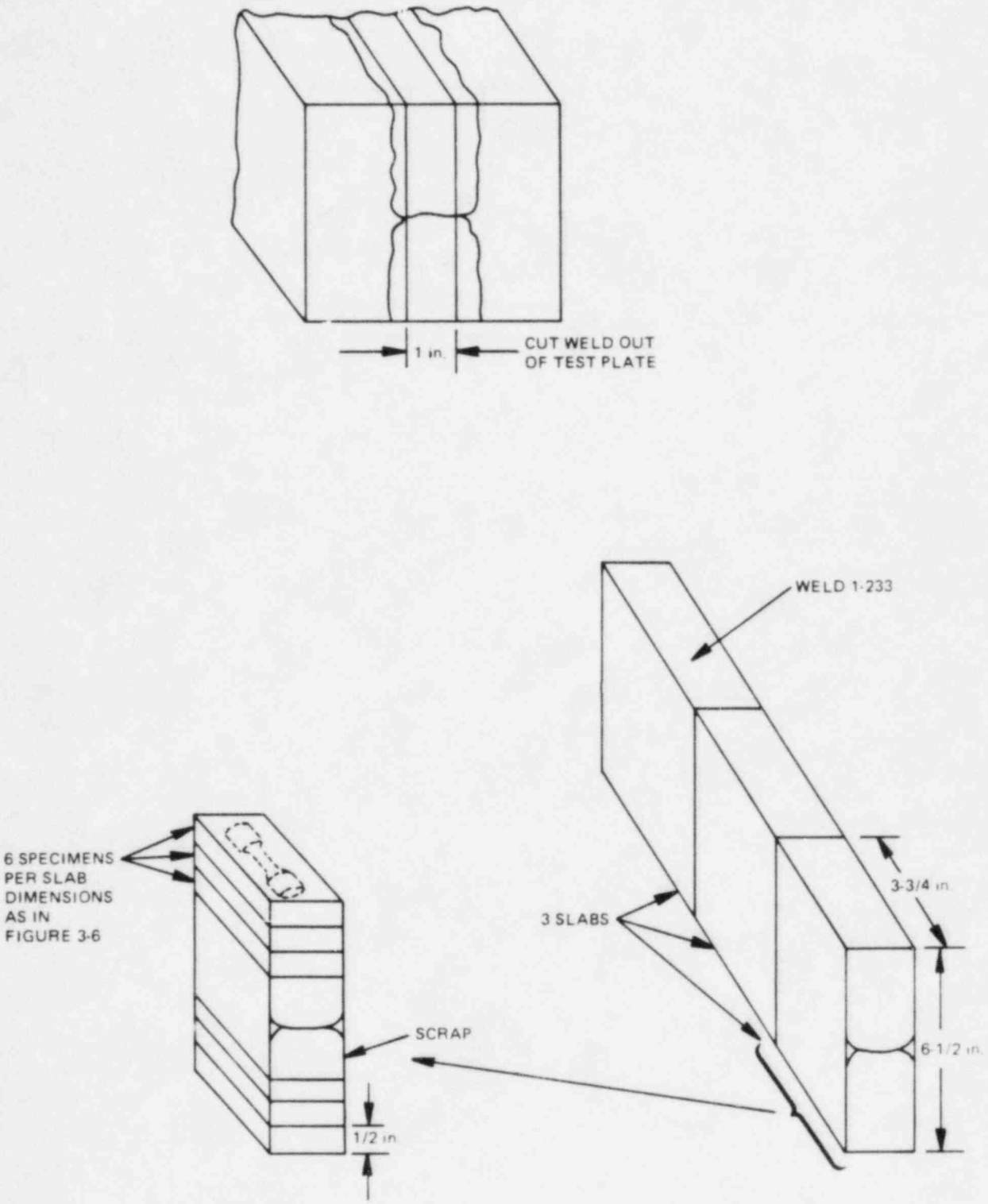

Figure 3-7. Fabrication Method for Weld Metal Tensile Specimens

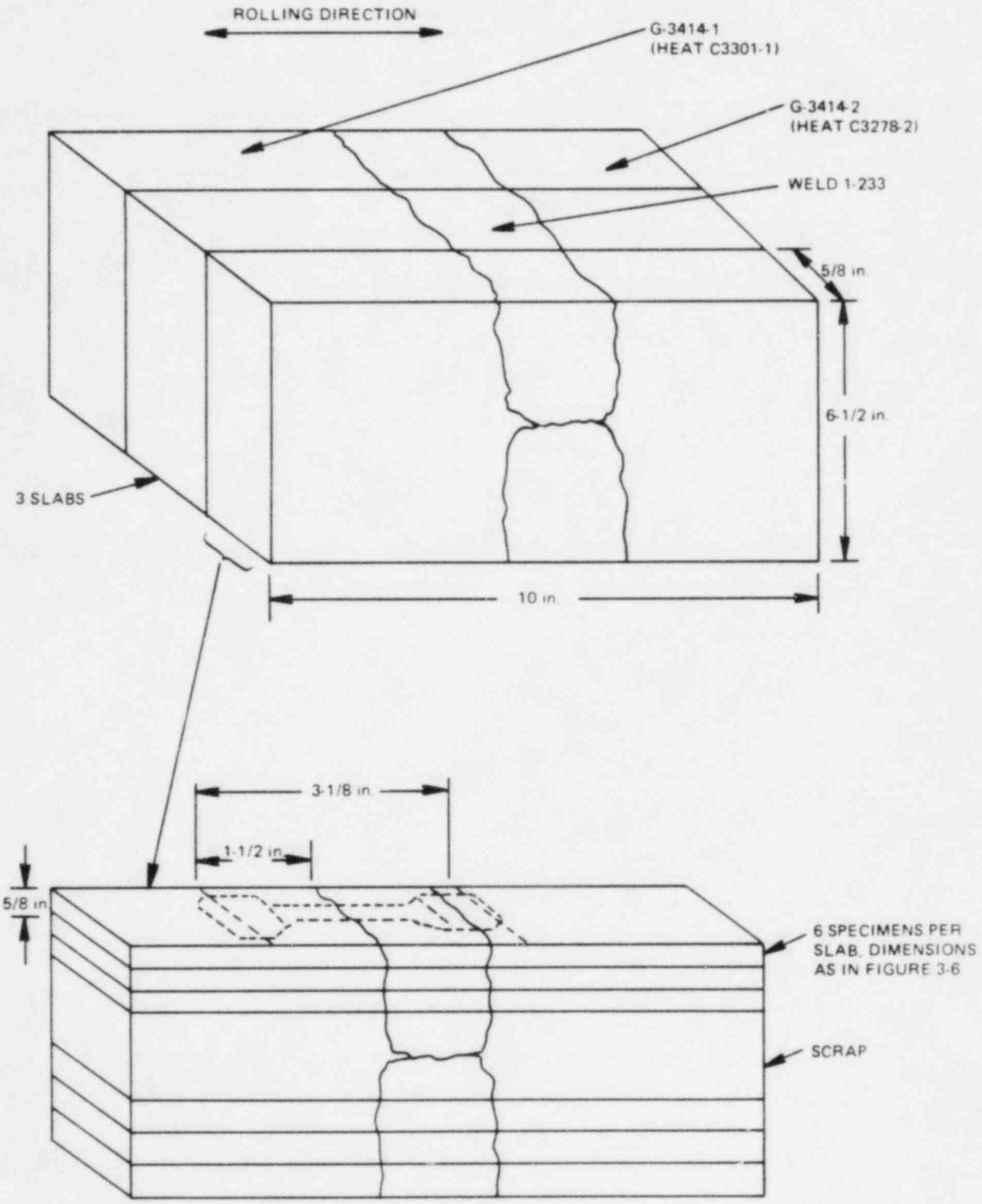

Figure 3-8. Fabrication Method for HAZ Tensile Specimens

4. PEAK RPV FLUENCE EVALUATION

Flux wires were analyzed to determine flux and fluence received by the surveillance capsule. A reference analysis combining two-dimensional and one-dimensional flux distribution computer calculations was evaluated to establish the location of peak vessel fluence and the lead factors of the surveillance capsule relative to the peak vessel location.

4.1 FLUX WIRE ANALYSIS

4.1.1 Procedure

The surveillance capsule contained nine flux wires: three each of iron, copper, and nickel. Each wire was removed from the capsule, cleaned with dilute acid, weighed, mounted on a counting card, and analyzed for its radioactivity content by gamma spectrometry. Each iron wire was analyzed for Mn-54 content, each nickel wire for Co-58, and each copper wire for Co-60 at a calibrated 4- or 10-cm source-to-detector distance with an 80-cc Ge(Li) detector system. The gamma spectrometer was calibrated using NBS material.

To properly predict the flux and fluence at the surveillance capsule from the activity of the flux wires, the periods of full and partial power irradiation and the zero power decay periods were considered. Operating days for each fuel cycle and the reactor average power fraction are shown in Table 4-1. Zero power days between fuel cycles are listed as well.

From the flux wire activity measurements and power history, reaction rates for Fe-54 (n,p) Mn-54, Cu-63 (n,α) Co-60, and Ni-58 (n,p) Co-58 were calculated. The >1 MeV fast flux reaction cross sections for the iron, copper, and nickel wires were estimated to be 0.177 barn, 0.0031 barn and 0.230 barn, respectively. These values were obtained from measured cross section functions determined at Vallecitos from more than 65 spectral determinations for BWRs and for the General Electric Test Reactor using activation monitor and spectral unfolding techniques. These data functions are applied to BWR pressure vessel locations based on water gap (fuel to vessel wall) distances. The cross sections for >0.1 MeV flux were determined from the measured 1-to-0.1 MeV cross section ratio of 1.6.

4.1.2 Results

The measured activity, reaction rate and determined full-power flux results for the surveillance capsule are given in Table 4-2. The >1 MeV and >0.1 MeV flux values of 1.4×10^9 and 2.2×10^9 n/cm^2-sec from the flux monitors were calculated by dividing the reaction rate measurement data by the appropriate cross sections. The corresponding fluence results, 2.6×10^{17} and 4.2×10^{17} n/cm^2 for >1 MeV and >0.1 MeV, respectively, were obtained by multiplying the full-power flux density values by the product of the total seconds irradiated (2.75×10^8 sec) and the full-power fraction (0.686).

Generally, for long-term irradiations, dosimetry results from copper flux wires are considered the most accurate because of Co-60's long half-life (5.27 years). The secondary nickel and iron flux monitor reactions yielding Co-58 and Mn-54 gave results fairly consistent with the copper reaction despite the shorter half-lives of 70.8 days for Co-58 and 312.5 days for Mn-54. Consistency in results indicates an accurate power-history evaluation and a consistent core radial power shape.

The accuracies of the values in Table 4-2 for a 2σ deviation are estimated to be:

± 5% for dps/g (disintegrations per second per gram)
± 12% for dps/nucleus (saturated)
± 25% for flux and fluence >1 MeV
± 35% for flux and fluence >0.1 MeV

A set of flux wires from FitzPatrick was evaluated by General Electric in 1982. The >1 MeV flux was 1.5×10^9 n/cm^2-sec. The result from this study of 1.4×10^9 n/cm^2-sec is very close. The flux wires from each analysis are from the same location, so consistent results are expected.

4.2 DETERMINATION OF LEAD FACTORS

The flux wires detect flux at a single location. The wires will therefore reflect the power fluctuations associated with the operation of the plant. However, the flux wires are not necessarily at the location of peak vessel flux. Lead factors are required to relate the flux at the wires' location to the the peak flux. These lead factors are a function of the core and vessel geometry and of the distribution of bundles in the core. Lead factors were generated for a 218 inch BWR/4 geometrically identical to FitzPatrick and with a similar bundle distribution (Reference 11). The Reference 11 analysis was reviewed and it was concluded that the lead factors are appropriate for FitzPatrick application. The methods used to calculate the lead factors are discussed below.

4.2.1 Procedure

Determination of the lead factors for the RPV inside wall and at 1/4 T depth was done using a combination of one-dimensional and two-dimensional finite element computer analysis. The two-dimensional analysis established the relative fluence in the azimuthal direction at the vessel surface and 1/4 T depth. A series of one-dimensional analyses were done to determine the core height of the axial flux peak and its relationship to the surveillance capsule height. The combination of azimuthal and axial distribution results provides the ratio of flux, or the lead factor, between the surveillance capsule location and the peak flux locations.

The two-dimensional DOT computer program was used to solve the Boltzman transport equation using the discrete ordinate method on an (R,θ) geometry, assuming a fixed source. Quarter core symmetry was used with periodic boundary conditions at 0° degree and 90°. Neutron cross sections were determined for 26 energy groups, with angular scattering approximated by a third-order Legendre expansion. A schematic of the two-dimensional vessel model is shown in Figure 4-1. A total of 99 radial elements and 90 azimuthal elements were used. The model consists of an inner and outer core region, the shroud, water regions inside and outside the shroud, the vessel wall, and an air region representing the drywell. Flux as a function of azimuth was calculated, establishing the azimuth of the peak flux and its magnitude relative to the flux at the wires' location of 30°.

The one-dimensional computer code (SN1D) was used to calculate radial flux distribution at several core elevations at the azimuth angle of 45°, where the azimuthal peak was determined to exist. The elevation of the peak flux was determined, as well as its magnitude relative to the flux at the surveillance capsule elevation.

4.2.2 Results

The one-dimensional flux calculations established the elevation of peak flux at 106 inches above the bottom of active fuel, or 34 inches higher than the capsule. The two-dimensional calculation indicated the flux to be a maximum 45 degrees on either side of the RPV quadrant references (0°, 90°, etc.). The peak closest to the 30° location of Capsule 1 is at 45°.

The distribution calculations establish the lead factor between the surveillance capsule location and the peak location at the inner vessel wall. This lead factor is 0.79. The fracture toughness analysis done is based on a 1/4 T depth flaw in the beltline region, so the attenuation of the flux to that depth is considered. The resulting lead factor from the capsule to the 1/4 T depth at the peak location is 1.05.

4.3 ESTIMATE OF END-OF-LIFE FLUENCE

The fluence at end-of-life (EOL) is estimated by taking the upper bound of the measured flux from Table 4-2 and the 1/4 T lead factor. The period assumed to represent EOL is 32 EFPY, or 1.01×10^9 seconds. The resulting EOL fluence is:

$$(1.4 \times 10^9 \text{ n/cm}^2\text{-s})(1.25)(1.01 \times 10^9 \text{ s})/1.05 = 1.7 \times 10^{18} \text{ n/cm}^2.$$

Table 4-1

SUMMARY OF DAILY POWER HISTORY

Cycle	Cycle Dates	Operating Days	Percent of Full Power	Days Between Cycles
1	1/26/75 - 6/21/77	877	0.523	
				93
2	9/22/77 - 9/16/78	359	0.796	
				81
3	12/6/78 - 5/6/80	517	0.513	
				95
4	8/9/80 - 10/31/81	448	0.825	
				128
5	3/8/82 - 6/3/83	452	0.863	
				91
6	9/2/83 - 2/15/85	532	0.781	
		3185	0.686 (average)	

Table 4-7

SURVEILLANCE CAPSULE LOCATION FLUX AND FLUENCE
FOR IRRADIATION FROM 1/26/75 TO 2/15/85

Wire (Element)	Wire Weight (g)	dps/g Element (at end of Irradiation)	Reaction Rate [dps/nucleus (saturated)]	Full Power Flux [a] (n/cm^2-s) >1 MeV	Full Power Flux [a] (n/cm^2-s) >0.1 MeV	Fluence (n/cm^2) >1 MeV	Fluence (n/cm^2) >0.1 MeV
Copper 64742	0.4582	1.35×10^{4}	4.49×10^{-18}				
Copper 64743	0.4029	1.29×10^{4}	4.29×10^{-18}				
Copper 64744	0.4181	1.26×10^{4}	4.20×10^{-18}				
			Average = 4.33×10^{-18}	1.4×10^{9}	2.2×10^{9}	2.6×10^{17}	4.2×10^{17}
Iron 64742	0.1438	1.06×10^{5}	2.33×10^{-16}				
Iron 64743	0.1471	1.05×10^{5}	2.31×10^{-16}				
Iron 64744	0.1042	1.04×10^{5}	2.29×10^{-16}				
			Average = 2.31×10^{-16}	1.3×10^{9}			
Nickel 64742	0.3113	1.44×10^{6}	2.63×10^{-16}				
Nickel 64743	0.2849	1.44×10^{6}	2.64×10^{-16}				
Nickel 64744	0.3039	1.49×10^{6}	2.73×10^{-16}				
			Average = 2.67×10^{-16}	1.2×10^{9}			

[a] Full power of 2436 MW_t.

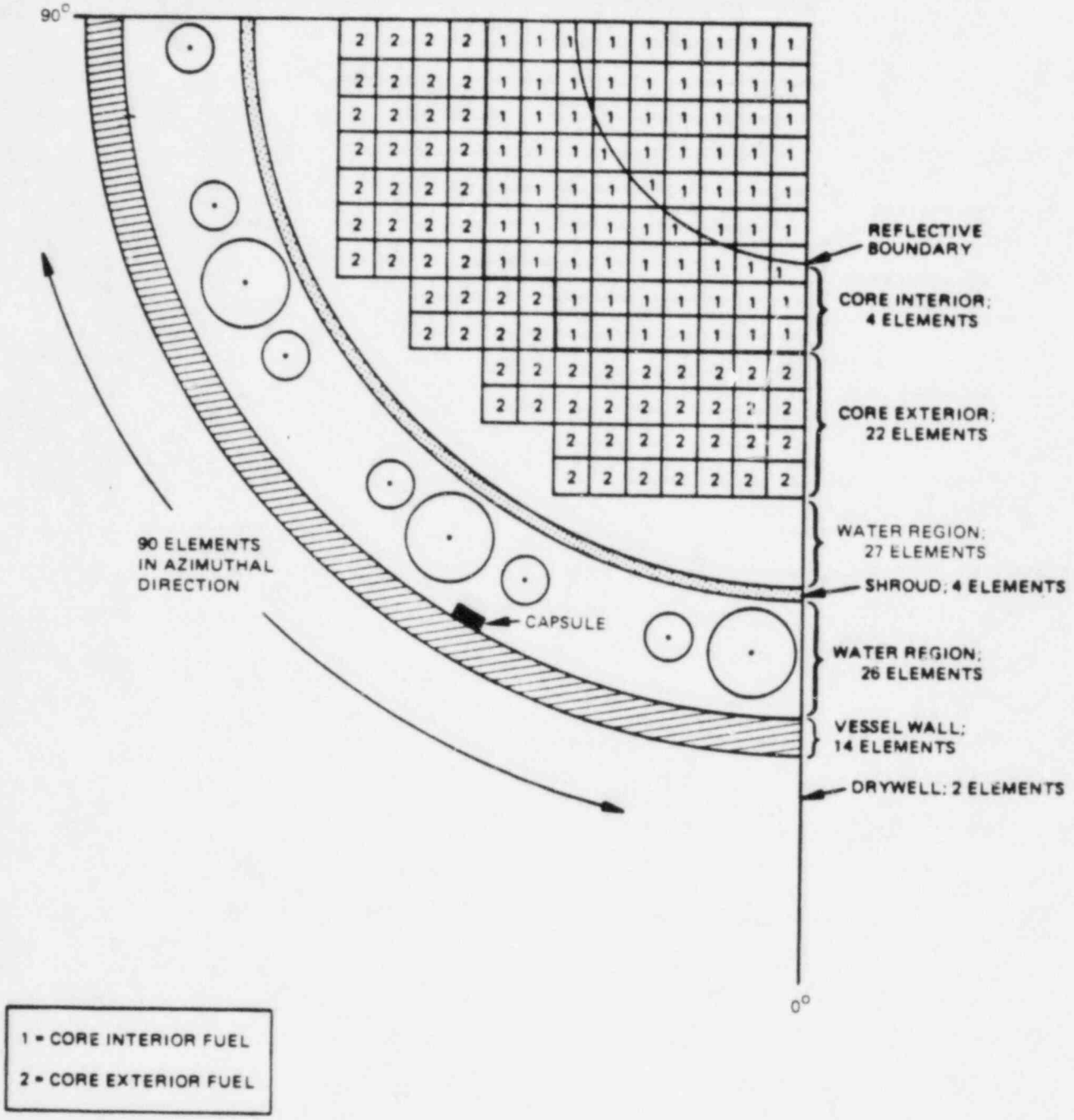

Figure 4-1. Schematic of Model for Two-Dimensional Flux Distribution Analysis

5. CHARPY V-NOTCH IMPACT AND HARDNESS TESTING

The 36 Charpy specimens recovered from the surveillance capsule were impact tested at temperatures selected to establish the toughness transition and upper shelf of the irradiated RPV materials. Testing was conducted in accordance with ASTM E23-82 (Reference 12). After impact testing, Rockwell C hardness testing was performed on the broken specimen halves per ASTM E18-79 (Reference 13).

5.1 IMPACT TEST PROCEDURE

The testing machine used was a Riehle Model PL-2 impact machine, serial number R-89916. The pendulum has a maximum velocity of 15.44 ft/sec and a maximum available hammer energy of 240 ft-lb. The test apparatus and operator were qualified using U.S. Army Watertown standard specimens. The standards are designed to fail at 74.1 ft-lb and 13.9 ft-lb at a test temperature of -40°F. According to Reference 12, the test apparatus averaged results must reproduce the Watertown design values within an accuracy of ±5% or ±1.0 ft-lb, whichever is greater. The successful qualification of the Riehle machine and operator is summarized in Table 5-1.

Charpy V-Notch tests were conducted at temperatures between -60°F and 400°F. For tests between 32°F and 212°F, the temperature conditioning fluid was water. Dichloromethane was used at temperatures below 32°F. Above 212°F, a silicone oil was used. Cooling of the conditioning fluids was done with liquid nitrogen, and heating by an immersion heater. The fluids were mechanically stirred to maintain uniform temperatures. The fluid temperature was measured by a chromel-alumel thermocouple and a copper-constantan thermocouple. These were calibrated with boiling water (212°F), and ice water (32°F). Once at test temperature, the specimens were manually transferred with centering tongs to the Riehle machine and impacted within 5 seconds.

For each Charpy V-Notch specimen tested, test temperature, energy absorbed, lateral expansion, and percent shear were evaluated. Lateral expansion and percent shear were measured according to Reference 12 methods. Percent shear was determined with method two of Subsection 11.2.4.3 of Reference 12, which is a comparison of the fracture surface appearance with the reference fracture surfaces in Figure 15 of Reference 12.

5.2 IMPACT TEST RESULTS

Twelve Charpy V-Notch specimens each of base metal, weld metal and HAZ were tested at temperatures selected to define the toughness transition and upper shelf portions of the fracture toughness cu . Absorbed energy, lateral expansion and percent shear data are listed in Table 5-2 for each material. Plots of absorbed energy data for base, weld, and HAZ metal are presented in Figures 5-1, 5-2 and 5-3, respectively. Lateral expansion plots for base, weld and HAZ metal are given in Figures 5-4, 5-5 and 5-6, respecti.ely.

The data sets are freehand fit with best-estimate S-shaped curves characteristic of fracture toughness transition curves. The HAZ data in Figures 5-3 and 5-6 are not fit with a curve. There is too much scatter in the data for a meaningful curve to be drawn. The HAZ data probably show the greatest scatter because the HAZ has been uniquely heat treated by the welding process. In addition, the uncertainty of the specimen notch location relative to the weld fusion line causes scatter in the HAZ results.

Photographs were taken of the fracture surfaces for each specimen. The fracture surface photographs were used to evaluate percent shear. The photographs and a summary of test results for each specimen are contained in Appendix A.

5.3 IRRADIATED VERSUS UNIRRADIATED CHARPY V-NOTCH PROPERTIES

As a part of the RPV fabrication test program, Charpy V-Notch testing was done at various temperatures on the unirradiated RPV plate materials. Data for the beltline plate from which the base metal specimens were fabricated, (plate G-3414-2) were recovered from QA records. The impact energy and lateral expansion data are plotted in Figures 5-7 and 5-8, respectively. The corresponding irradiated data from the base metal surveillance specimens are plotted in Figures 5-7 and 5-8 as well.

The curves of irradiated and unirradiated Charpy V-Notch properties are used to estimate the values in Table 5-3: 30 ft-lb, 50 ft-lb and 35 MLE index temperatures and USEs. The RT_{NDT} shift values are determined as the change in the temperature at which 30 ft-lb impact energy is achieved, as required in Reference 4. In previous experience, the shift in the transition curve has been approximately equal at the 30 ft-lb and 50 ft-lb levels. Table 5-3 shows a slight difference (23°F versus 26°F, respectively). The shift in lateral expansion at the 35 MLE level of 13°F supports a lower shift value, so the 30 ft-lb shift of 23°F is used as the RT_{NDT} shift. This shift from initial to adjusted RT_{NDT} for the base metal is compared to analytical values calculated in Section 7 according to Regulatory Guide 1.99, Revision 1. A similar comparison cannot be made for the weld metal because unirradiated weld metal Charpy test data are not available.

5.4 ROCKWELL HARDNESS TESTING

After the Charpy specimens were tested, one broken half of each specimen was subjected to Rockwell hardness testing, according to ASTM E18-79 (Reference 13). The test used for the surveillance materials was the Rockwell C test, which employs a diamond sphero-conical penetrator with a minor load of 10 kgf and a major load of 150 kgf.

The machine used was a calibrated Wilson Rockwell Hardness Tester. As a further calibration before testing, a test block with a reference hardness of 35.0 ± 1.0 HRC was tested. The three values taken were 34.0, 34.2 and 36.0 HRC, for an average of 34.7 HRC, which is acceptable.

Three indentations were made on each specimen half and the results were averaged to develop the hardness values in Table 5-4. Each piece tested was consistently the half with the specimen identification stamped in the end. The indentations were made on the same side of each specimen in a group approximately 3/8 inches from the fracture surface.

The results show a definite difference between weld and base metal. The weld metal grouping averages 5 HRC above the base metal average. As discussed in Section 3, the HAZ specimens are half weld and half base metal. The results of Table 5-4 indicate that the weld side of the HAZ specimens was tested.

Table 5-1

QUALIFICATION TEST RESULTS USING
U.S. ARMY WATERTOWN SPECIMENS
(TESTED IN FEBRUARY 1986)

Qualification Test Specimen Identification	Test Temperature (°F)	Energy Absorbed Mechanical Gage (ft-lb)
EE30427	-40	72.0
EE30075	"	74.5
EE30233	"	80.0
EE30956	"	75.8
EE30365	"	74.2
Average		75.3
Allowable	-40	74.1 ± 3.7 Acceptable
DD50442	-40	15.0
DD50905	"	13.8
DD50486	"	14.0
DD50977	"	14.0
DD50831	"	14.0
Average		14.2
Allowable	-40	13.9 ± 1.0 Acceptable

Table 5-2

CHARPY V-NOTCH IMPACT TEST RESULTS
FOR IRRADIATED RPV MATERIALS

Specimen Identification	Test Temperature (°F)	Fracture Energy (ft-lb)	Lateral Expansion (mils)	Percent Shear (Method 2) (%)
Base:				
52K	-60	14.3	15	0
52C	-20	21.0	26	0
52B	0	46.5	46	0
531	10	61.0	57	10
52A	20	67.5	61	20
51B	40	44.5	51	20
51L	80	83.6	70	50
51C	120	100.0	68	60
51Y	160	125.0	86	50
51D	200	136.5	92	90
52M	300	136.5	94	100
52U	400	121.3	92	80
Weld:				
55J	-60	7.2	11	0
55D	-20	24.0	26	20
55A	0	15.0	20	10
56M	10	14.0	23	0
552	20	20.0	25	30
541	40	31.4	33	20
54L	80	42.0	39	40
54B	120	54.1	52	70
54P	160	75.0	62	85
54D	200	82.1	53	70
55U	300	86.0	65	60
56E	400	79.3	70	100
HAZ:				
5BL	-60	13.2	16	10
5B4	-20	38.3	35	20
5AC	0	78.5	70	50
5BU	10	26.5	28	40
5AA	20	86.7	64	60
572	40	60.1	51	50
57Y	80	61.5	46	60
57K	120	110.6	65	50
5A1	160	81.2	66	100
57T	200	107.5	70	100
5BM	300	87.2	71	60
5BP	400	72.0	70	100

Table 5-3

SIGNIFICANT RESULTS OF IRRADIATED AND
UNIRRADIATED CHARPY V-NOTCH DATA

Material	Index Temperature (°F)			Upper Shelf Energy (ft-lb) L/T [a]
	E=30 ft-lb	E=50 ft-lb	MLE=35 mil	
Unirradiated Plate	-32	1	-13	130/85
Irradiated Plate	-9	27	0	122/79
Difference	23	26	13	8/5 (6%)
Irradiated Weld	48	100	61	82/82

[a] Longitudinal (L) USE is read directly from Figures 5-1 and 5-3. Transverse (T) USE is taken as 65% of the longitudinal USE, according to Reference 7. L/T USE values are equal for weld metal, which has no orientation effect.

Table 5-4

ROCKWELL C HARDNESS TEST RESULTS

Identification	Specimen Type	Rockwell C Hardness (HRC)
52K	Base	14.3
52E	"	13.9
52A	"	13.7
531	"	13.4
52M	"	13.3
52B	"	12.8
51Y	"	12.6
51B	"	12.5
52U	"	12.4
51D	"	12.3
51C	"	12.2
51L	"	12.0
	Average =	13.0
54L	Weld	21.3
54D	"	20.1
54B	"	18.8
552	"	18.6
54P	"	18.4
55A	"	18.3
55U	"	18.2
55J	"	18.1
541	"	18.1
55D	"	17.6
56M	"	17.4
56E	"	16.7
	Average =	18.5
57Y	HAZ	21.1
57T	"	20.7
57K	"	19.3
5AA	"	19.3
572	"	18.9
5BM	"	18.9
5A1	"	18.6
5BL	"	18.3
5BU	"	18.3
5BP	"	18.1
5AC	"	17.5
5B4	"	17.0
	Average =	18.8

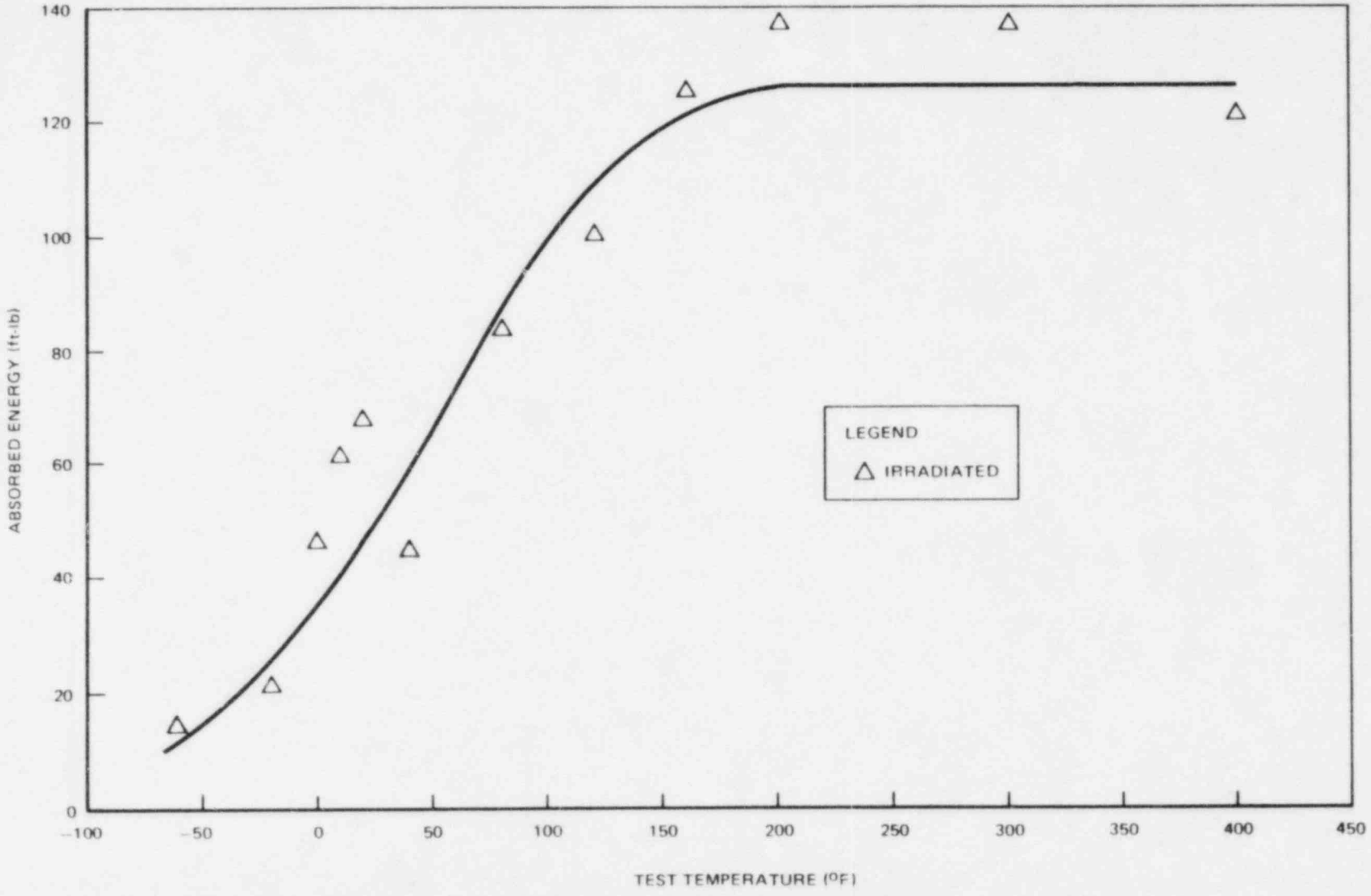

Figure 5-1. FitzPatrick Irradiated Base Metal Impact Energy

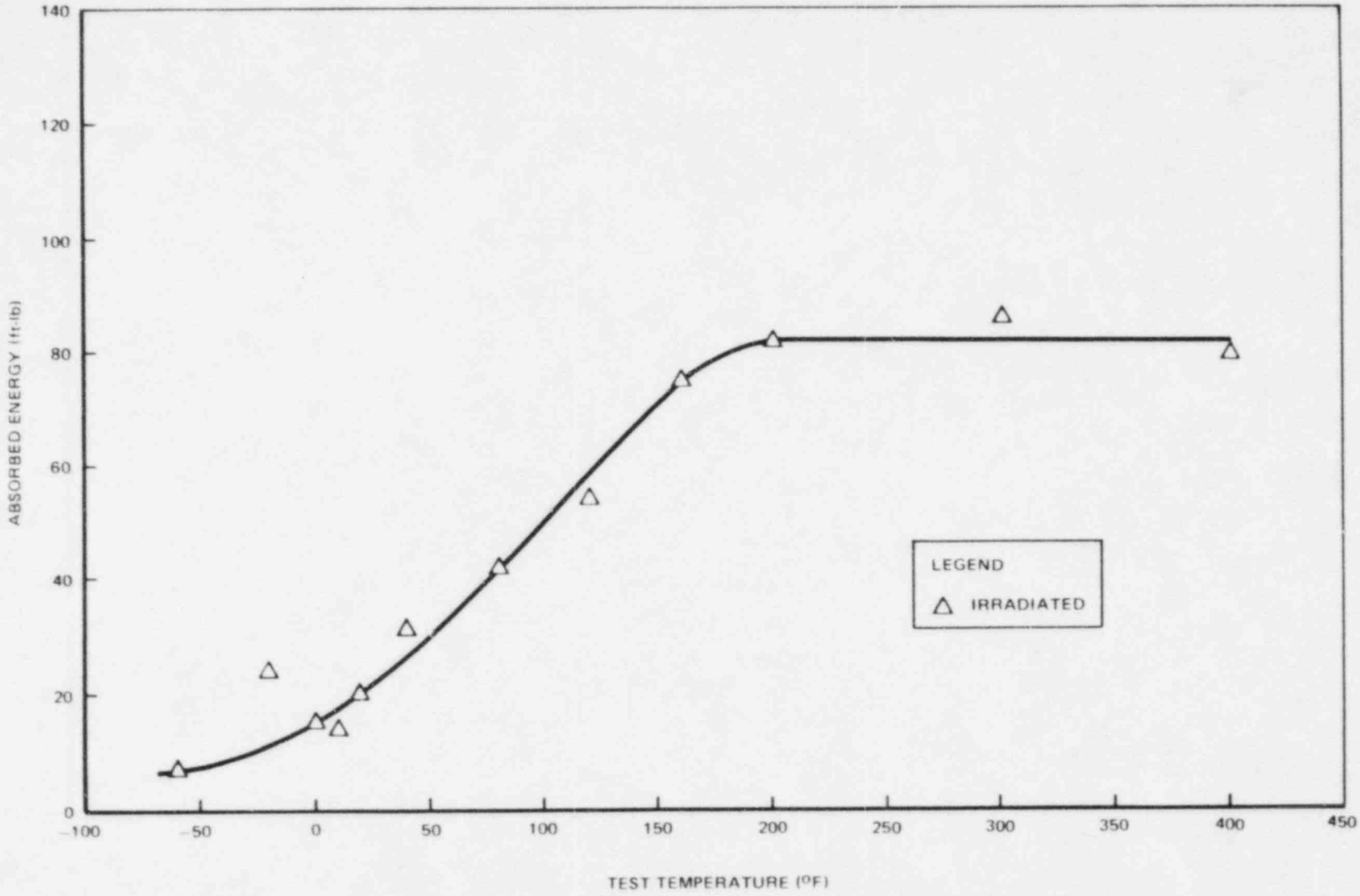

Figure 5-2. FitzPatrick Irradiated Weld Metal Impact Energy

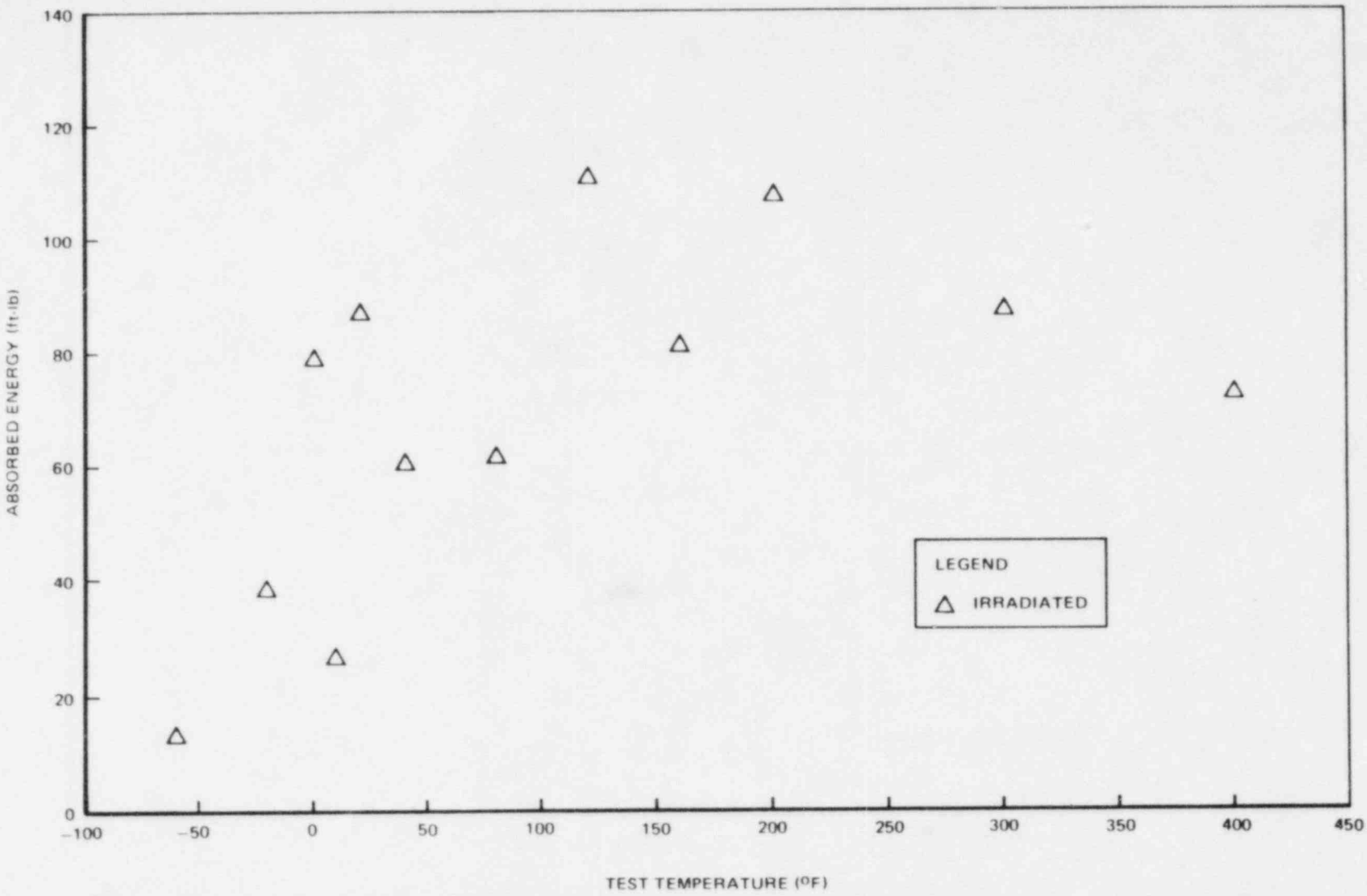

Figure 5-3. FitzPatrick Irradiated HAZ Metal Impact Energy

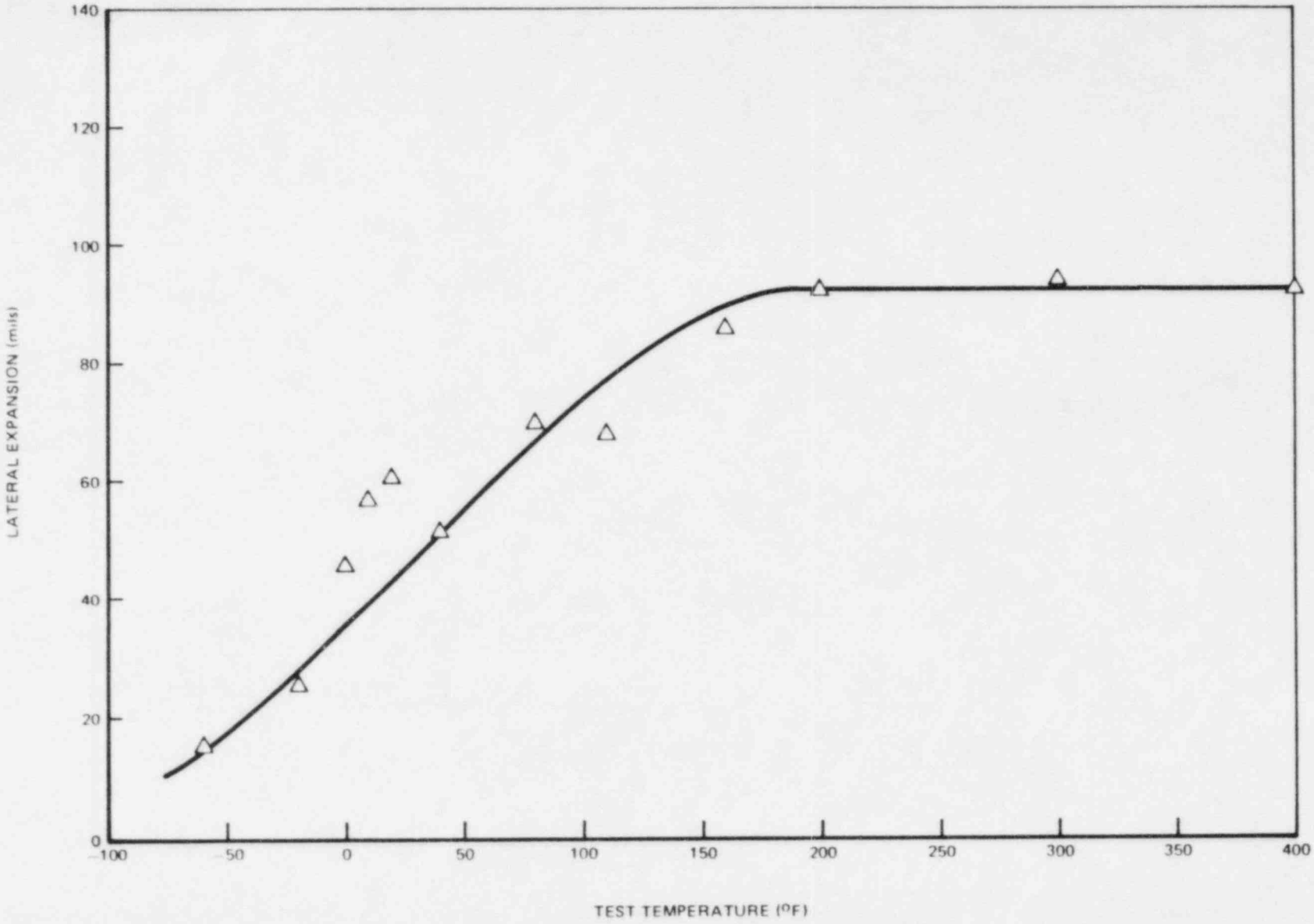

Figure 5-4. FitzPatrick Irradiated Base Metal Lateral Expansion

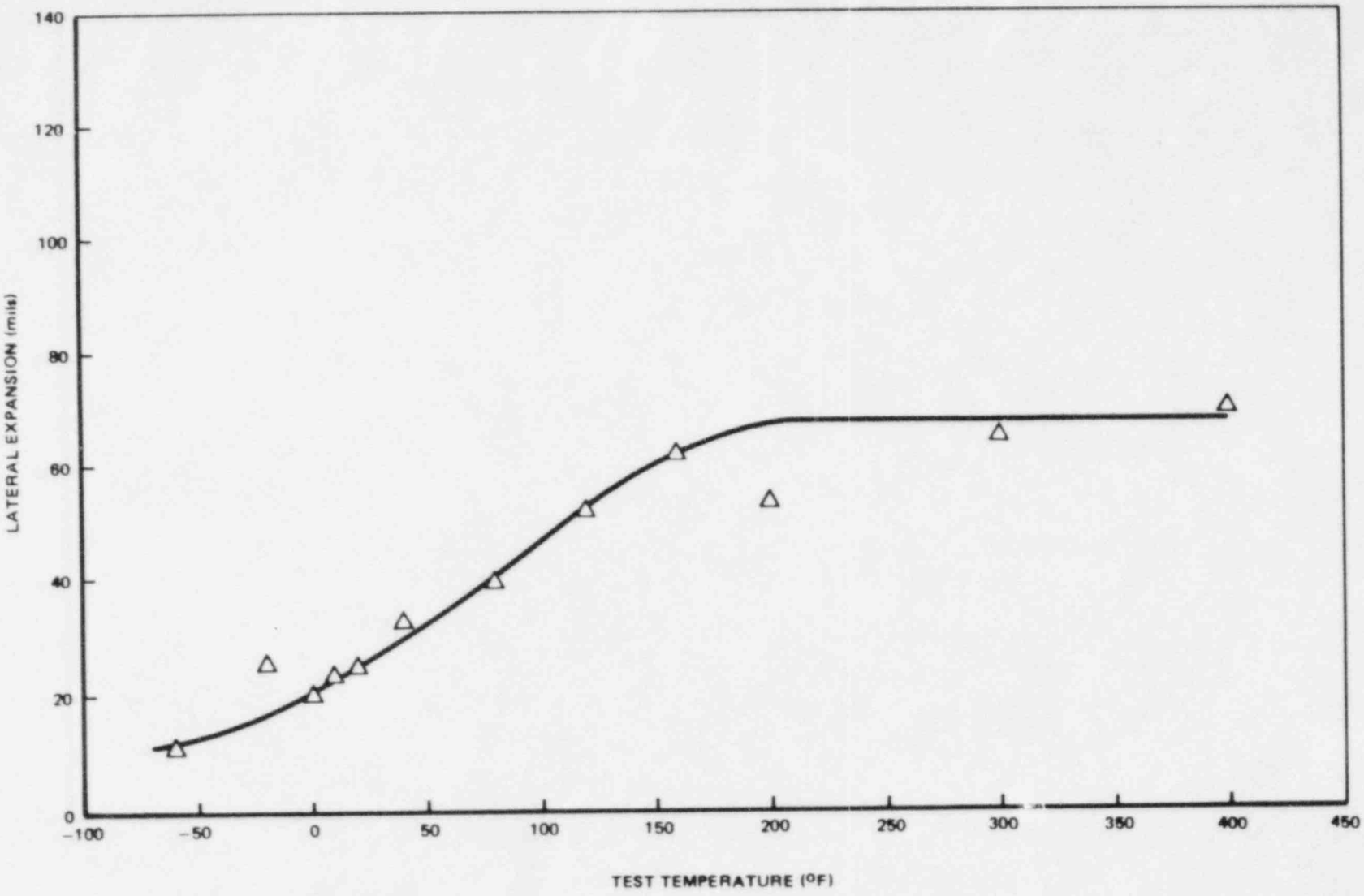

Figure 5-5. FitzPatrick Irradiated Weld Metal Lateral Expansion

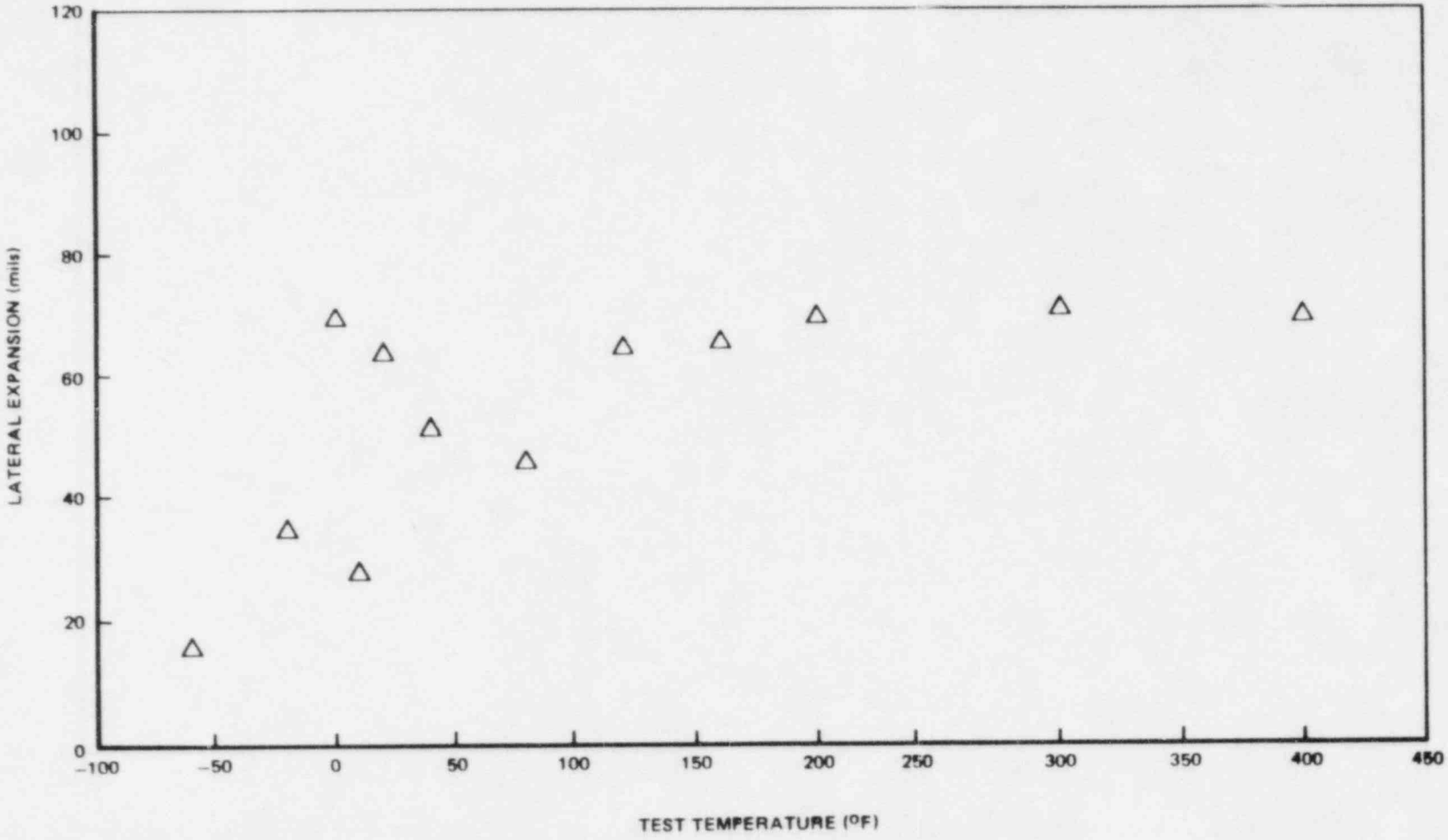

Figure 5-6. FitzPatrick Irradiated HAZ Metal Lateral Expansion

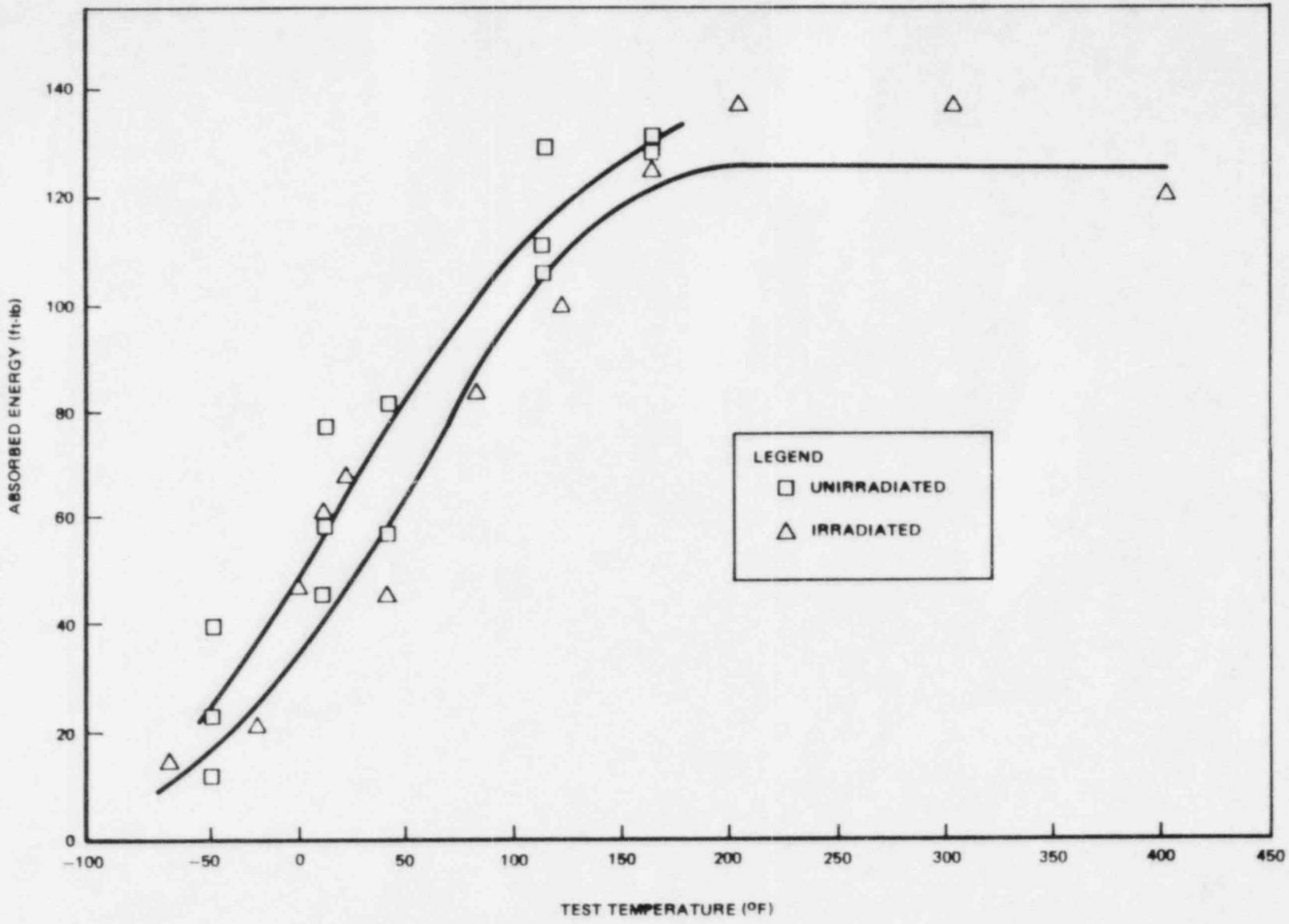

Figure 5-7. FitzPatrick Irradiated Versus Unirradiated Base Metal Impact Energy

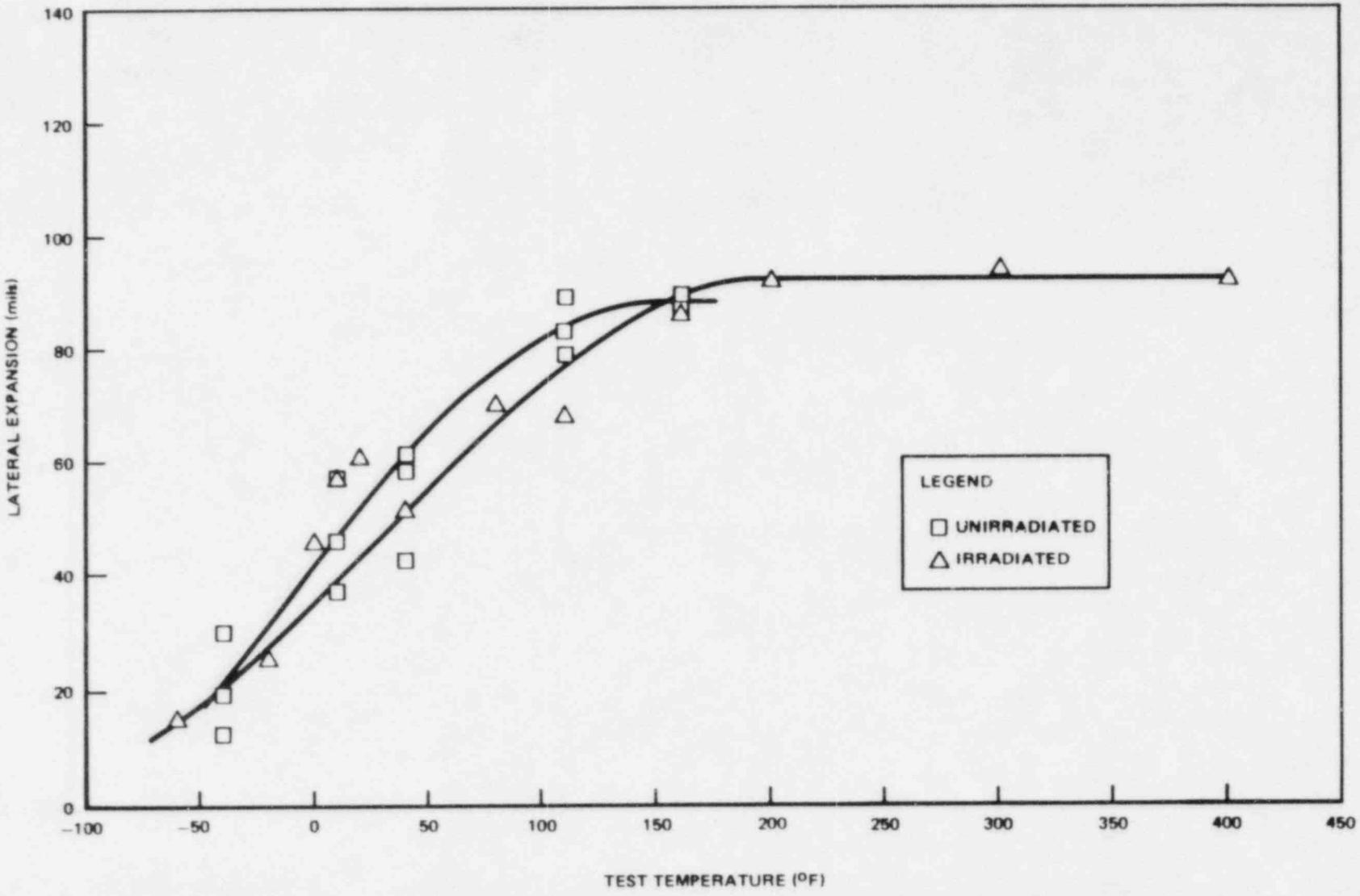

Figure 5-8. FitzPatrick Irradiated Versus Unirradiated Base Metal Lateral Expansion

6. TENSILE TESTING

Eight round bar tensile specimens were recovered from the surveillance capsule. Uniaxial tensile tests were conducted in air at room temperature, RPV operating temperature, and onset of upper shelf temperature. Tests were conducted in accordance with ASTM E8-81 (Reference 14).

6.1 PROCEDURE

All tests were conducted using a screw-driven Instron test frame equipped with a 20-kip load cell and special pull bars and grips. Heating was done with a Satec resistance clamshell furnace centered around the specimen load train. Test temperature was monitored and controlled by a chromel-alumel thermocouple spot-welded to an Inconel clip that was friction-clipped to the surface of the specimen at its midline. Before the elevated temperature tests, a profile of the furnace was conducted at the test temperature of interest using an unirradiated steel specimen of the same geometry. Thermocouples were spot-welded to the top, middle, and bottom of a central 1 inch gage of this specimen. In addition, the clip-on thermocouple was attached to the midline of the specimen. When the target temperatures of the three thermocouples were within ±5°F of each other, the temperature of the clip-on thermocouple was noted and subsequently used as the target temperature for the irradiated specimens.

All tests were conducted at a calibrated crosshead speed of 0.005 inch/min until well past yield, at which time the speed was increased to 0.05 inch/min until fracture. A 1 inch span knife edge extensometer was attached directly to each specimen's central gage region and was used to monitor gage extension during test.

The test specimens were machined with a minimum diameter of 0.250 inch at the center of the gage length. The three specimens each of base metal and HAZ were tested at room temperature (RT = 76°F), onset of upper shelf temperature (estimated at 185°F), and RPV operating temperature (550°F).

The two weld metal specimens were tested at room temperature and 550°F. The yield strength (YS) and ultimate tensile strength (UTS) were calculated by dividing the nominal area (0.0491 $in.^2$) into the 0.2% offset load and into the maximum test load, respectively. The values listed for the uniform and total elongations were obtained from plots that recorded load versus specimen extension and are based on a 1 inch gage length. Reduction of area (RA) values were determined from post-test measurements of the necked specimen diameters using a calibrated blade micrometer and employing the formula:

$$RA = 100\% * (A_o - A_f)/A_o$$

After testing, each broken specimen was photographed end-on showing the fracture surface and lengthwise showing fracture location and local necking behavior.

6.2 RESULTS

Tensile test properties of YS, UTS, RA, uniform elongation (UE) and total elongation (TE) are presented in Table 6-1. Shown in Figure 6-1 is a stress-strain curve for a 550°F base metal specimen typical of the stress-strain characteristics of all the specimens tested. Shown graphically in Figures 6-2 and 6-3 are the data in Table 6-1. Photographs of fracture surfaces and necking behavior are given in Figures 6-4, 6-5 and 6-6 for base, weld and HAZ specimens respectively. The base, weld, and HAZ materials generally follow the trend of decreasing properties with increasing temperature.

6.3 IRRADIATED VERSUS UNIRRADIATED TENSILE PROPERTIES

Unirradiated tensile test data were recovered from QA records for the surveillance specimen plate (G-3414-2) and the beltline weld (1-233). Data for 0.505 inch diameter gage tensile specimens from the fabrication test program were used to get unirradiated room temperature YS, UTS, RA and TE properties. These are compared in Table 6-2 to the irradiated base metal and weld metal specimen RT data to determine the degree of irradiation effect. The trends of increasing YS and UTS and of decreasing TE and RA are characteristic of irradiation embrittlement. The weld metal shows a larger effect, which is in agreement with the larger RT_{NDT} shift predicted because of the weld's higher Cu content.

Table 6-1

TENSILE TEST RESULTS FOR IRRADIATED RPV MATERIALS

Specimen Number	Material	Test Temp (°F)	Yield Strength (ksi)	Ultimate Strength (ksi)	Uniform Elongation (%)	Total Elongation (%)	Reduction of Area (%)
5CL	Base	76	71.4	93.6	10.0	20.6	68.7
5CT	Base	185	68.5	88.7	9.1	20.7	72.5
5CM	Base	550	65.1	89.1	8.9	17.4	65.9
5DL	Weld	76	88.6	105.0	9.4	18.5	64.5
5DM	Weld	550	76.3	96.2	8.5	14.4	44.7
5ED	HAZ	76	77.2	99.6	7.7	17.3	68.2
5EB	HAZ	185	73.2	94.0	6.5	16.3	69.1
5EM	HAZ	550	74.4	98.0	8.2	13.9	54.8

Table 6-2

COMPARISON OF UNIRRADIATED AND IRRADIATED
TENSILE PROPERTIES AT ROOM TEMPERATURE

	Yield Strength (ksi)	Ultimate Strength (ksi)	Total Elongation (%)	Reduction of Area (%)
Base (G-3414-2):				
Unirradiated [a]	67.7	89.3	27.0	69.8
Irradiated [b]	71.4	93.6	20.6	68.6
Difference [c]	5.2%	4.6%	-31.1%	-1.8%
Weld (1-233):				
Unirradiated [a]	72.9	85.4	26.0	68.5
Irradiated [b]	88.6	105.0	18.5	64.5
Difference [c]	17.8%	18.7%	-40.5%	-6.2%

[a] Specimens have 0.505 inch gage diameter.

[b] Specimens have 0.250 inch gage diameter.

[c] Difference = [(Irradiated - Unirradiated)/Irradiated] * 100%

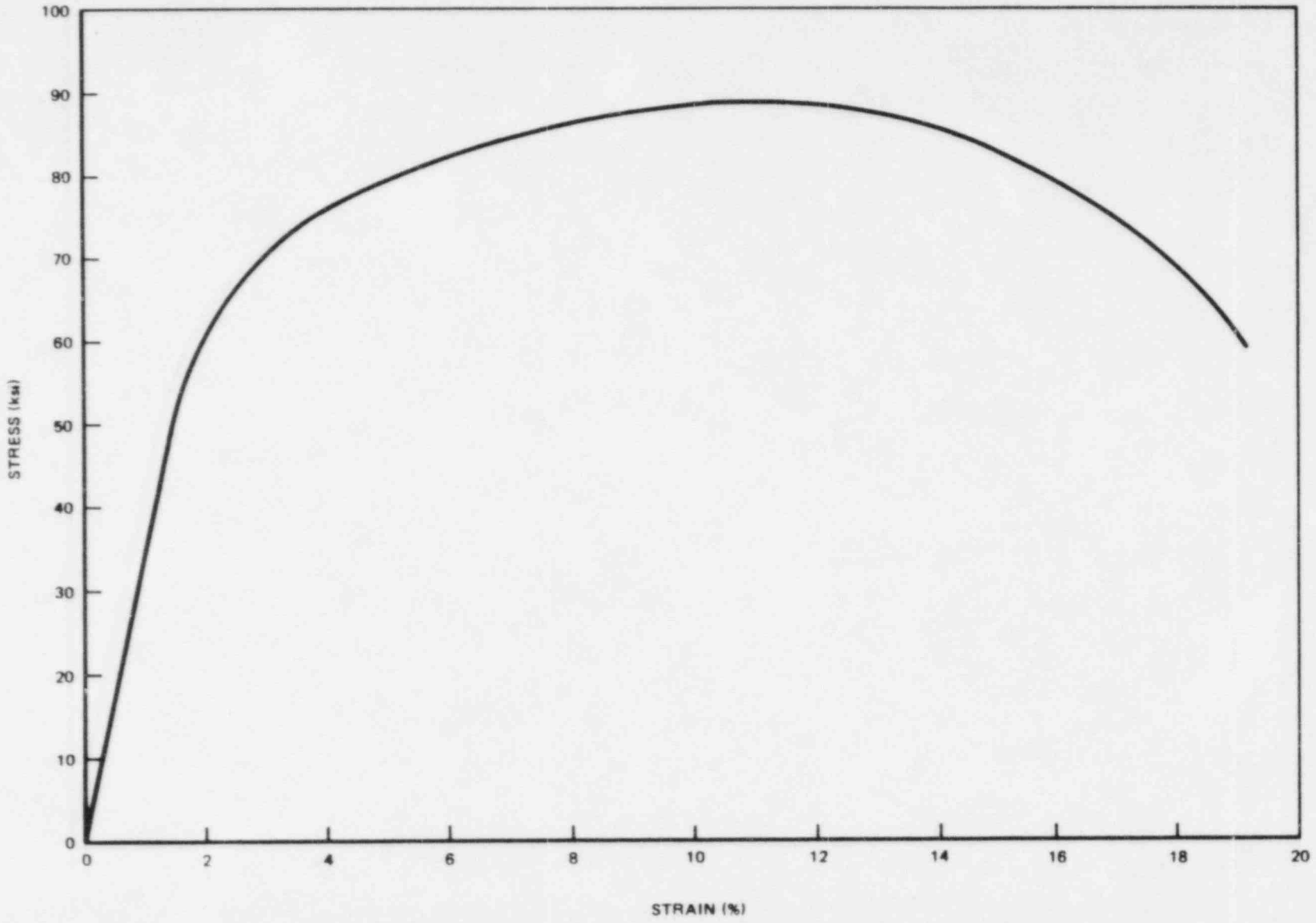

Figure 6-1. Typical Engineering Stress Versus Percent Strain for Irradiated RPV Materials

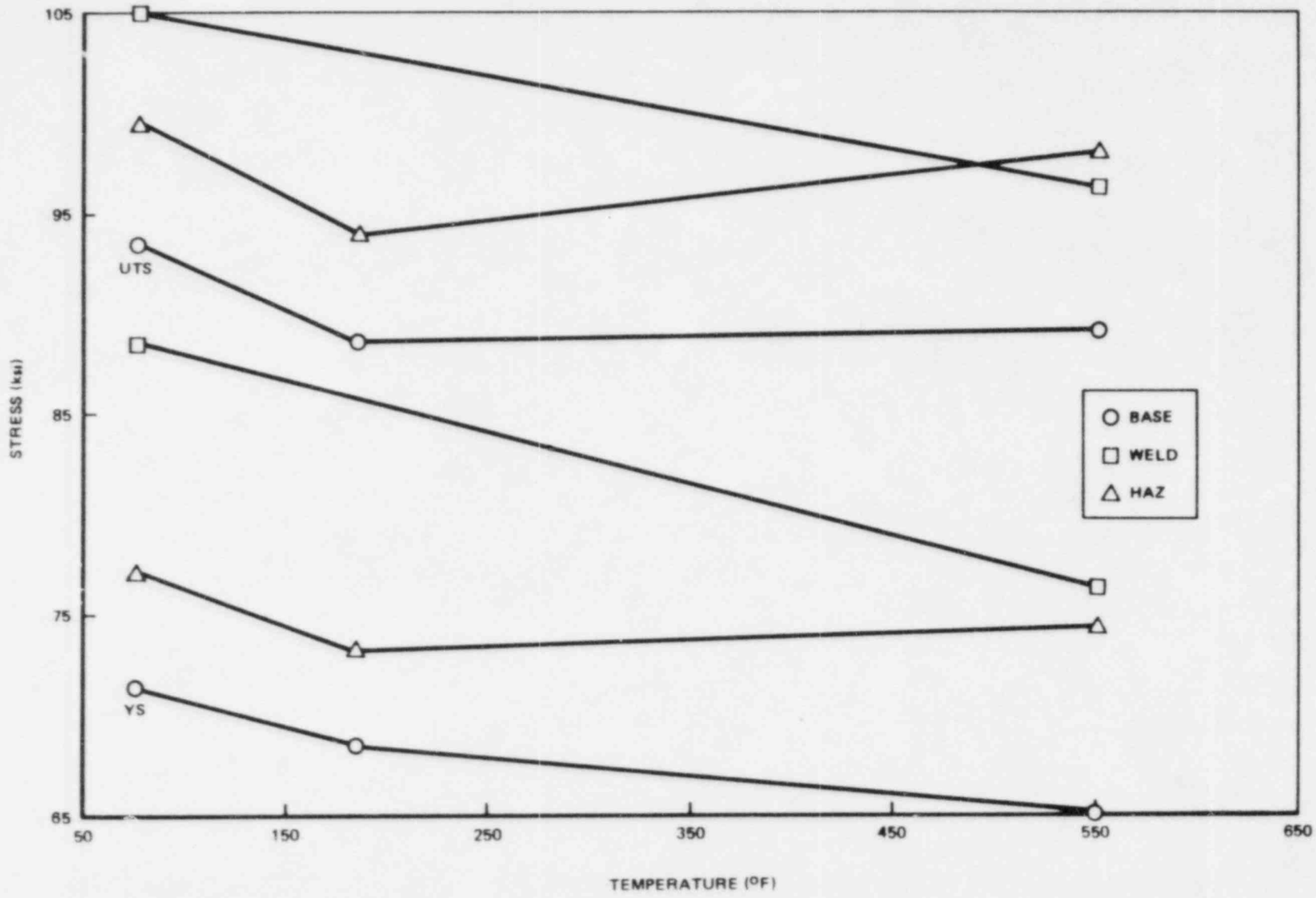

Figure 6-2. Strength Versus Test Temperature for Irradiated Base, Weld, and HAZ Tensile Specimens

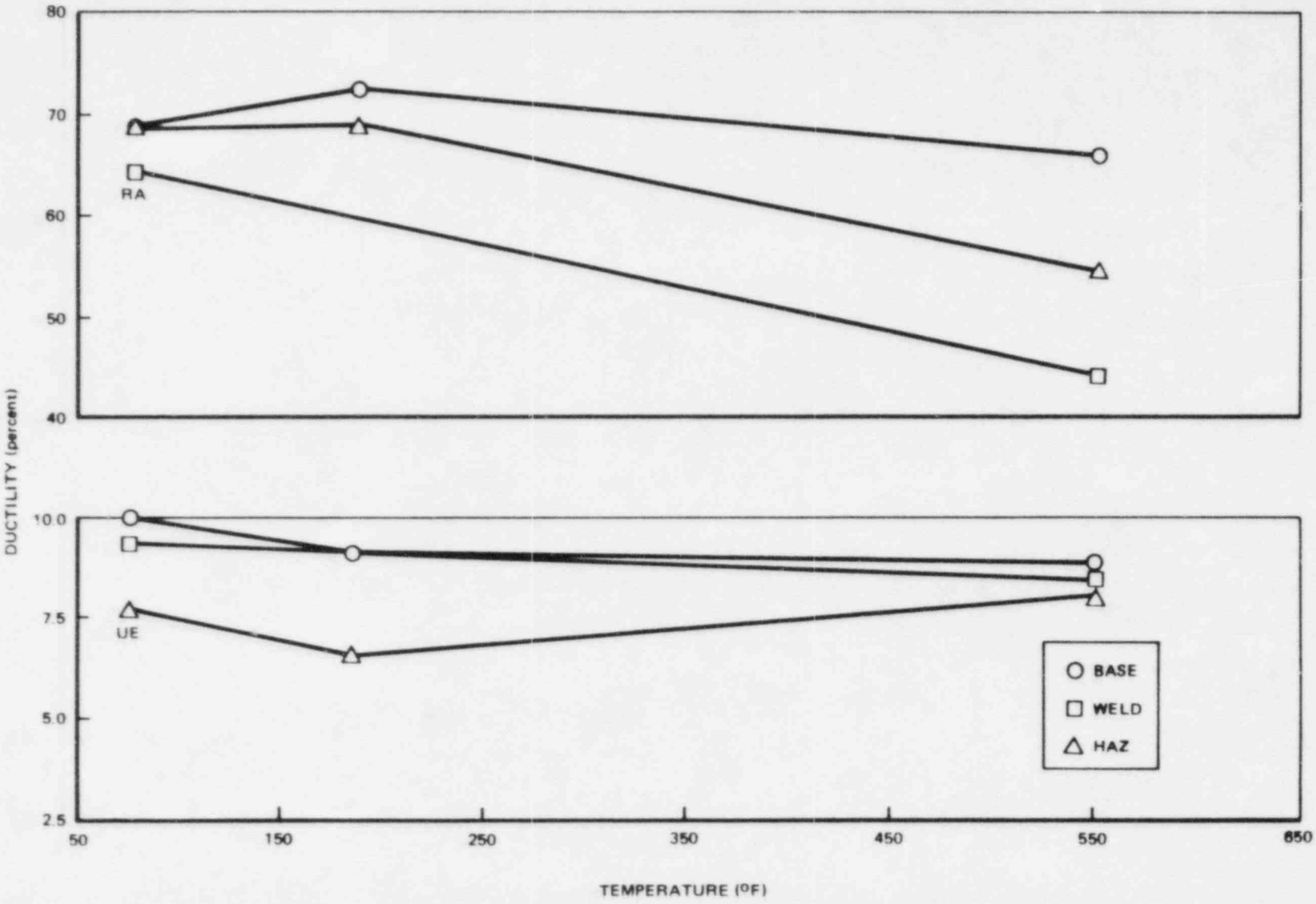

Figure 6-3. Ductility Versus Test Temperature for Irradiated Base, Weld, and HAZ Tensile Specimens

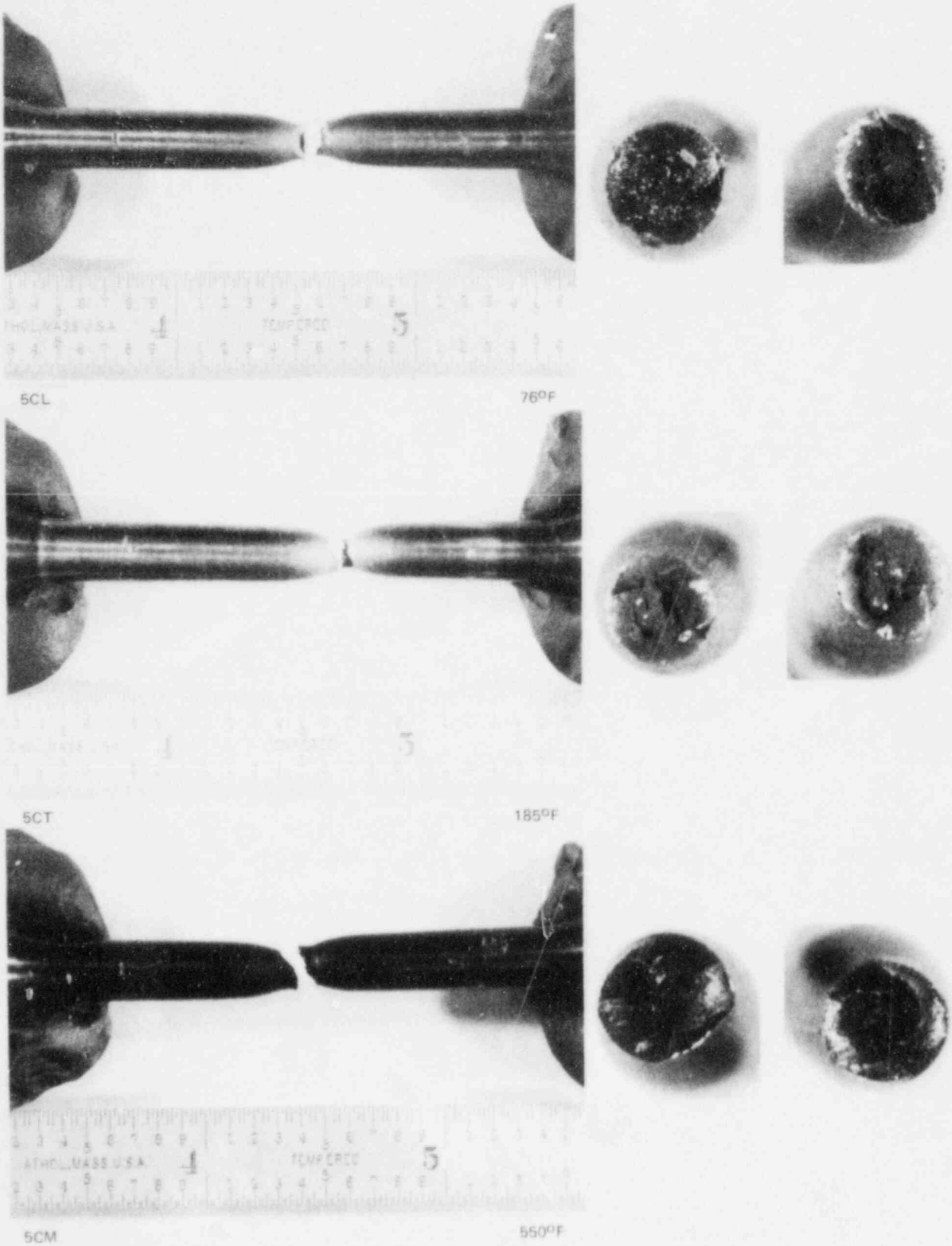

Figure 6-4. Fracture Location, Necking Behavior, and Fracture Appearance for Irradiated Base Metal Tensile Specimens

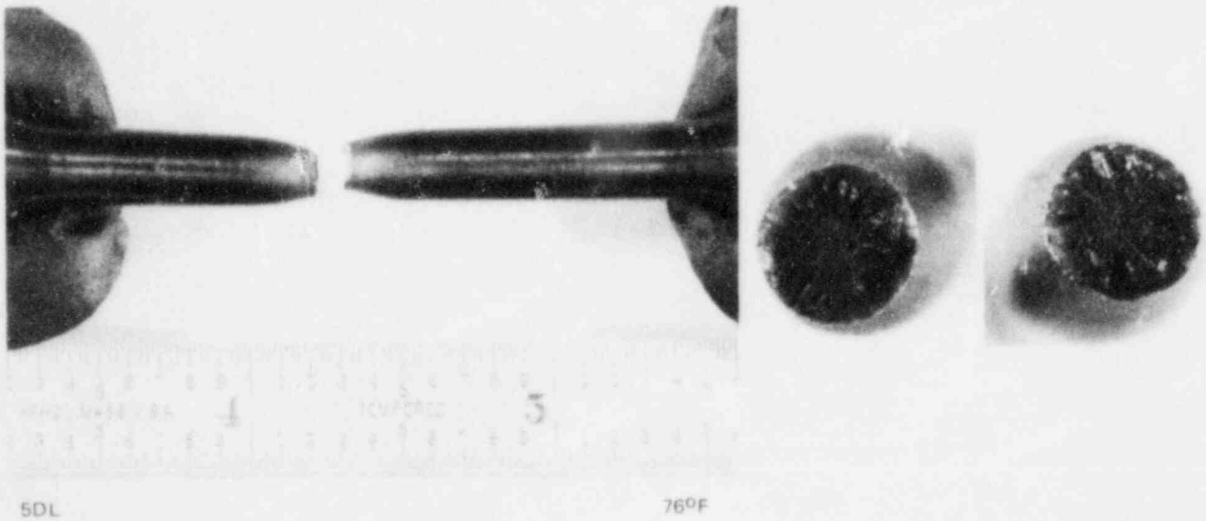

5DL 76°F

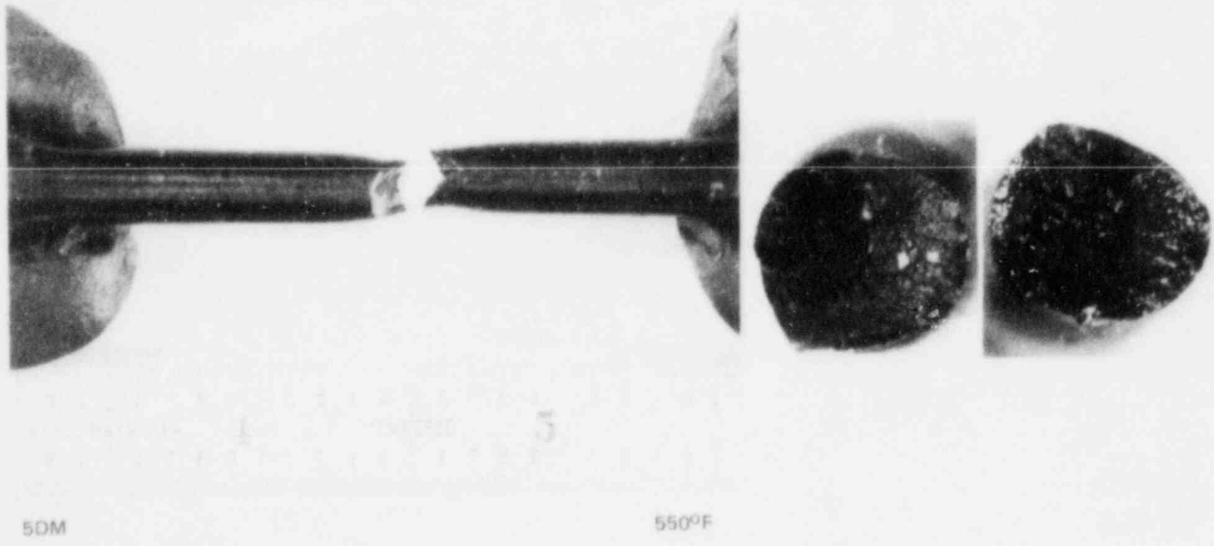

5DM 550°F

Figure 6-5. Fracture Location, Necking Behavior, and Fracture Appearance for Irradiated Weld Metal Tensile Specimens

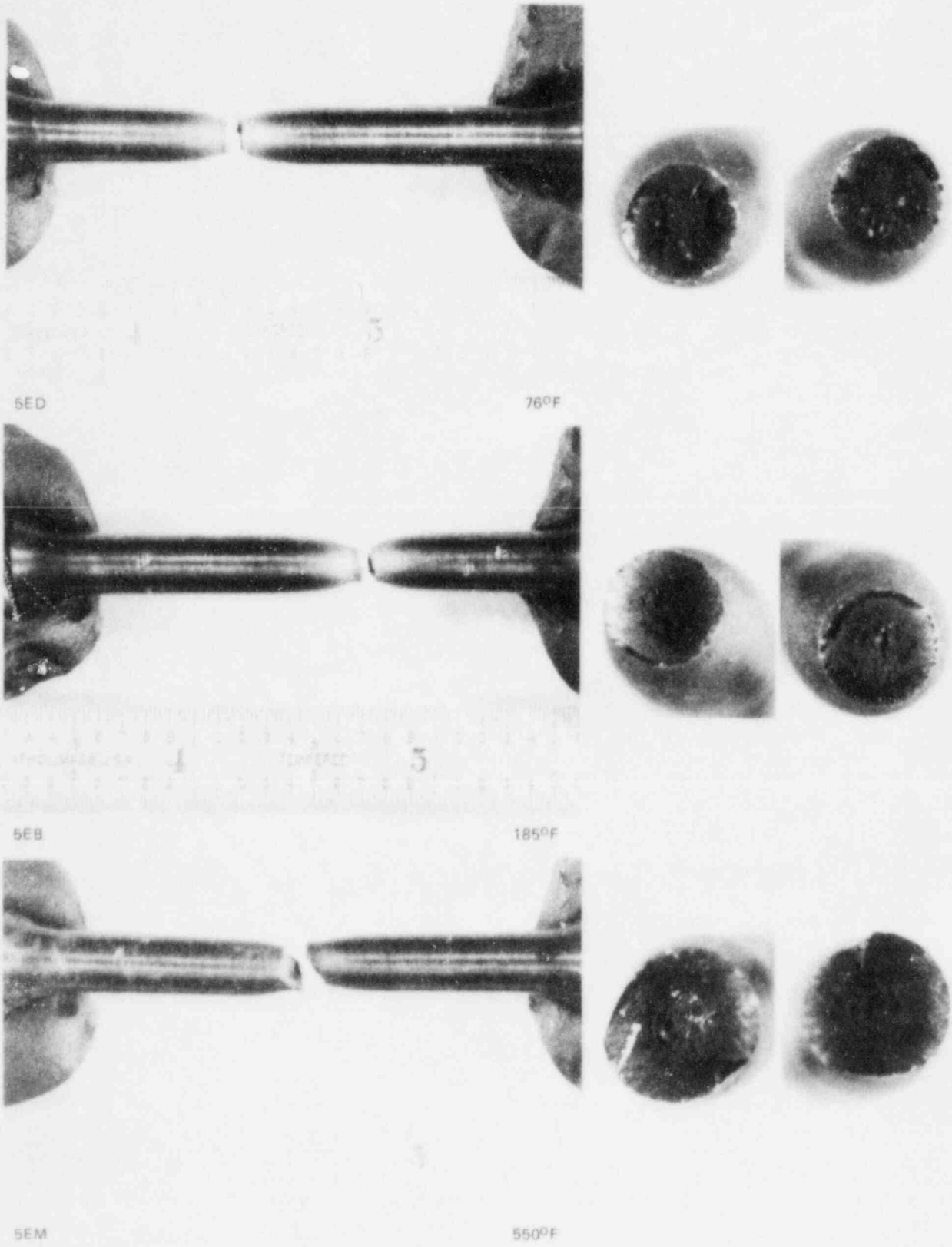

Figure 6-6. Fracture Location, Necking Behavior, and Fracture Appearance for Irradiated HAZ Metal Tensile Specimens

7. DEVELOPMENT OF OPERATING LIMITS CURVES

7.1 BACKGROUND

Operating limits for pressure and temperature are required for three categories of operation: (a) hydrostatic pressure tests and leak tests, referred to as Curve A; (b) non-nuclear heatup/cooldown and low-level physics tests, referred to as Curve B; and (c) core critical operation, referred to as Curve C. There are three vessel regions that affect the operating limits: the closure flange region, the core beltline region, and the remainder of the vessel, or non-beltline regions. The closure flange region limits are controlling at lower pressures primarily because of Reference 1 requirements. The non-beltline and beltline region operating limits are evaluated according to procedures in References 1 and 2, with the beltline region minimum temperature limits increasing as the vessel is irradiated.

7.2 NON-BELTLINE REGIONS

Non-beltline regions are those locations that receive too little fluence to cause any RT_{NDT} increase. Non-beltline components include the nozzles, the closure flanges, some shell plates, top and bottom head plates and the control rod drive (CRD) penetrations. Detailed stress analyses of the non-beltline components were performed for the BWR/6. The analyses took into account all mechanical loadings and thermal transients anticipated. Detailed stresses were used according to Reference 2 to develop plots of allowable pressure (P) versus temperature relative to the reference temperature ($T - RT_{NDT}$). These results were applied to the FitzPatrick vessel components, since the geometries are not significantly different from BWR/6 configurations, and the mechanical and thermal loadings anticipated are comparable.

The non-beltline region results were established by adding the highest RT_{NDT} for the non-beltline discontinuities to the P versus (T - RT_{NDT}) curves for the most limiting BWR/6 components. The CRD penetration and feedwater nozzle results bound the results for all other non-beltline BWR/6 components. Shown in Figures 7-1 through 7-3 are the FitzPatrick unique calculated non-beltline operating limits for Curves A, B, and C, respectively. Curve A limiting values are set by the BWR/6 CRD penetration results in conjunction with the 30°F RT_{NDT} of the recirculation inlet nozzle. The BWR/6 feedwater nozzle analysis, combined with the recirculation inlet RT_{NDT} of 50°F, establishes the limits for Curves B and C.

7.3 CORE BELTLINE REGION

The pressure-temperature (P-T) limits for the unirradiated beltline region are shown in Figures 7-1 through 7-3. As the beltline fluence increases during operation, these curves shift to the right by an amount discussed in Subsection 7.6. Eventually, the beltline curves shift to become more limiting than the non-beltline curves. The stress intensity factors calculated for the beltline region according to Reference 2 procedures are based on a combination of pressure and thermal stresses. The pressure stresses were calculated using thin-walled cylinder equations. Thermal stresses were calculated assuming the through-wall temperature distribution of a flat plate subjected to a 100°F/hr thermal gradient. The initial RT_{NDT} of 24°F for the beltline was used to adjust the (T - RT_{NDT}) values from Figure G-2210-1 of Reference 2.

7.4 CLOSURE FLANGE REGION

Reference 1 sets several minimum requirements for pressure and temperature in the closure flange region in addition to those outlined in Reference 2. In some cases, the results of analysis for other regions exceed these requirements and they do not affect the shape of the P-T curves. However, some closure flange requirements from Reference 1 do impact the curves. In addition, General Electric recommends 60°F margin on the required bolt preload temperature.

As stated in Paragraph G-2222(c) of Reference 2, for application of full bolt preload and reactor pressure up to 20% of hydrostatic test pressure, the RPV metal temperature must be at RT_{NDT} or greater. The GE practice is to require (RT_{NDT} + 60°F) for bolt preload, for two reasons:

a. The original ASME Code of construction requires (RT_{NDT} + 60°F); and

b. The highest stressed region during boltup is the closure flange region, and the flaw size assumed in that region (0.24 inches) is less than 1/4 T. This flaw size is detectable using ultrasonic testing (UT) techniques. In fact, References 15 and 16 report that a flaw in the closure flange region of 0.09 inch can be reliably detected using UT.

(RT_{NDT} + 60°F) is not a current ASME Code requirement; it provides extra margin for Curves A and B. However, (RT_{NDT} + 60°F) is a requirement for Curve C, as described in paragraph IV.A.3 of Reference 1.

Reference 1, paragraph IV.A.2, sets temperature minimum requirements for pressure above 20% hydrotest pressure. Curve A temperature must be no less than (RT_{NDT} + 90°F) and Curve B temperature no less than (RT_{NDT} + 120°F). The Curve A requirement causes a 30°F shift at 20% hydrotest pressure (312 psig) as shown in Figure 7-1. The Curve B requirement has no impact on Figure 7-2 because the analytical results for the feedwater nozzle require that temperature be greater than (RT_{NDT} + 120°F) at 312 psig.

7.5 CORE CRITICAL OPERATION REQUIREMENTS OF 10CFR50, APPENDIX G

Curve C, the core operation curve shown in Figure 7-3 is generated from Figure 7-2, accounting for the requirements of Reference 1, paragraph IV.A.3. Essentially paragraph IV.A.3 requires that core critical P-T limits be 40°F above any Curve A or B limits. Curve B is more limiting than Curve A, so Curve C is Curve B plus 40°F. The (RT_{NDT} + 60°F)

minimum permissible temperature mentioned in Subsection 7.4 for Curve C is an exception for BWRs, allowing critical operation at temperatures below the hydrostatic test temperature.

7.6 EVALUATION OF RADIATION EFFECTS

The shift in fracture toughness properties in the beltline materials is a function of neutron fluence and the presence of certain elements, such as copper (Cu) and phosphorus (P). The specific relationship from Reference 5 is:

$$\text{SHIFT } (^\circ\text{F}) = [40 + 1000(\%\text{Cu}-0.08) + 5000(\%\text{P}-0.008)]*(f/10^{19})^{\frac{1}{2}} \qquad (7\text{-}1)$$

where:

%Cu = wt % of Cu present,
%P = wt % of P present,
f = fluence (n/cm^2) at selected EFPY.

The limiting beltline plate and weld are determined based on the Cu-P content and initial RT_{NDT} of the materials. Calculations based on the information in Tables 3-1 and 3-2 show the following:

Limiting plate: 0.13% Cu, 0.015% P, Initial RT_{NDT} = 24°F
Limiting weld: 0.31% Cu, 0.015% P, Initial RT_{NDT} = -22°F
Surveillance plate: 0.13% Cu, 0.011% P

This material information is used to evaluate irradiation shift versus fluence.

7.6.1 Measured Versus Predicted Surveillance Shift

Table 5-3 presents a measured shift for the base metal of 23°F. No measured shift is available for the weld metal. The predicted shift of the surveillance plate, calculated according to Equation 7-1, assumes 0.13% Cu, 0.011% P and an upper bound fluence of:

$$f = (2.6 \times 10^{17} \text{ n/cm}^2 \text{ for capsule})(1.25 \text{ uncertainty}) = 3.25 \times 10^{17} \text{ n/cm}^2.$$

The predicted shift is 19°F, versus the measured shift of 23°F.

7.6.2 Modification of the Shift Relationship

Since the measured shift exceeds the predicted shift, using Reference 5 methods to predict the limiting beltline plate shift may be non-conservative, and therefore is modified. Using Reference 5, the shift calculated is proportional to the material characteristics and to the square root of the fluence. Assuming that the fluence relationship is correct means that the coefficient representing the materials in Equation 7-1 must be increased by the factor (23/19) or 1.21.

7.6.3 Radiation Shift Versus EFPY

Equation 7-1 can be simplified and expressed as a function of EFPY for the base metal and weld metal. Subsection 4.3 concludes that the EOL (32 EFPY) 1/4 T fluence is 1.7×10^{18} n/cm^2. Therefore, in terms of EFPY, the fluence is

$$f = 5.31 \times 10^{16} * \text{EFPY} \qquad (7\text{-}2)$$

Equation 7-2 is used in Equation 7-1 with the appropriate Cu, P values.

For the weld metal:

$$\text{SHIFT}_W = 22.23 * (\text{EFPY})^{\frac{1}{2}}. \qquad (7\text{-}3)$$

For the base metal: (including 1.21 factor)

$$SHIFT_b = 11.02 * (EFPY)^{\frac{1}{2}}. \quad (7\text{-}4)$$

The adjusted reference temperature (ART) is defined as the initial RT_{NDT} plus the irradiation shift. The initial RT_{NDT} values of the limiting plate and weld materials are 24°F and -22°F, respectively. Figure 7-4 shows the ART for each material based on these initial RT_{NDT} values and the shifts of Equations 7-3 and 7-4. As shown in the figure, the plate is initially limiting, because of its higher initial RT_{NDT}. However, the larger shift associated with the weld, because of its higher Cu content, causes the weld ART to exceed the plate ART at about 17 EFPY. The ART values of Figure 7-4 are used to develop the operating limits curves. The higher of the plate or weld ART is used for a given EFPY.

7.6.4 End-Of-Life Conditions

Paragraph IV.B of Reference 1 sets limits on the ART and on the upper shelf energy (USE) of the beltline materials. The ART must be less than 200°F, and the USE must be above 50 ft-lb. Based on Figure 7-4, the ART values at 32 EFPY of 104°F for the weld and 86°F for the plate are acceptable.

Calculations of USE, using Reference 5, are summarized in Table 7-1. The equivalent transverse USE of the plate material is taken as 65% of the longitudinal USE, according to Reference 7. The weld metal USE is not adjusted because weld metal has no orientation effect. Surveillance results for the base metal in Table 5-3 show USE decrease of 6%. The calculated value, using Reference 5, is 10%, so Reference 5 appears to be conservative. Original fabrication testing done by Combustion Engineering developed Charpy data for the beltline plates up to 160°F. The values at 160°F are averaged to estimate USE for the unirradiated beltline plates. The weld USE is established for an intermediate fluence by the surveillance test results. This intermediate value is used to predict the original unirradiated USE, and an EOL value is then calculated. The minimum EOL plate and weld USE values are estimated as 58 ft-lb and 72 ft-lb,

respectively, which are above the minimum limit. Therefore, irradiation effects are not severe enough to necessitate RPV annealing before 32 EFPY.

7.7 OPERATING LIMITS CURVES VALID TO 16 EFPY

The ART selected for the core beltline curves depends on the amount of operation for which the curves will be valid. Sixteen EFPY was selected because Reference 4 recommends withdrawal of the second surveillance capsule at 15 EFPY. The beltline ART estimated with Figure 7-4 is 68°F, based on the plate material. Adjusting the unirradiated beltline curves in Figures 7-1 through 7-3, with their initial RT_{NDT} of 24°F, and considering the non-beltline curves, gives the operating limits valid to 16 EFPY, as shown on Curves A, B and C in Figure 7-5, 7-6 and 7-7, respectively. The values plotted on Figures 7-5 through 7-7 are tabulated in Table 7-2 for Curve A and Table 7-3 for Curves B and C.

7.8 REACTOR OPERATION VERSUS OPERATING LIMITS

For most reactor operating conditions, pressure and temperature are at saturation conditions, which are in the operating zone of the limits curves. The most severe unplanned transient is an upset condition consisting of several transients which result in a SCRAM. The worst combination of pressure and temperature is 1180 psig with temperatures in the lower head at 250°F. At the same time, the steam space coolant temperature is still nearly 550°F. Steam space coolant temperature is used to identify the appropriate curve to be applied. In this case, the core is not critical and, according to the steam space coolant temperature, there is no significant cooldown occurring, so the hydrostatic pressure curve applies (Curve A). As seen for Curve A in Figure 7-5, at 1180 psi the minimum transient temperature in the vessel of 250°F lies in the safe operating zone. Therefore, violation of the operating limits curves is only a concern in cases where operator interaction occurs, such as hydrostatic pressure testing and initiation of criticality.

Table 7-1

ESTIMATE OF UPPER SHELF ENERGY FOR BELTLINE MATERIALS

Identification	% Cu	Upper Shelf (ft-lb) Longitudinal/Transverse f=0	f=3.3×10^{17}	f=1.7×10^{18}
Lower Shell:				
G-3415-1R	0.11	132[a]	120	115/75
G-3415-2	0.14	127[a]	113	108/70
G-3415-3	0.13	119[a]	107	102/66
Low-Int Shell:				
G-3413-7	0.12	103[a,b]	93	89/58
G-3414-1	0.18	127[a]	112	104/68
G-3414-2	0.13	130[a]	117	112/73
Longitudinal Weld:				
1-233	0.31	104	82[a]	72/72

[a] USE values taken from test data. Other USE values are calculated using Reference 5.

[b] Based on Charpy data at only 110°F. Actual USE should be somewhat higher.

Table 7-2

PRESSURE-TEMPERATURE VALUES FOR FIGURE 7-5, CURVE A

Pressure (psi)	Temperature (°F)	Remarks
0	90	Boltup Temperature
312	90	
312	120	RT_{NDT}+90 per 10CFR50 App. G
755	120	Beltline becomes limiting
760	121	
770	122.5	
780	124	
790	126	
800	127.5	
810	129	
820	130.5	
830	132	
840	133.5	
850	135	
860	136.5	
870	138	
880	139	
890	140.5	
900	142	
910	143	
920	144.5	
930	145.5	
940	147	
950	148	
960	149	
970	150.5	
980	151.5	
990	152.5	
1000	153.5	Pressure increment of 20 psi
1020	156	
1040	158	
1060	162.5	
1080	164.5	
1100	166.5	
1120	168.5	
1140	170	
1160	172	
1180	173.5	
1200	175	
1220	177	
1240	178.5	
1260	180	
1280	181.5	
1300	183	
1320	184.5	
1340	186	
1360	187	
1380	188.5	
1400	190	

Table 7-3

PRESSURE-TEMPERATURE VALUES FOR FIGURE 7-6 (CURVE B) AND 7-7 (CURVE C)

Pressure (psi)	Curve B Temp. (°F)	Curve C Temp. (°F)	Remarks
0	90	90	Boltup Temperature
57		90	FW Nozzle limiting Curve C
60		94	
70		102	
80		110	
90		117	
100		124	
110		129	
112	90	130	FW Nozzle limiting Curve B
120	94	134	
130	99	139	
140	104	144	
150	108	148	
160	112	152	
170	115.5	155.5	
180	119	159	
190	122	162	
200	125	165	
210	127.5	167.5	
220	130	170	
230	132.5	172.5	
240	135	175	
250	137	177	
260	139	179	
270	141	181	
280	143	183	
290	145	185	
300	147	187	Increment pressure 20 psi
320	150	190	
340	153	193	
360	157	197	
380	160	200	
400	162.5	202.5	
420	165	205	
440	168	208	
460	170	210	
480	172	212	
500	174.5	214.5	
520	176.5	216.5	
540	178	218	
560	180	220	
580	182	222	

Table 7-3 (continued)

Pressure (psi)	Curve B Temp. (°F)	Curve C Temp. (°F)	Remarks
600	184	224	Increment pressure 50 psi
650	188	228	
700	192	232	
750	194	234	
800	196	236	
850	198	238	
900	200	240	
950	202	242	
1000	204	244	
1050	205.5	245.5	
1100	207	247	
1150	209	249	
1200	211	251	
1250	212.5	252.5	Beltline becomes limiting
1300	215.5	255.5	
1350	218.5	258.5	
1400	221	261	

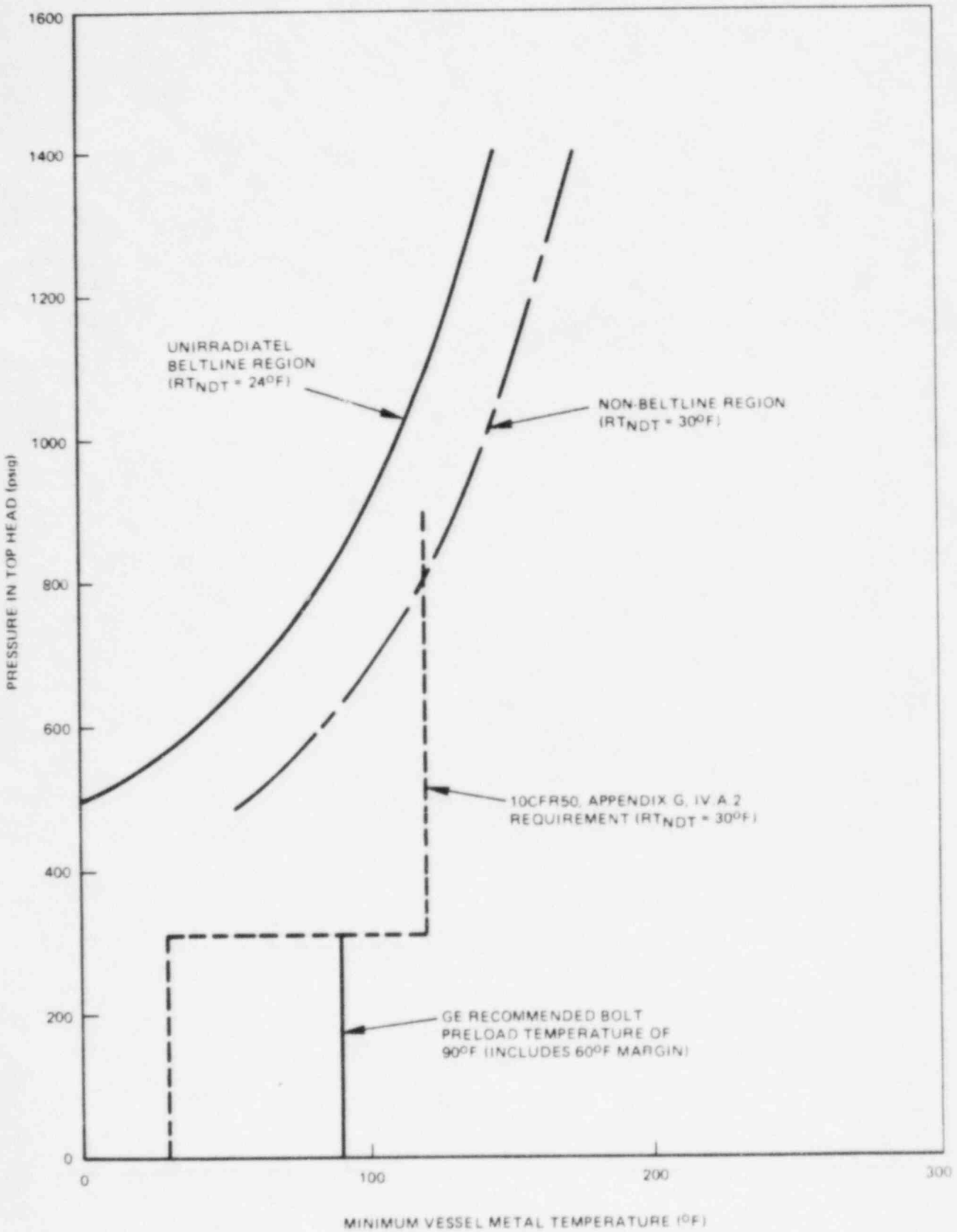

Figure 7-1. Components of Operating Limits Curve for Pressure Tests (Curve A) for FitzPatrick

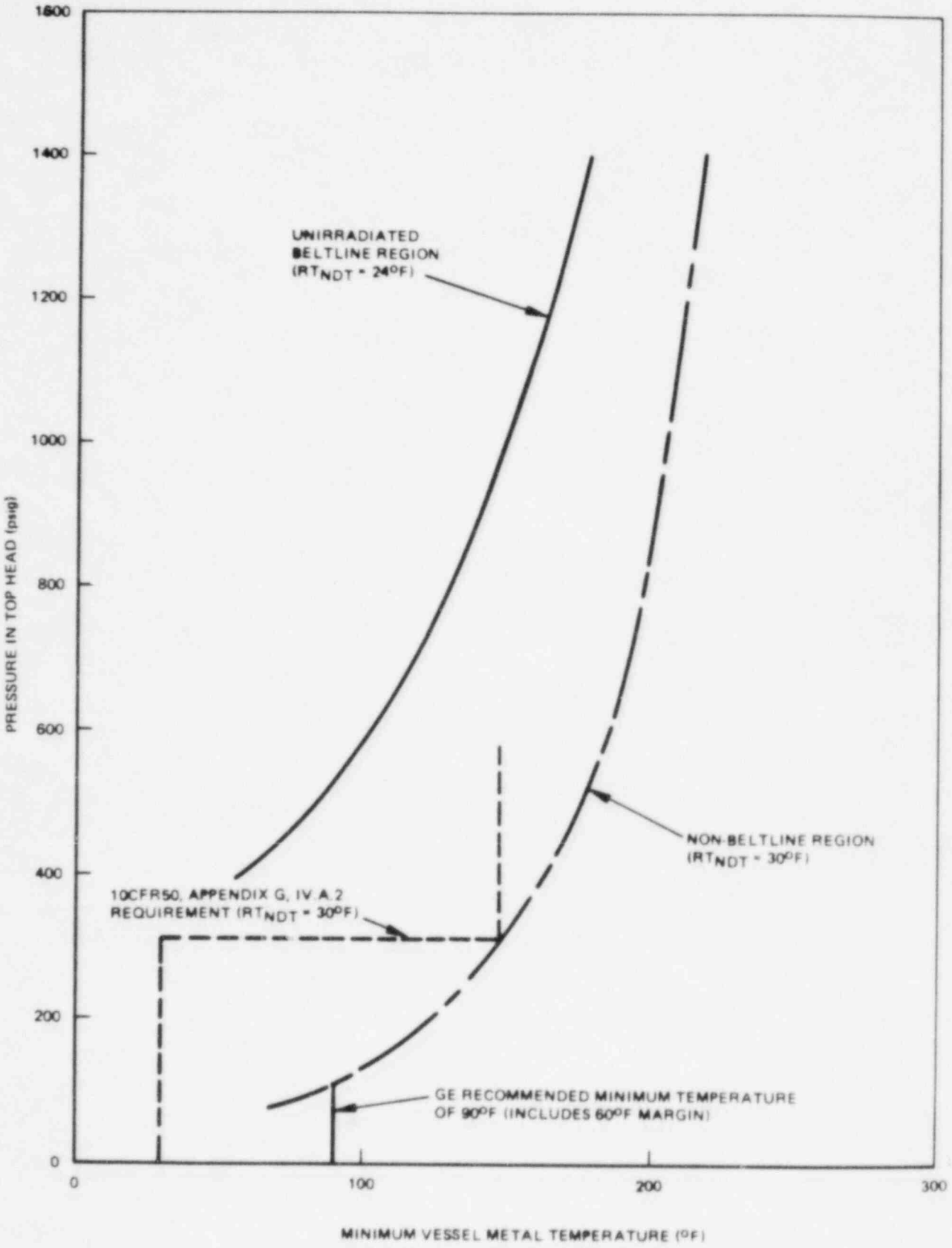

Figure 7-2. Components of Operating Limits Curve for Non-Nuclear Heatup/Cooldown (Curve B) for FitzPatrick

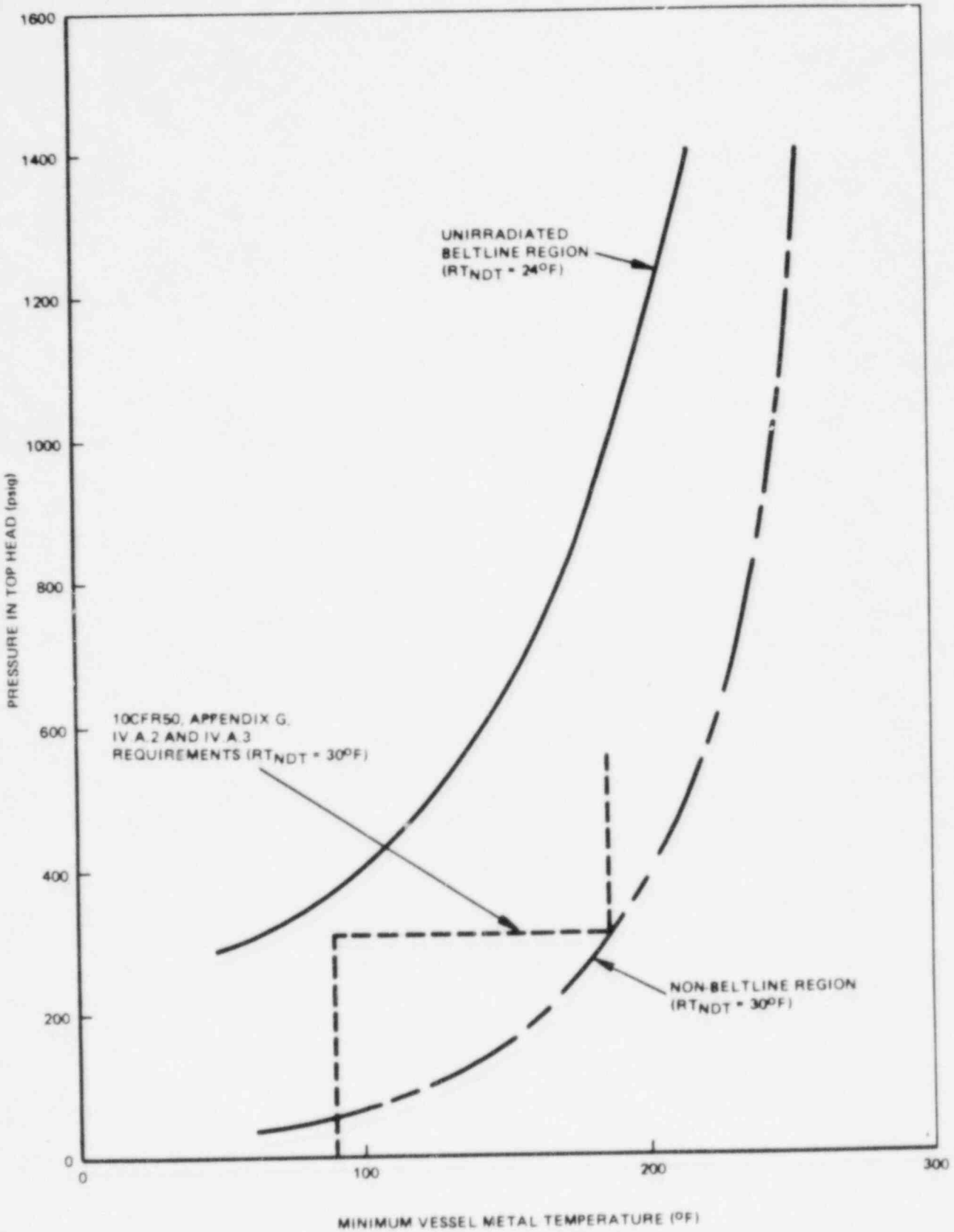

Figure 7-3. Components of Operating Limits Curve for Core Critical Operation (Curve C) for FitzPatrick

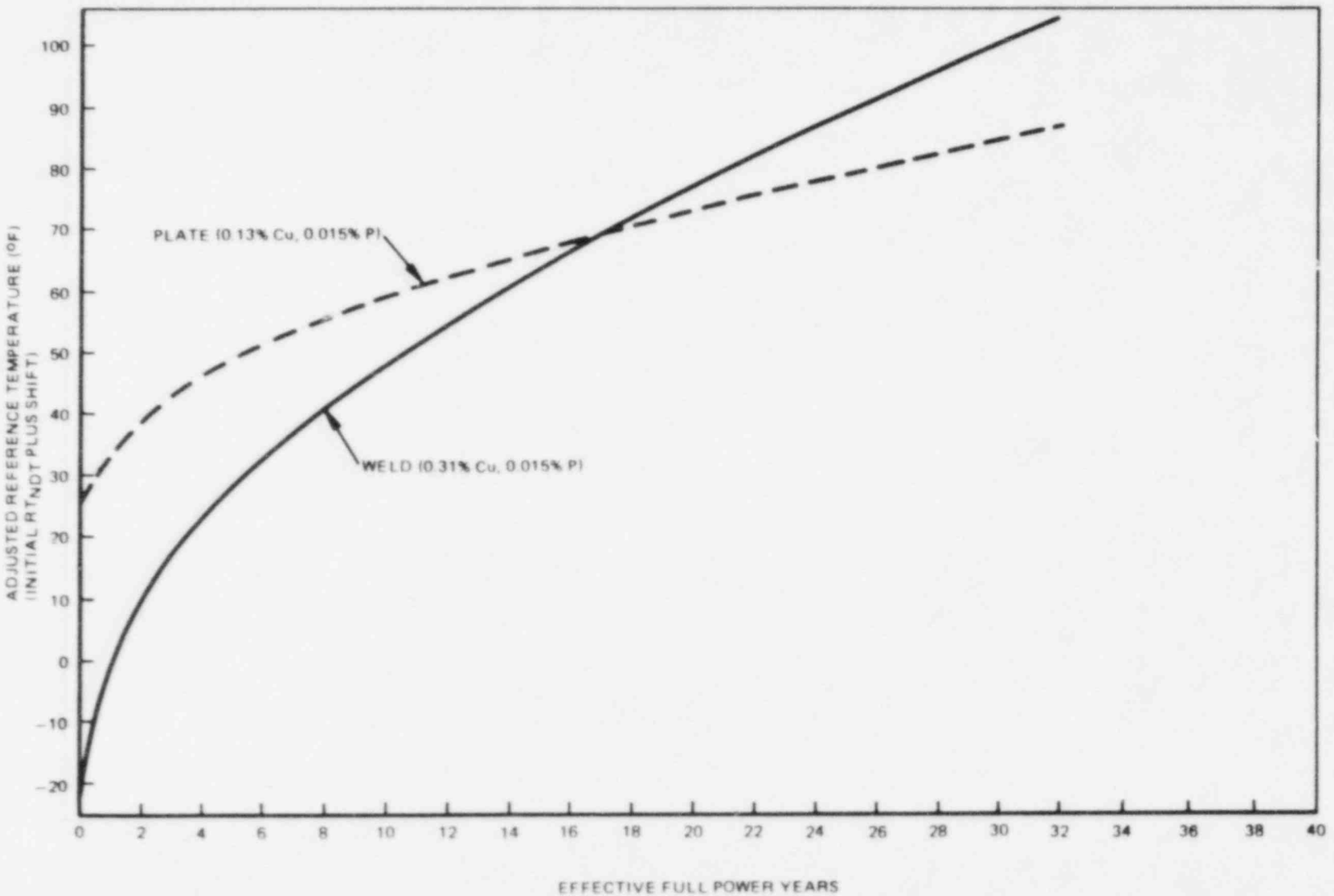

Figure 7-4. Adjusted Reference Temperature of Limiting Beltline Plate and Weld, Based on Surveillance Specimen Test Results for FitzPatrick

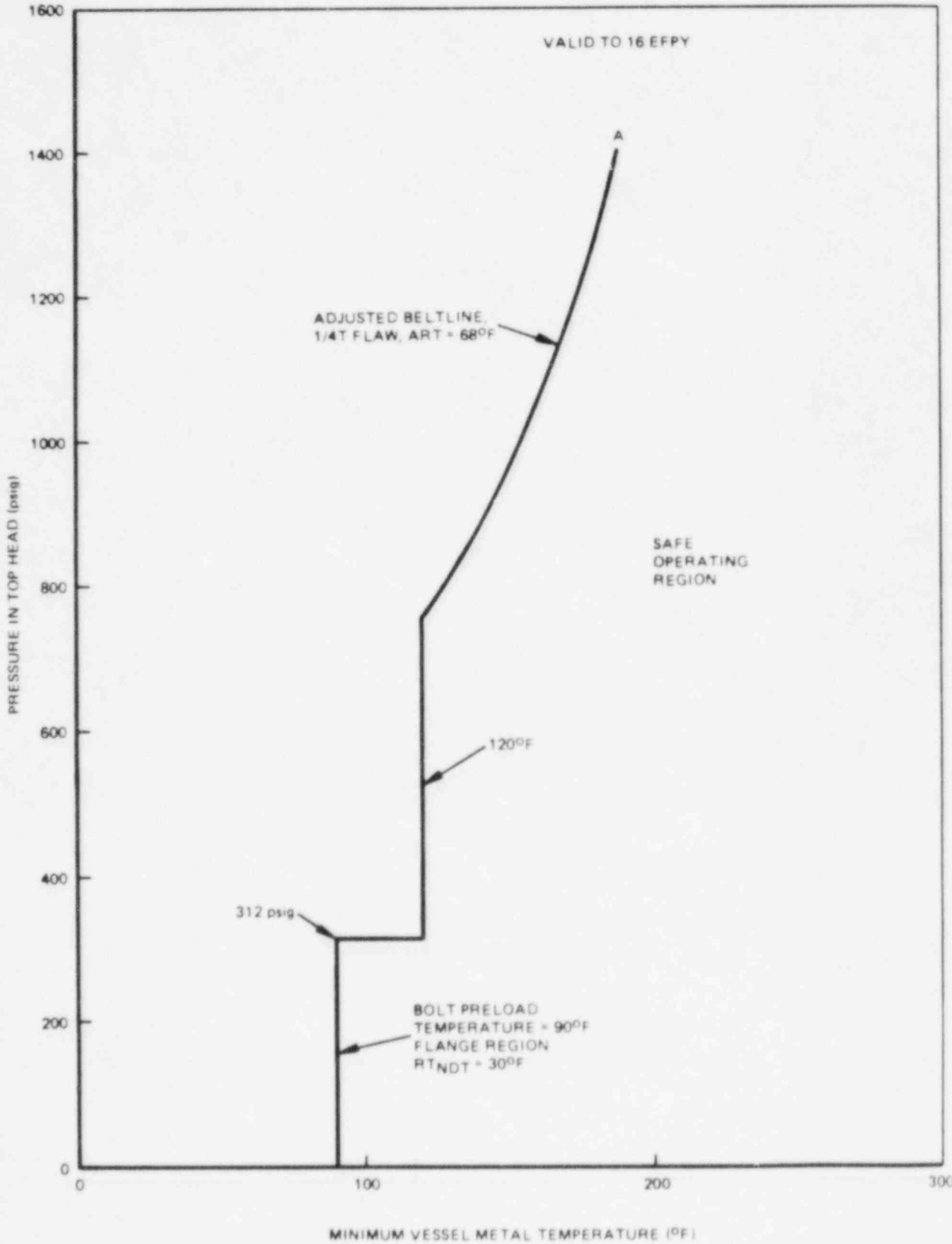

Figure 7-5. Pressure Versus Minimum Temperature for Hydrostatic Pressure Tests for FitzPatrick

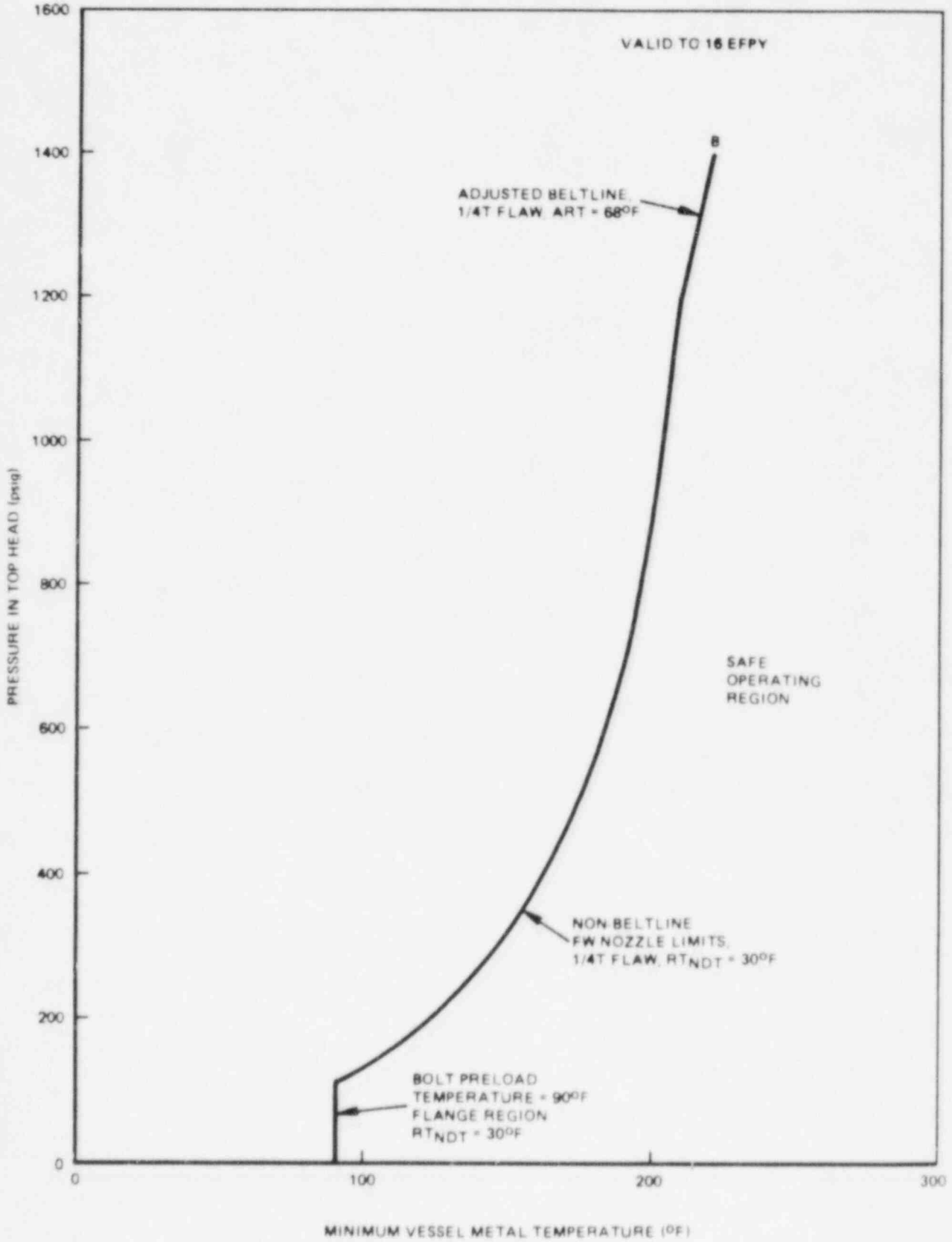

Figure 7-6. Pressure Versus Minimum Temperature for Non-Nuclear Heatup and Cooldown for FitzPatrick

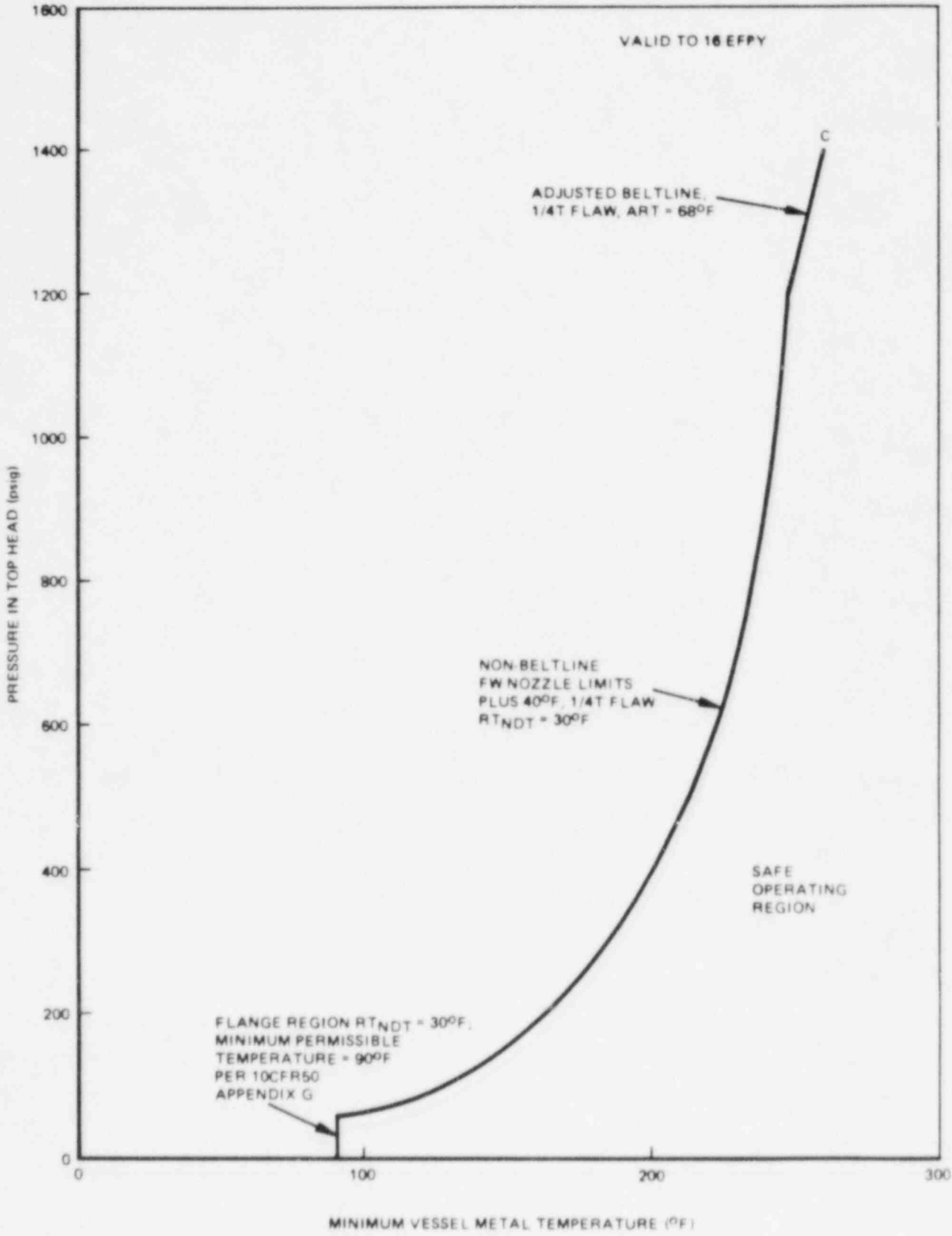

Figure 7-7. Pressure Versus Minimum Temperature for Core Critical Operation for FitzPatrick

8. REFERENCES

1. "Fracture Toughness Requirements," Appendix G to Part 50 of Title 10 of the Code of Federal Regulations, July 1983 (24FR24008).

2. "Protection Against Non-Ductile Failure," Appendix G to Section III of the ASME Boiler & Pressure Vessel Code, Addenda to and including Winter 1984.

3. "Reactor Vessel Material Surveillance Program Requirements," Appendix H to Part 50 of Title 10 of the Code of Federal Regulations, July 1983 (48FR24008).

4. "Conducting Surveillance Tests for Light Water Cooled Nuclear Power Reactor Vessels," Annual Book of ASTM Standards, E185-82, July 1982.

5. "Effects of Residual Elements on Predicted Radiation Damage to Reactor Vessel Materials," USNRC Regulatory Guide 1.99, Revision 1, April 1977.

6. Deleted.

7. "Fracture Toughness Requirements," USNRC Branch Technical Position MTEB 5-2, Revision 1, July 1981.

8. "Capsule Basket," General Electric Drawing 117C4349, Revision 1, October 1969.

9. Letter, R. A. Hillis of Combustion Engineering, Inc. to G. A. Barry of General Electric Company, "Welding Material Certification Data for FitzPatrick Beltline," January 1986.

10. "Surveillance Test Program for Nine Mile Point III Reactor Vessel," Combustion Engineering Specification (GE VPF 1980-234-1), May 1969.

11. Caine, T. A., "Hatch 1 RPV Surveillance Materials Testing and Fracture Toughness Analysis," General Electric Company (NEDC-30997), October 1985.

12. "Standard Methods for Notched Bar Impact Testing of Metallic Materials," Annual Book of ASTM Standards, E23-82, March 1982.

13. "Standard Test Methods for Rockwell Hardness and Superficial Rockwell Hardness of Metallic Materials," Annual Book of ASTM Standards, E18-79.

14. "Standard Methods of Tension Testing of Metallic Materials," Annual Book of ASTM Standards, E8-81.

15. "Ultrasonic Examination for Cracks in the Top Head Flange," CBI Nuclear, Development Report 74-9047, December 1975.

16. "Ultrasonic Examination for Cracks in the Shell Flange," CBI Nuclear, Development Report 74-9056, November 1975.

APPENDIX A

CHARPY V-NOTCH FRACTURE SURFACE PHOTOGRAPHS

Photographs of each Charpy specimen fracture surface were taken to facilitate the determination of percent shear, and to comply with the requirements of ASTM E185-82. The pages following show the fracture surface photographs along with a summary of the Charpy test results for each specimen. The pictures are arranged by increasing test temperature for each material, with the materials in the order of base, weld and HAZ.

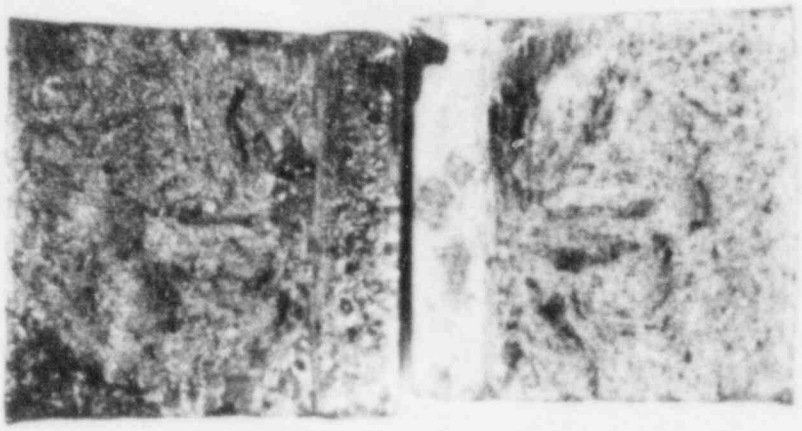

BASE: 52K
TEMP: −60°F
ENERGY: 14.3 ft·lb

MLE: 15
% SHEAR: 0

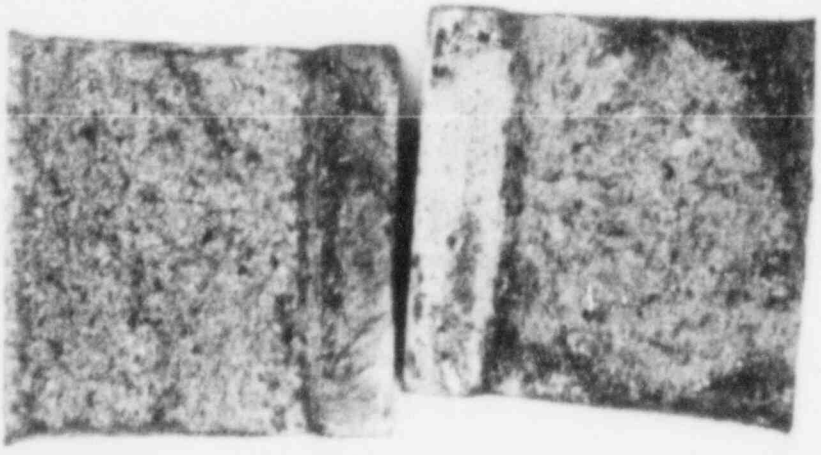

BASE: 52C
TEMP: −20°F
ENERGY: 21.0 ft·lb

MLE: 26
% SHEAR: 0

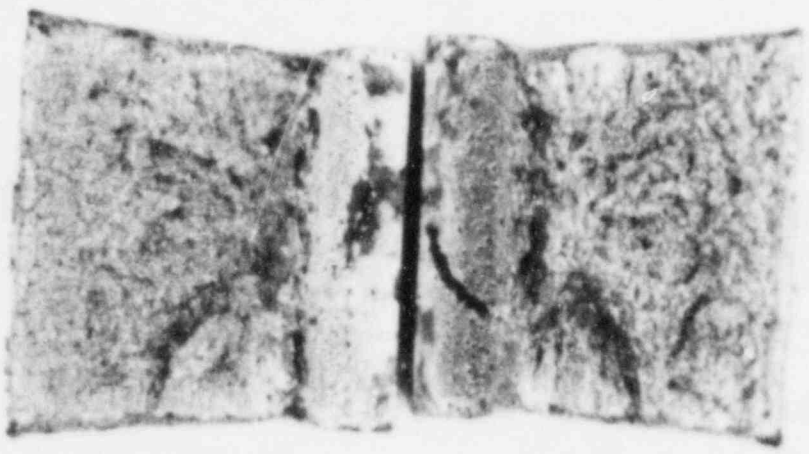

BASE:	528	MLE:	46
TEMP:	0°F	% SHEAR:	0
ENERGY:	46.5 ft-lb		

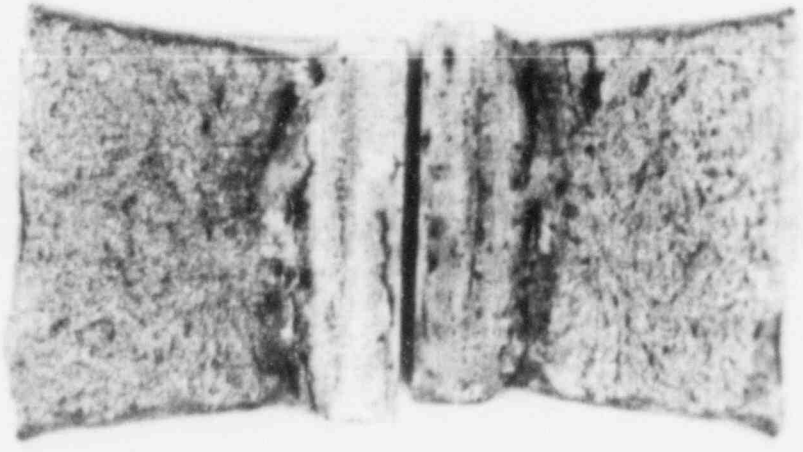

BASE:	531	MLE:	57
TEMP:	10°F	% SHEAR:	10
ENERGY:	6.10 ft-lb		

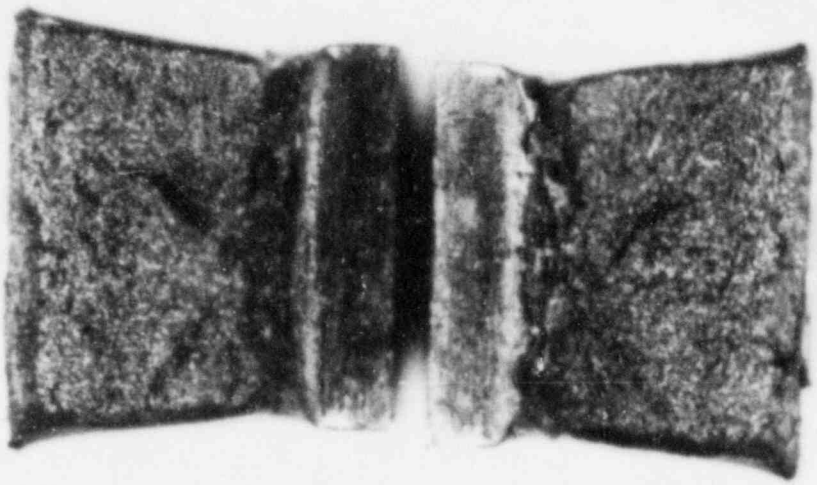

BASE: 52A
TEMP: 20°F
ENERGY: 67.5 ft-lb

MLE: 61
% SHEAR: 20

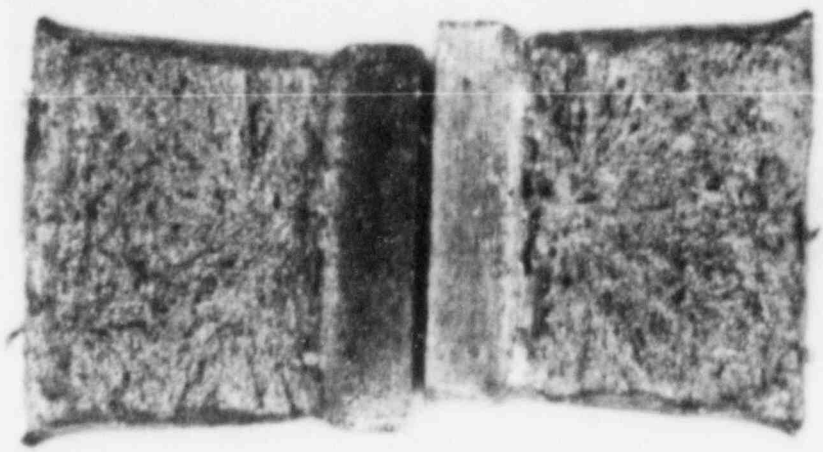

BASE: 51B
TEMP: 40°F
ENERGY: 44.5 ft-lb

MLE: 51
% SHEAR: 20

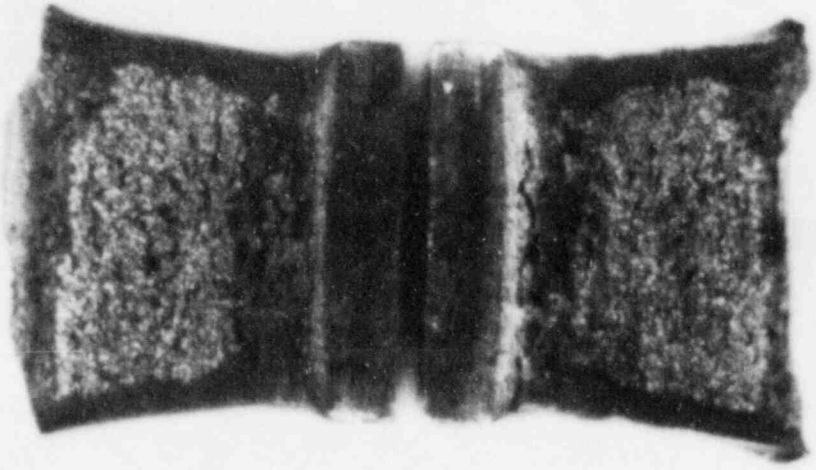

BASE: 51L
TEMP: 80°F
ENERGY: 83.6 ft-lb

MLE: 70
% SHEAR: 50

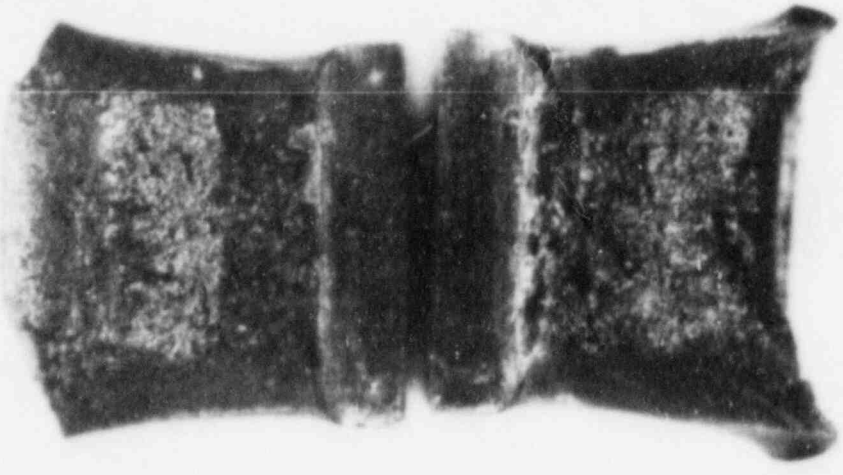

BASE: 51C
TEMP: 120°F
ENERGY: 100.0 ft-lb

MLE: 68
% SHEAR: 60

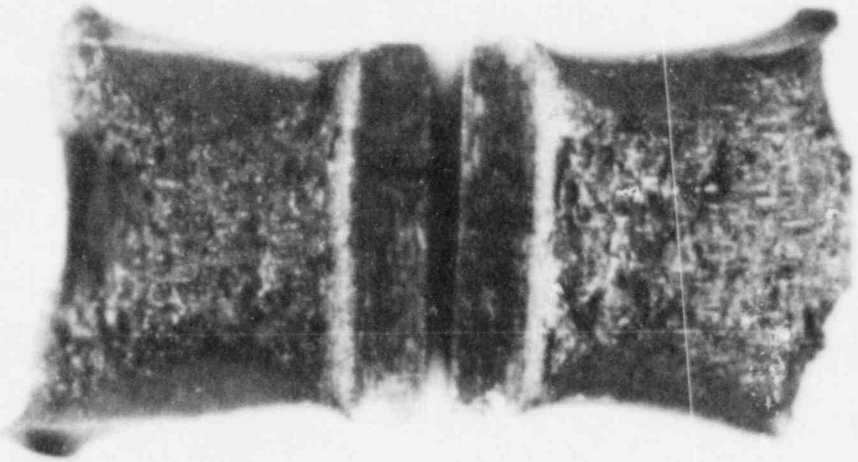

BASE:	51Y	MLE	86
TEMP	160°F	% SHEAR	50
ENERGY:	125.0 ft-lb		

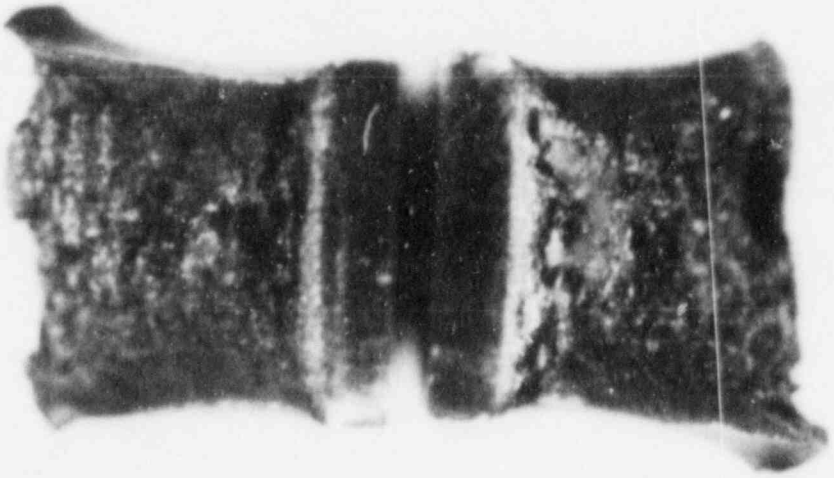

BASE:	51D	MLE	92
TEMP	200°F	% SHEAR	90
ENERGY:	136.5 ft-lb		

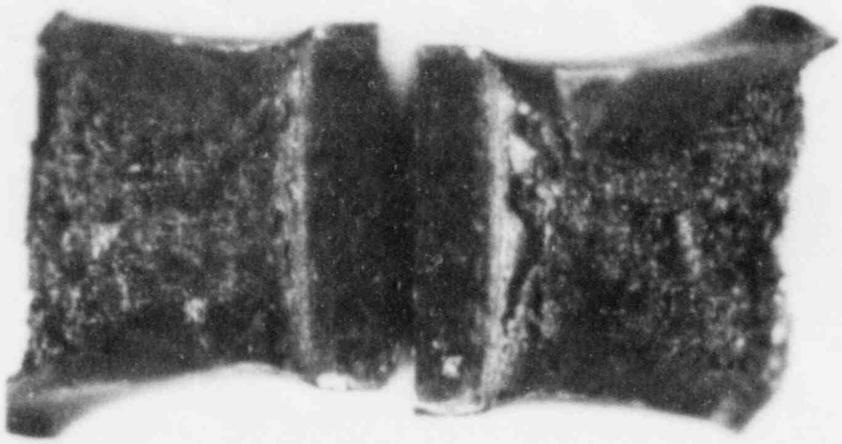

BASE: 52M
TEMP: 300°F
ENERGY: 136.5 ft-lb

MLE: 94
% SHEAR: 100

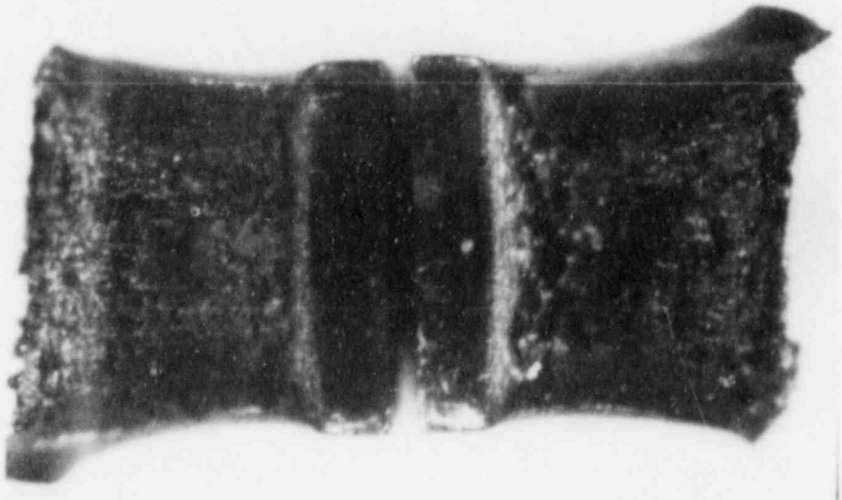

BASE: 52U
TEMP: 400°F
ENERGY: 121.3 ft-lb

MLE: 92
% SHEAR: 80

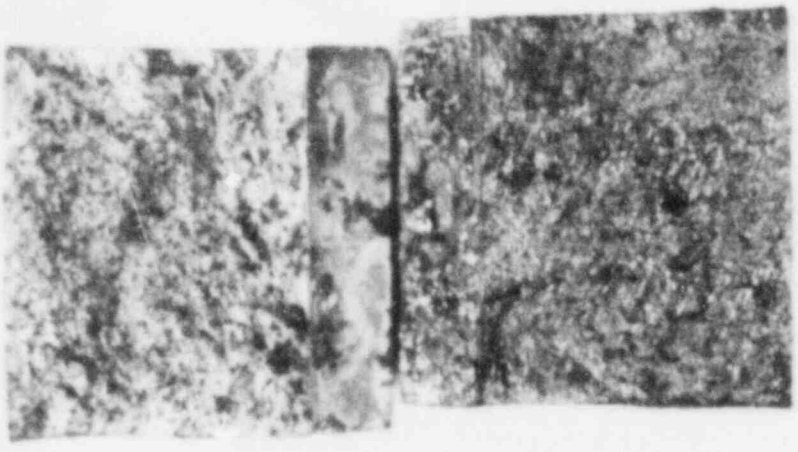

WELD:	55J	MLE:	11
TEMP:	-60°F	% SHEAR:	0
ENERGY:	7.2 ft-lb		

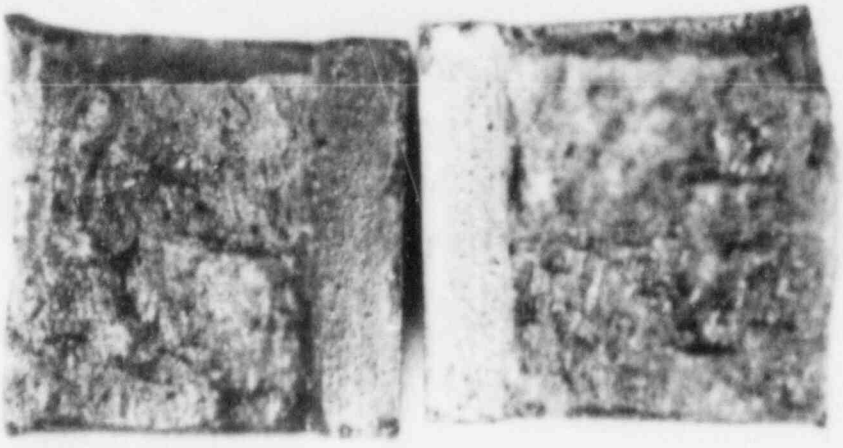

WELD:	55D	MLE:	26
TEMP:	-20°F	% SHEAR:	20
ENERGY:	24 ft-lb		

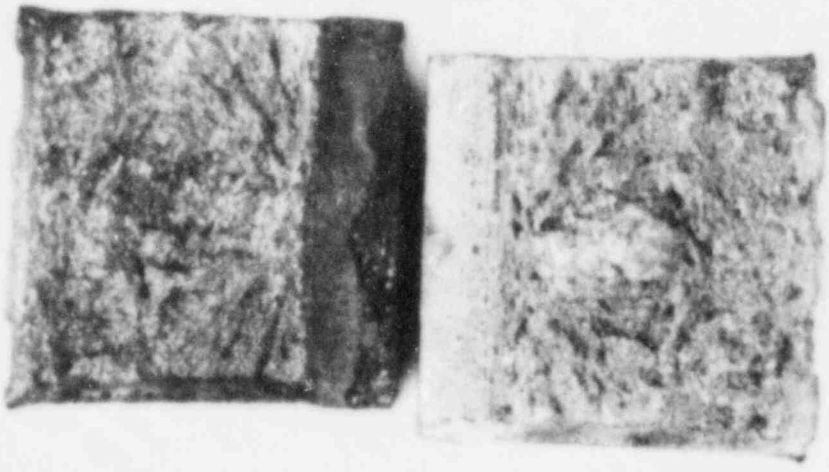

WELD:	55A	MLE:	20
TEMP:	0°F	% SHEAR:	10
ENERGY:	15.0 ft-lb		

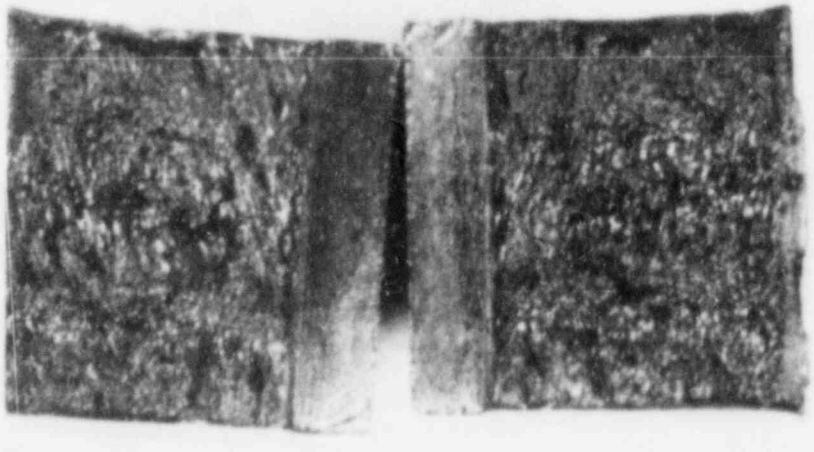

WELD:	56M	MLE:	23
TEMP:	10°F	% SHEAR:	0
ENERGY:	14.0 ft-lb		

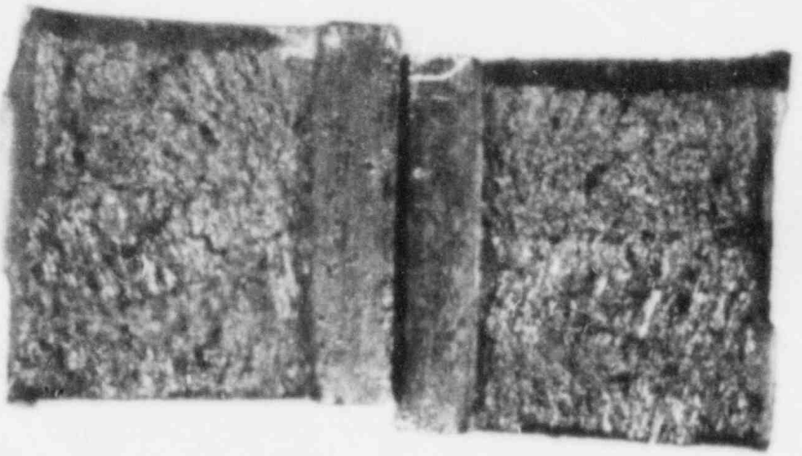

WELD: 552
TEMP: 20°F
ENERGY: 20.0 ft-lb

MLE: 25
% SHEAR: 30

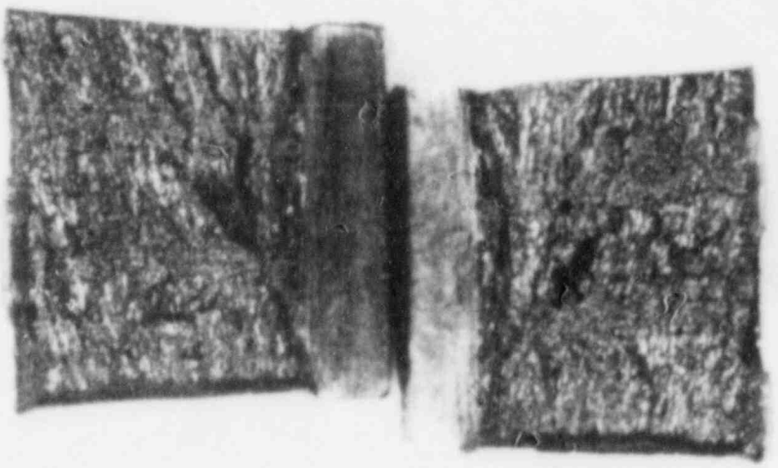

WELD: 541
TEMP: 40°F
ENERGY: 31.4 ft-lb

MLE: 33
% SHEAR: 20

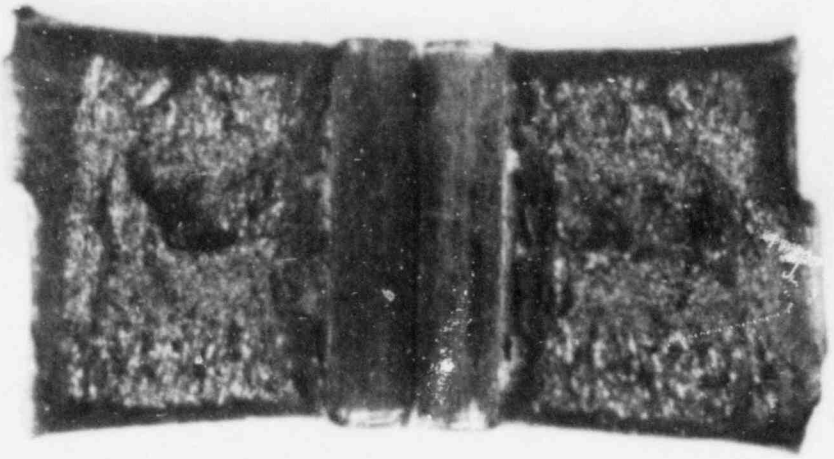

WELD:	54L	MLE:	39
TEMP:	80°F	% SHEAR:	40
ENERGY:	42.0 ft-lb		

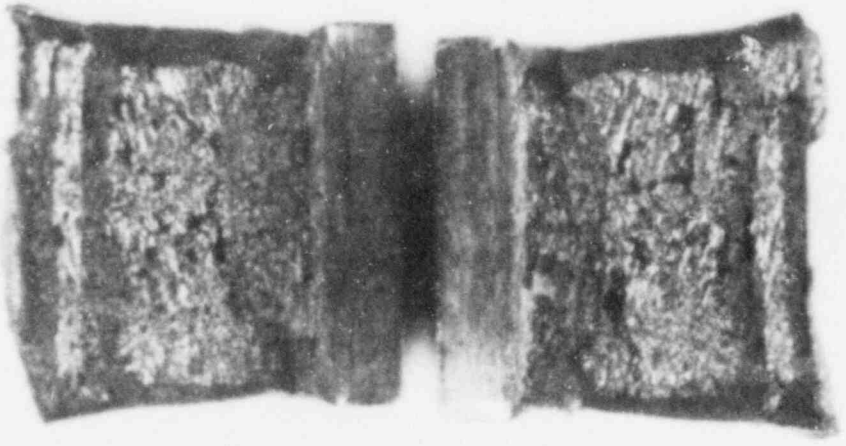

WELD:	54B	MLE:	52
TEMP:	120°F	% SHEAR:	70
ENERGY:	54.1 ft-lb		

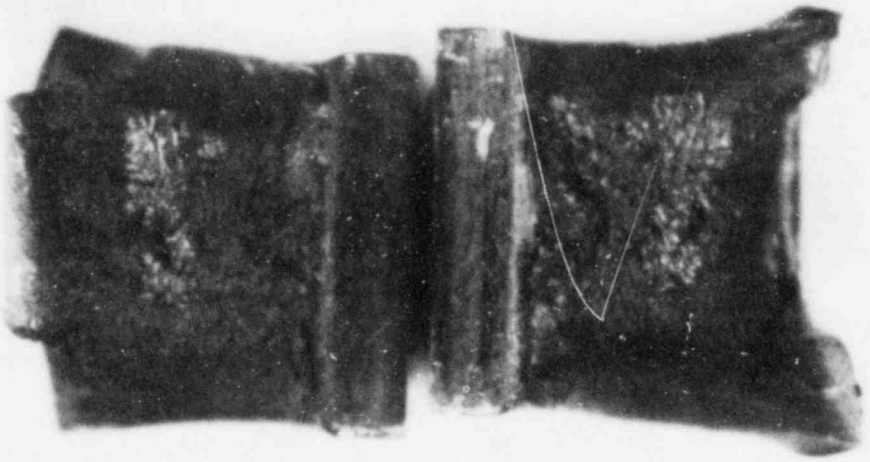

WELD:	54P	MLE:	62
TEMP:	160°F	% SHEAR:	85
ENERGY:	75.0 ft-lb		

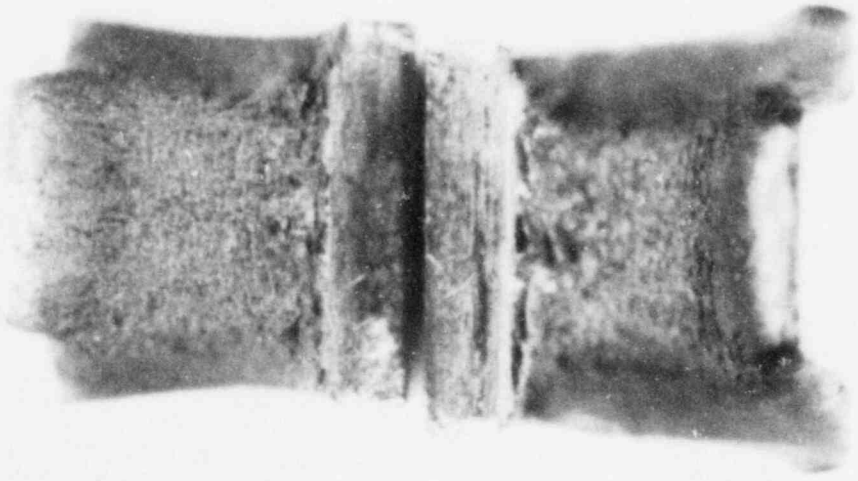

WELD:	54D	MLE:	53
TEMP:	200°F	% SHEAR:	70
ENERGY:	82.1 ft-lb		

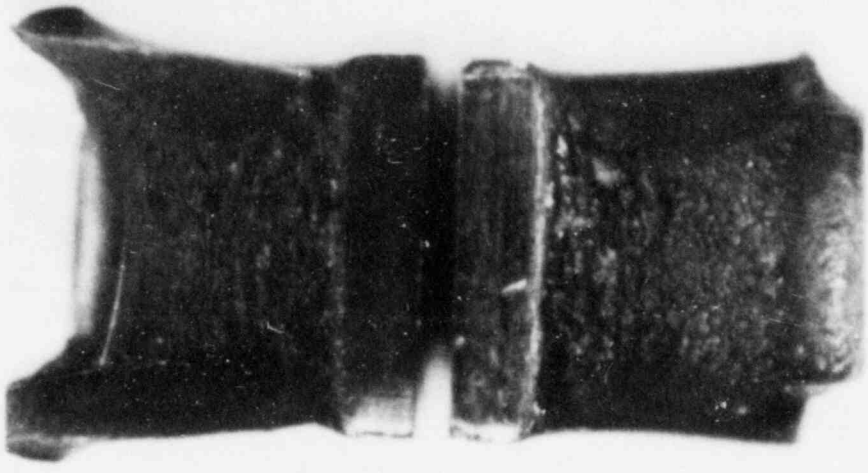

WELD:	55U	MLE:	65
TEMP:	300°F	% SHEAR:	60
ENERGY:	86.0 ft-lb		

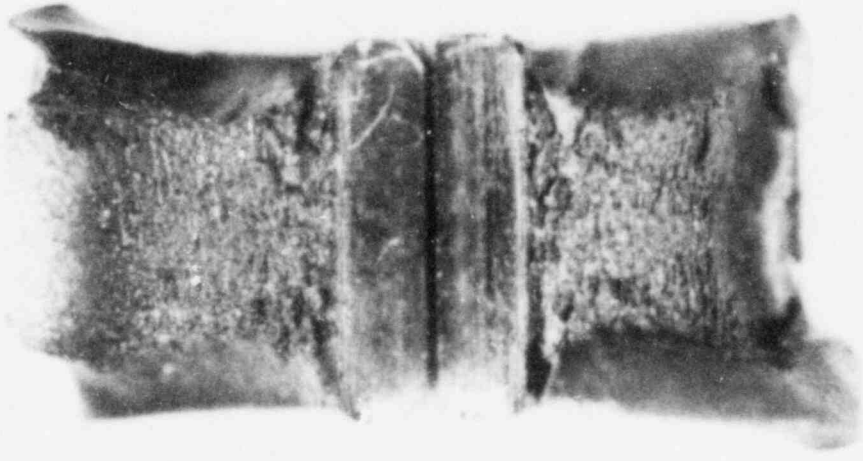

WELD:	56E	MLE:	70
TEMP:	400°F	% SHEAR:	100
ENERGY:	79.3 ft-lb		

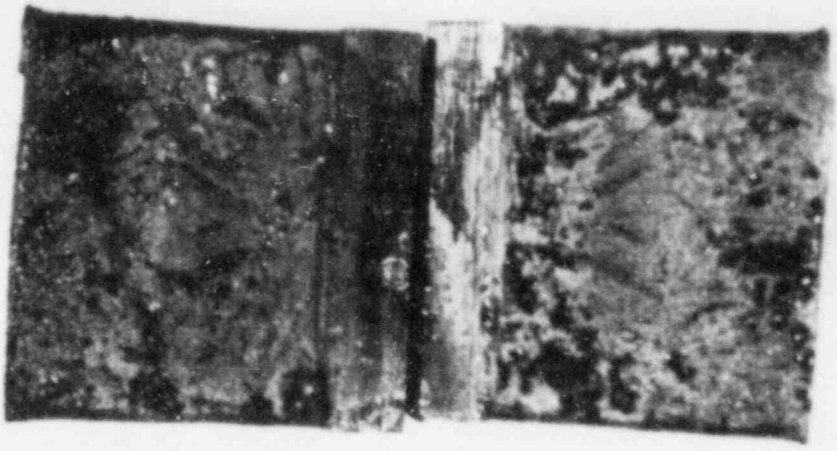

HAZ: 5BL
TEMP: –60°F
ENERGY: 13.2 ft-lb

MLE: 16
% SHEAR: 10

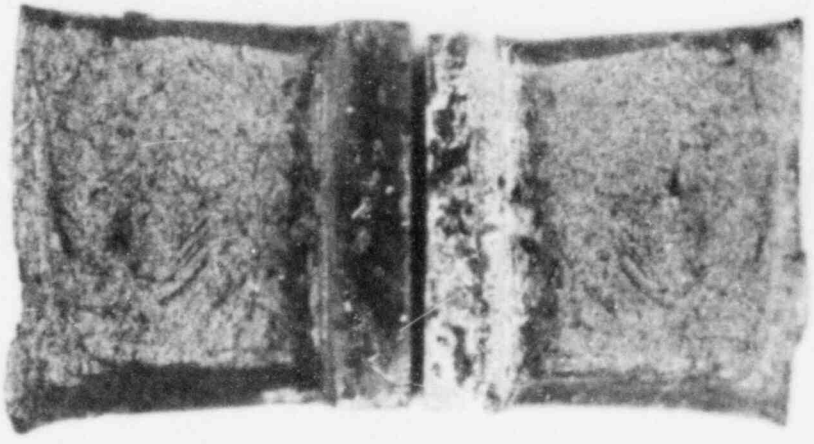

HAZ: 5B4
TEMP: –20°F
ENERGY: 38.3 ft-lb

MLE: 35
% SHEAR: 20

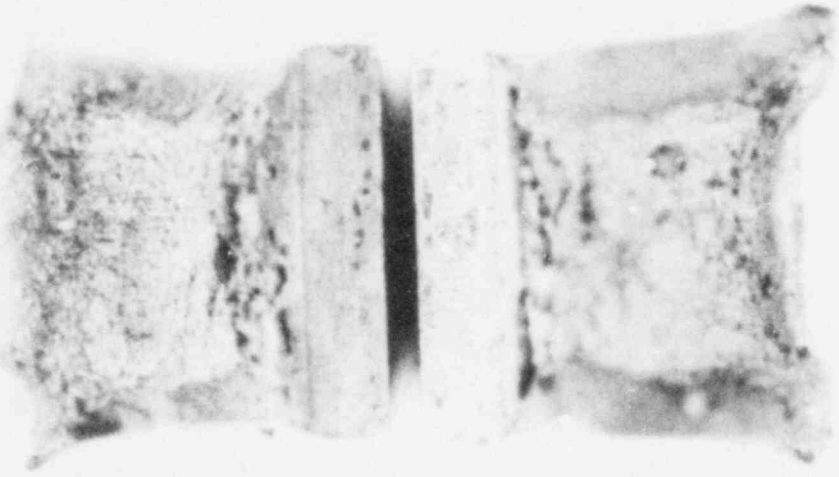

HAZ:	5AC	MLE:	70
TEMP:	0°F	% SHEAR:	50
ENERGY:	78.5 ft-lb		

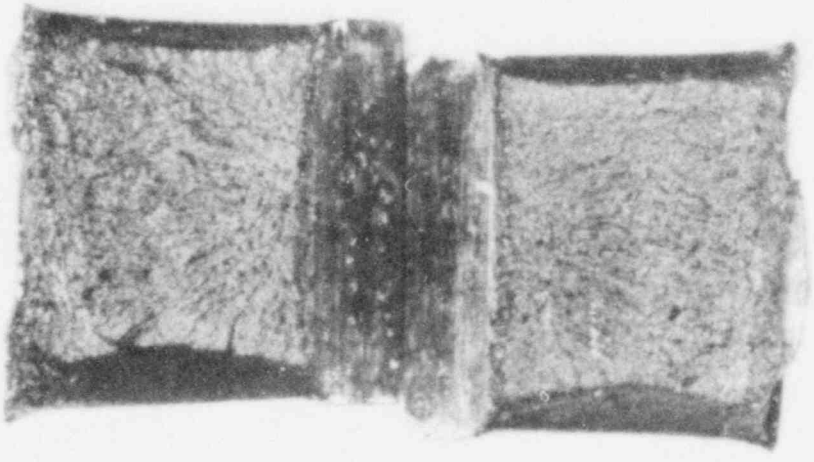

HAZ:	5BU	MLE:	28
TEMP:	10°F	% SHEAR:	40
ENERGY:	26.5 ft-lb		

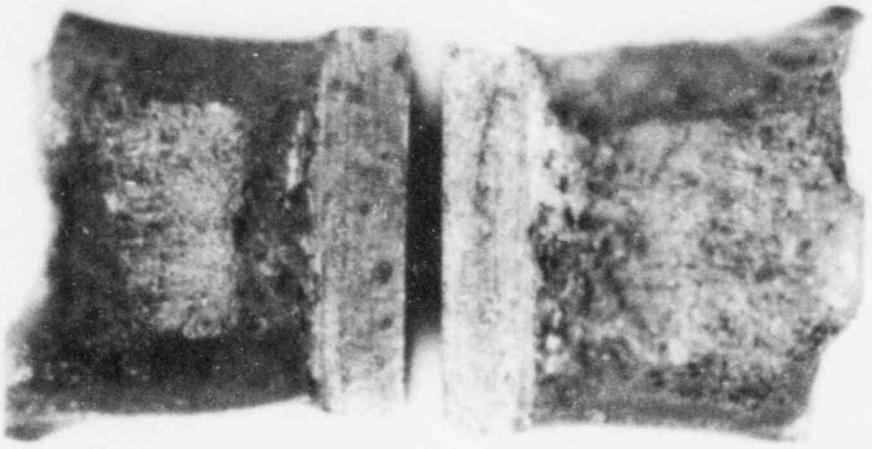

HAZ:	5AA	MLE:	64
TEMP:	20°F	% SHEAR:	60
ENERGY:	86.7 ft-lb		

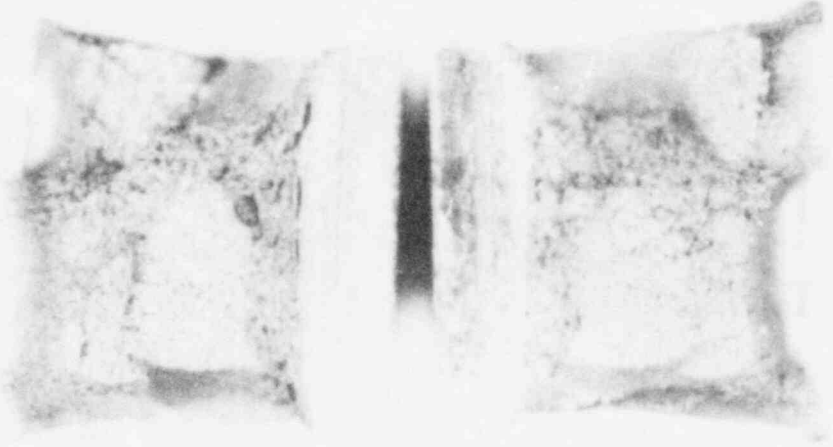

HAZ:	572	MLE:	51
TEMP:	40°F	% SHEAR:	50
ENERGY:	60.1 ft-lb		

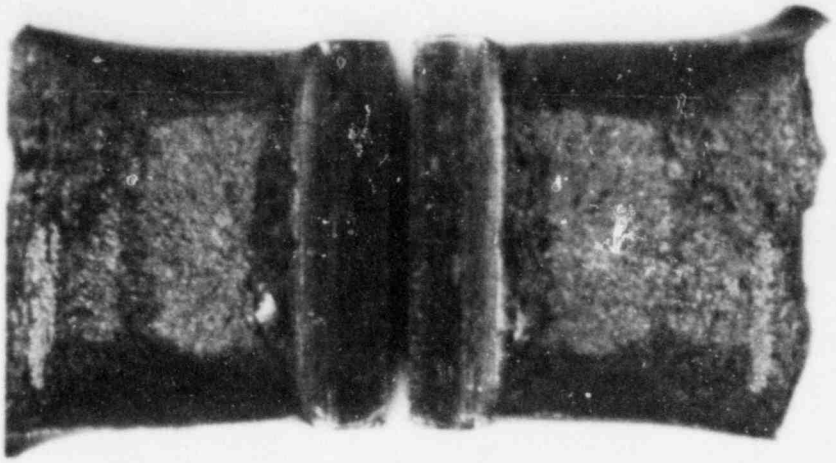

HAZ:	57Y	MLE:	46
TEMP:	80°F	% SHEAR:	60
ENERGY:	61.5 ft-lb		

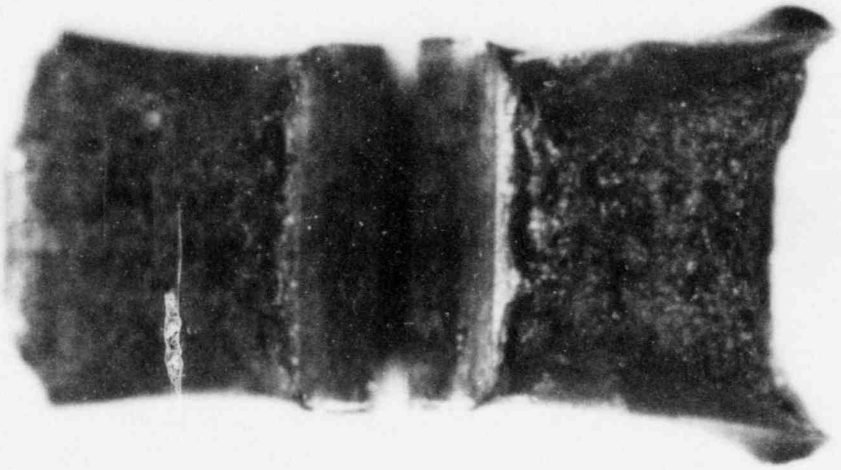

HAZ:	57K	MLE:	65
TEMP:	120°F	% SHEAR:	50
ENERGY:	110.6 ft-lb		

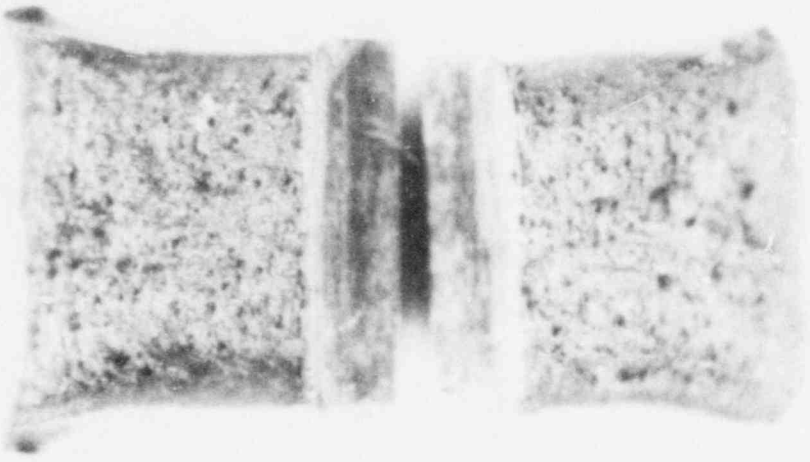

HAZ:	5A1	MLE:	66
TEMP:	160°F	% SHEAR:	100
ENERGY:	81.2 ft-lb		

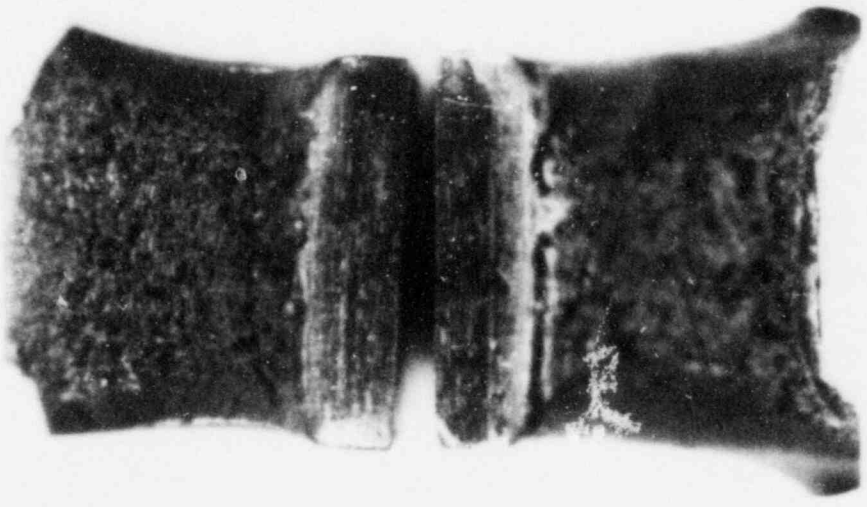

HAZ:	57T	MLE:	70
TEMP:	200°F	% SHEAR:	100
ENERGY:	107.5 ft-lb		

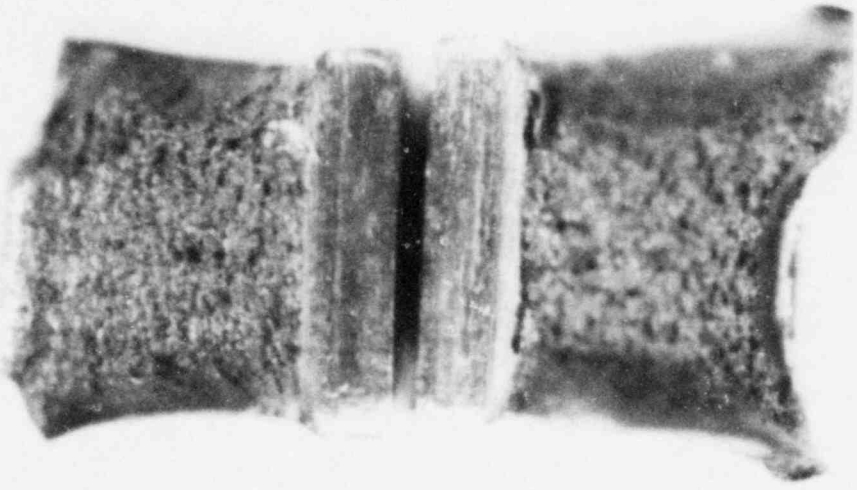

HAZ: 5BM
TEMP: 300°F
ENERGY: 87.2 ft-lb

MLE: 71
% SHEAR: 60

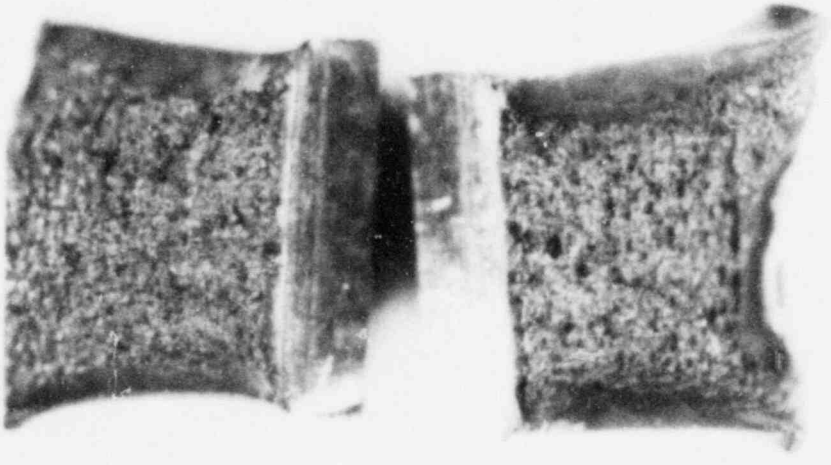

HAZ: 5BP
TEMP: 400°F
ENERGY: 72.0 ft-lb

MLE: 23
% SHEAR: 100